AN ABSTRACT OF THE THESIS OF

Daniel R. Bailey for the degree of Master of Science in Water Resource Engineering presented on December 22, 2011.

Title: Towards Autonomous Irrigation: Comparison of Two Moisture Sensing Technologies, Irrigation Distribution Analysis, and Wireless Network Performance at an Ornamental Container Nursery

Abstract approved:

John S. Selker

As ornamental container nurseries face diminishing water allocations, many are looking to automated irrigation solutions to increase their water application efficiency. This thesis presents the findings of a study conducted at a commercial container nursery to determine 1) whether a capacitance or load cell sensor was better suited for monitoring volumetric water content in the substrate; 2) if the actual irrigation distribution conformed to the expected pattern, how uniform were the weights of plants, and how these combined with plant canopy affected the leaching fraction; and 3) the reliability of the wireless network used to transmit the data to a central database. It was found that 1) the load cells outperformed the capacitance-based sensors because the load cells took an integrated measure; 2) the actual irrigation pattern followed the expected pattern, the variation of irrigation sections were low (C.V. = 0.06) and similar (C.V. ranging from 0.029 to 0.12), and unpruned plant canopies produced greater leaching fraction than pruned canopies ($P < 0.18$); and 3) wireless network transmission reliability was low (75.2%), suggesting that the system was not suitable for real-time irrigation control, but was sufficient for calculating irrigation length and monitoring net effective irrigation application and evapotranspirative consumption.

Towards Autonomous Irrigation: Comparison of Two Moisture Sensing Technologies, Irrigation Distribution Analysis, and Wireless Network Performance at an Ornamental Container Nursery

by

Daniel R. Bailey

A THESIS

submitted to

Oregon State University

in partial fulfillment of
the requirements for the
degree of

Master of Science

Presented December 22, 2011
Commencement June 2012

Master of Science thesis of Daniel R. Bailey presented on December 22, 2011.

APPROVED:

Major Professor, representing Water Resources Engineering

Director of the Water Resource Graduate Program

Dean of the Graduate School

I understand that my thesis will become part of the permanent collection of Oregon State University libraries. My signature below authorizes release of my thesis to any reader upon request.

Daniel R. Bailey, Author

ACKNOWLEDGEMENTS

I would like to express my sincere and utmost thanks to my many family members and friends who have walked with me during my adventures at Oregon State University. I could not have come this far without you. I would like to especially thank my mother and aunts and uncles who have provided much needed support and advice throughout. Additionally, to my friends who have leant sympathetic ears and shared many cups of coffee, time around board games, and running trails, I thank you and appreciate you more than I could ever say. You have all truly blessed me.

CONTRIBUTION OF AUTHORS

John S. Selker, James S. Owen, and Heather Stoven provided much advice and direction on the experimental setup. James and Heather were invaluable during the installation and manual collection of plant masses. James Wagner provided much needed assistance for the configuration of the wireless network and load cell hardware communication. John, James Owen, and James Wagner provided helpful and insightful comments on data analysis and the editing of this document.

TABLE OF CONTENTS

TABLE OF CONTENTS (Continued)

Page

TABLE OF CONTENTS (Continued)

Page

LIST OF FIGURES

LIST OF FIGURES (Continued)

Page

LIST OF TABLES

LIST OF APPENDICES

LIST OF APPENDIX FIGURES

LIST OF APPENDIX FIGURES (Continued)

Page

LIST OF APPENDIX FIGURES (Continued)

Page

LIST OF APPENDIX TABLES

Towards Autonomous Irrigation: Comparison of Two Moisture Sensing Technologies, Irrigation Distribution Analysis, and Wireless Network Performance at an Ornamental Container Nursery

Chapter 1

Comparison of Two Sensors

1.0 Abstract

As ornamental container nurseries face increased pressure to reduce irrigation, many are looking to automated solutions to increase their water application efficiency. To this end, a study was conducted at a commercial container nursery to determine which of two sensors was better suited for monitoring the volumetric water content (VWC) of the substrate in an automated system. It was found that load cells outperformed capacitance based probes in reliability to provide an accurate response to irrigation, representation of the entire container, and resolution.

1.1 Introduction

1.1.1 Background

Since the 1980s, a major shift in water resource allocation has been taking place. Whereas historically, water access has been provided free of charge as a public good for many types of uses from farming to industry to private home use, now users are under much stricter environmental regulation to reduce water withdrawals and avoid chemical runoff. Water withdrawals and chemical pollution are two key factors impacting aquatic habitat quality (Andreen 2011). Beeson et al. (2004), in a review on the future of container nurseries, concluded that water availability for nursery use and chemical runoff will be two of the most important pressures facing nurseries in the following decade. Nursery managers can reduce their water consumption per plant while at the same time reducing chemical runoff pollution through several recognized methods, including improved water delivery (e.g. – drip irrigation), runoff management (capture, treatment, and reuse), and water deficit irrigation. To be most efficient, all three methods require more detailed attention to irrigation cycles with more frequent monitoring of substrate water content. In order to be attractive to a nursery manager, the solution must offer a net profit gain commensurate with the effort required to install and maintain the solution.

Welsh and Zajicek (1993) found that irrigating to a 25% water deficit produced the most growth compared to six other treatments of *Photinia x fraseri*. This is also called a managed allowable deficit (MAD) and is the process of providing less irrigation than the plant is capable of using. Beeson (2006) concluded that a 20% to 40% MAD produced the most marketable plants in three shrub species. Warsaw et al. (2009) compared three different deficit irrigation schemes

to a control and also found that plant growth under all deficit irrigation exceeded the control; however, they attributed the growth to accumulated nutrients in the root zone (as measured in electrical conductivity, nitrate losses and phosphate losses). Murray et al. (2004) observed stomatal conductance in azalea plants and concluded that woody perennials might not even need daily irrigation. But it is detrimental to growth if the plants are allowed to reach leaf wilting point; therefore, knowledge of the soil water content is important to ensure healthy plant growth. Controlling water to this precision requires accurate, easy-to-obtain, often-updated soil moisture data from the containers.

Many methods have been used to measure and monitor soil water content; some of these methods are bulk measurements, radiation (neutron probe), time domain reflectometry (TDR), frequency domain reflectometry, capacitance and dielectric measurements, soil air relative humidity (thermocouple psychrometers), vacuum-suction (tensiometer), electrical conductance (EC), and gravimetric monitoring (lysimeter measured with load cell) [Beeson, 2006; Earl, 2003; Gardiner and Miller, 2004]. Abraham et al. (2000) compared two automated drip irrigation systems used on a crop of Okra - one controlled irrigation by monitoring electrical resistance using a custom EC sensor, the other controlled irrigation by monitoring the leaf-air temperature difference. The EC sensor system maintained higher soil water content and produced a higher yield. However, as implemented, both sensors needed periodic maintenance; the EC sensor needed recalibration after each fertilizer application, and the leaf temperature sensor needed to be moved as the canopy developed. Some studies have used load cells, often called lysimeters, alone (Owen et al., 2007; Prehn, 2008; Beeson, 2006; Beeson, 2007; Earl, 2003), while others have used only capacitive sensors (Lea-Cox et al., 2008; Parsons and Bandaranayake, 2009). Lea-Cox and Black et al. (2008) used the EC-5 (Decagon Devices) probes

to monitor soil moisture content at three depths at a commercial tree nursery (in-ground), but the calibration method was neither simple nor easy as it required six soil cores and regression fitting to a quadratic equation (sensor output vs. volumetric water content). One goal of research in soil water measurement is to reduce the complexity of installing and calibrating measurement systems so as to make them more attractive to commercial operators (Lea-Cox et al., 2009).

1.1.2 Scope and goals of this work

This chapter will present the results from an on-farm experiment conducted in the summer of 2010 comparing load cells with capacitance-based sensors utilizing a wireless sensor network. The goal of the experiment was to determine which sensor type was best suited for automated irrigation decisions.

1.2 Materials and Methods

1.2.1 Site description

The research site was at Bailey Nurseries, Inc (BNI, 45.3584N 123.2137W, Figure 1.1) located near Yamhill, Oregon. The climate is temperate Mediterranean, and the study time

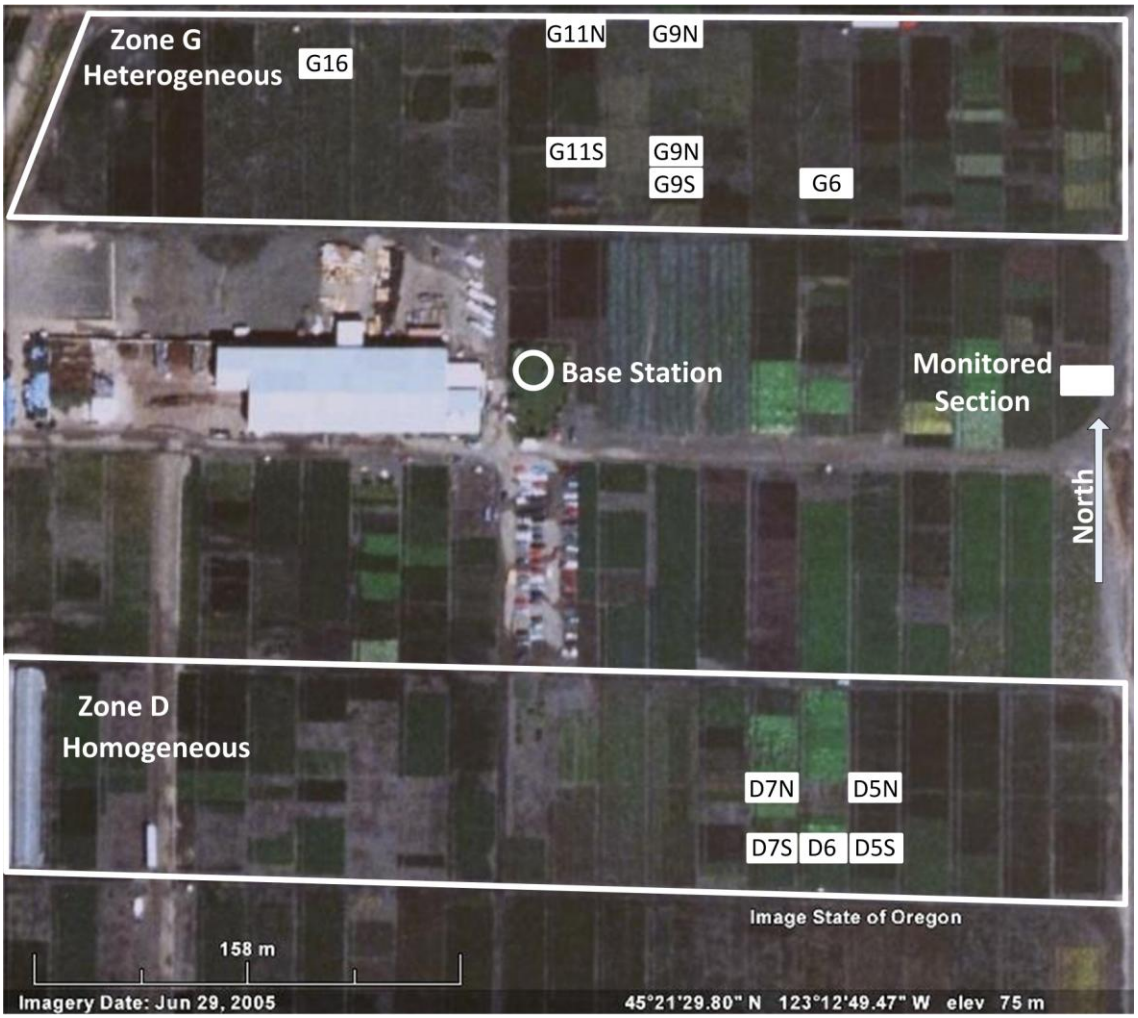

Figure 1.1 Satellite view of the study site showing irrigation zones, monitored sections, and Base Station location. Monitored sections are the small, white rectangles with their names overlaid onto them. Sections G11N, G9S, and D6 were not monitored with sensors and eKo Nodes. Sections G11S and D5S each had a weather station attached in addition to the plant sensors. Two sections are labeled G9N due to a change midway through the experiment. (Satellite view courtesy of Google Earth.)

period coincided with the warm, dry summer. The study area focused on two zones of irrigation, one with 3 species of plants in a single genus and in 5 sizes (homogeneous zone, Zone D, 446 m by 74 m, approx. 3.2 ha) and the other with 18 genus, 30 species, 75 varieties, and 5 sizes (heterogeneous zone, Zone G, 389 m by 74 m, approx. 2.8 ha). Each zone is further divided into uniformly sized rows (14.5 m by 74 m, approx. 1100 m^2), and each row into uniform sections between the overhead sprinklers (14.5 m by 14.0 m, approx. 200 m^2). For the purpose of this study, a section marked D7 section 3 will mean the third section from the north, seventh row from the east, in irrigation zone D.

1.2.2 Sensors

In each zone, four plants were chosen (total eight plants) to monitor with a load cell (15kg RL1042, Rice Lake Weighing Systems, Rice Lake, Wisc.) and volumetric water content sensor (5-cm EC-5, Decagon Devices, Inc., Pullman, Wash.). The load cell was mounted between two aluminum plates – a base plate (30.4cm x 30.4cm) and a container support plate (either 15.2cm x 15.2cm or 30.4cm x 30.4cm depending on container size). Each load cell required an analog signal amplification board (es9100, Memsic Corporation) to transmit data to the eKo Node. Each amplification board was placed in a NEMA 4X rated junction box sealed with silicone. Each irrigation zone also had a weather station (ES2000v6, Memsic Corporation, Andover, Mass.) which collected wind speed (WS) and direction (WD), irrigation (I), temperature (T), relative humidity (RH), solar radiation (SR), and barometric pressure (BP).

1.2.3 Communication network

Each set of sensors (one gravimetric and one capacitance sensor) was connected to a wireless communication node (eKo Node 2120, Memsic Corporation) that communicated with a

centralized base station (BaseStation, PureSense Environmental, Inc., Fresno, Calif.). Under normal operation the nodes transmitted sensor data to the BaseStation once every fifteen minutes. During the first hour after being turned on or after being reset, the nodes transmitted data once every minute. The BaseStation then sent the data to PureSense servers via a cellular modem. The end user received the data by using either the PureSense website or Irrigation Manager[1].

One of the advantages of the eKo Nodes over similar devices is their capability to communicate to the BaseStation via another node; if a node is too far from the BaseStation to communicate with it directly, the node can pass its data to a nearby node that is able to communicate with the BaseStation. This ability, called a mesh network (Lea-Cox et al, 2009; Ferrari 2010), enables the network to extend far from the BaseStation by utilizing intermediary nodes. Figure 1.2 shows a simplified network diagram. The reliability of this particular network is discussed in chapter 3 – "Wireless Hardware and Software Evaluation."

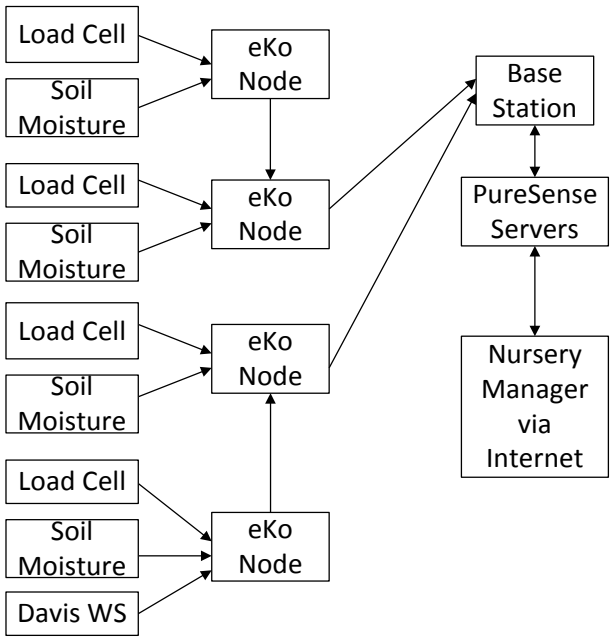

Figure 1.2 Simplified network diagram.

The network collected data over a period of nine weeks (18 July 2010 to 21 September 2010) during the active production season for the nursery.

[1] The PureSense Irrigation Manager is a custom Windows-based software application developed and distributed by PureSense to customers using the PureSense BaseStation.

1.2.4 Sensor sensitivity

Kizito et al. (2008) demonstrated that the Decagon ECH_2O family of soil moisture probes (EC-5, ECH_2O-TE [obsolete], and 5TE [replaces ECH_2O-TE])[2] are not strongly affected by either temperature or electrical conductivity in a wide range of substrate materials due to their operating frequency of 70 MHz. However, Bogena et al. (2007) showed that the effect from temperature resulted in an overestimation of about 1.8 % vol. at 40°C in a solution of known permittivity[3], and Kizito et al. (2008) determined the effect in sand to range from -0.002 $cm^3 \cdot cm^{-3} \cdot C^{-1}$ at θ_{wc}=0.25 $cm^3 \cdot cm^{-3}$ to +0.0005 $cm^3 \cdot cm^{-3} \cdot C^{-1}$ at θ_{wc}=0.1 $cm^3 \cdot cm^{-3}$. Cobos (2008) determined the volume of sensitivity is approximately 0.18 liter around the sensor, but others (Parsons and Bandaranayake, 2009; Sakaki et al., 2008) claim that the sensitive volume is an order of magnitude less at 0.018 liter. Regardless, the EC-5 is most sensitive to the volume immediately surrounding the sensor prongs and the sensor head. In coarse-textured, low-density, porous substrate the probes themselves may generate disruptions in the substrate density immediately around the sensor. These macropores cause less substrate to be in direct contact with the sensor and form large pore spaces next to the probe from which water preferentially drains. As a result the probes may under-report bulk soil moisture content. Also, because of the sensitivity of the sensor head, it is important that the entire sensor be completely inserted into the soilless substrate for consistent water detection.

1.2.5 Sensor resolution

The load cells employed bridge resistance circuitry to provide a weight dependent voltage output with a 15 kg rated maximum load. The output, or signal, was then amplified by

[2] The ECH_2O family of probes share a common soil moisture sensing circuit (Kizito et al., 2008).
[3] ε=40 F/m which corresponds to a soil water content of 51%.

the ES9100 board to be within the sensitivity range of the eKo Node. The eKo Node is capable of sensing an analog voltage between 0.0000 mV and 3000 mV with a 10-bit analog to digital resolution, i.e – the range of 0 to 3000 mV is divided equally into 1023 increments of 2.933 mV per bit[4]. The goal of amplification was to make the load cell output at full-scale (15 kg) to be as close to 3000 mV as possible without exceeding it.

The resolution of the load cells, according to the operational theory, is dependent upon the load cell excitation voltage (ExcV), the unique load cell bridge response (V_{BR}), and the gain resistor (R_G).

The resolution is then:

$$\text{Resolution} = \frac{3000(\text{mV}) * \text{LC}_{\text{MAX}}\ (\text{g})}{1023\ (\text{bits}) * \text{ExcV(V)} * \text{V}_{\text{BR}} \left(\frac{\text{mV}}{\text{V}}\right) * \left(1 + \frac{100000(\text{ohm})}{\text{R}_{\text{G}}(\text{ohm})}\right)} \qquad \text{Equation 1.1}$$

where LC_{MAX} is the maximum weight the load cell is capable of detecting.

The overall expected mean resolution of the load cells was 15.17 g · bit^{-1}. Allowing for the differences in resistors, load cell circuit response, and battery voltages, the overall theoretical range of resolution was between 13.38 g · bit^{-1} and 17.83 g · bit^{-1}. It is important not to confuse these theoretical operating resolutions with system accuracy. More detailed information about the load cell sensor resolution and operating theory is in Appendix B – "Sensor Resolution". The mean resolution of the capacitance probes was 0.0037 cm^3 · cm^{-3} · bit^{-1} and was in the range between 0.0036 and 0.0038 cm^3 · cm^{-3}. More detailed information about

[4] Another way of looking at this is to say that for every increase of 2.933 mV, the value shown in the eKo Node increases by 1. The 4 significant figures are necessary to recover a value of 3000 mV when multiplying 2.933 mV · bit^{-1} by 1023 bits.

the capacitance probe resolution is in Appendix B – "Sensor Resolution".

1.2.6 Sensor installation

The installation procedure sought to minimize disturbance and obtain a measurement from the most dynamic and critical zone of the substrate. The 8.9 cm long (probe head included) EC-5 sensors were installed from the surface of the substrate and pushed into the center of the rootball at a 45 degree angle as shown in Figure 1.3. Perfect insertion would leave the sensor head about one centimeter below the surface; in reality, due to the plants being close to shipping maturity, the root ball mass often prevented insertion this deep, and sometimes the sensor head was allowed to be above the substrate surface. If fully inserted at a 45 degree angle, the probe would measure a cross-section of substrate 6.3 cm in depth.

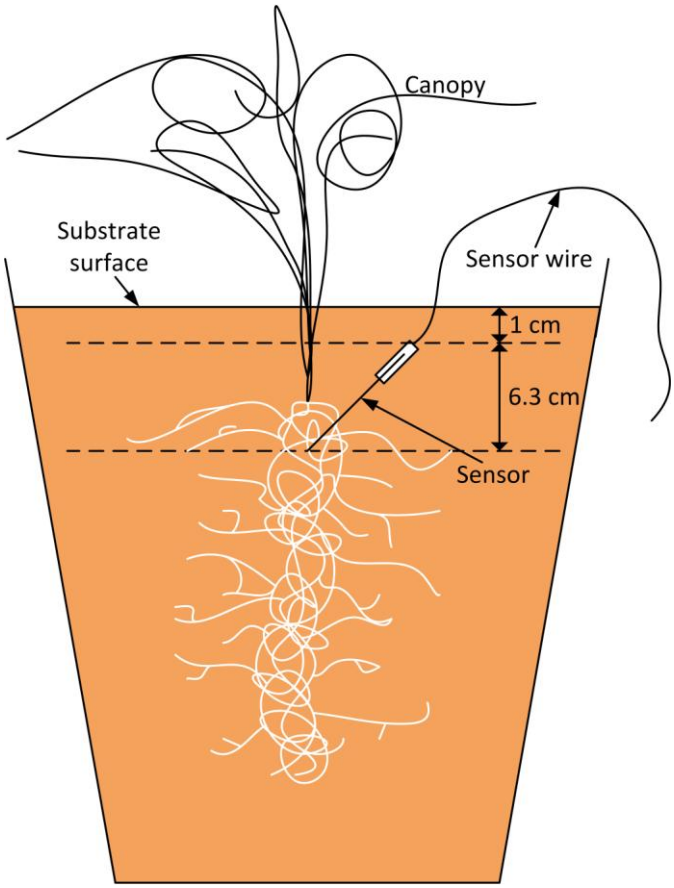

Figure 1.3 Diagram showing installation of the capacitance sensor at a 45 degree angle from the substrate surface into the rootball leaving the top of the sensor approximately 1 cm below the surface.

In a study using TDR probes to automatically control drip and spray emitters, Murray et al. (2004) found that vertical installation of TDR probes in the wetting zone resulted in less

leachate than diagonal installation. Three concerns arose, however, from the comparison of the two orientations and between the flat-pronged electronic capacitance sensors and rod-based TDR sensors. The first concern is that the soil moisture data desired is in the center of the rootball, and vertical orientation will not penetrate the center of the rootball. The second concern is that it is not clear whether capacitance-based probes suffer from the same installation issues as TDR probes (e.g., TDR probes are generally long, cylindrical metal prongs that are easily forced apart, whereas the EC-5 and other capacitance probes are often short, planar, circuit-board material). The third concern is that soil moisture outside of the main rootball (where a vertical installation would necessarily be) would exhibit a different diurnal soil moisture pattern than that inside the rootball.

A horizontal installation from the surface would require much more disturbance of the substrate; however, if inserted through a vertical slit in the side of the container, the substrate surface would remain undisturbed and could possibly be the best installation technique for plants already in containers. Preliminary results from a separate experiment conducted by J.S Owen Jr. and colleagues at Oregon State University's North Willamette Research and Extension Center did not produce any definitive conclusions as to which installation technique was best, and furthermore, the net diurnal change in VWC was found to be very similar amongst techniques (Tyler Hoskins, personal communication).

A guiding principle to probe installation and data interpretation comes from the fact that disturbed substrate does not have the same water-holding characteristics as undisturbed, aged substrate. As substrate sits in the pot over the growing season, the substrate will settle into a more compact configuration and the roots will develop and grow into empty spaces. The

combined actions of compaction and root growth decrease the air space and increase the container capacity of the substrate (Atland et al., 2011). The container capacity increases because smaller pores are better able to retain water against the force of gravity. This implies that a nursery manager cannot rely on initial soil moisture boundaries set near the potting date and that as the substrate matures, soil moisture boundaries will need to be re-established periodically.

1.2.7 Sensor calibration

The load cells were calibrated with known, constant weights over a three day period and then the values converted to weight units (grams) using a 2-point conversion. The entire process is documented in Appendix A - "Load Cell Calibration".

Although Rodriguez (2009) and Decagon (2011a) have shown that the ECH_2O family of VWC sensors has different calibration values in different soils and soilless substrates, the capacitance sensors used in this study were not calibrated for the specific soilless substrate used at the nursery. Regardless of the specific equation used to convert the collected data to VWC, the diurnal trend in the data is still informative when the end user sets the maximum and minimum boundary values. From the diurnal trends, it is possible to empirically derive wet (VWC maximum) and dry (VWC minimum) boundaries of allowable VWC without knowing either the precise VWC or weight.

Another concern was sensor to sensor variation. Several papers have attempted to answer this question (Sakaki et al., 2008; Decagon, 2011b; Rosenbaum et al., 2010), but the variation depended on the media and the VWC level; the range of variability was 0.003 $cm^3 \cdot$

cm^{-3} to 0.03 $cm^3 \cdot cm^{-3}$ in the three papers mentioned[5]. However, the diurnal change in VWC was found to be more consistent from sensor to sensor.

The lower accuracy deriving from the lack of calibration was not considered very problematic for this study because the focus was to identify which technology (load cells or capacitive sensors) is better suited to help a nursery manager better manage gross irrigation across a wide variety of species and plant sizes. Therefore, the standard calibration equation for mineral soil provided by Decagon was considered to be as close an approximation to true VWC as necessary for the purposes of this study (see Appendix B).

1.2.8 Plant species

Irrigation Zone D was a species homogeneous mix of *Rhododendron 'P.J.M.' Hybrids (R. minus Michx. Caroliniana x R. dauricum L.)* in five sizes. Two monitored plants in Zone D were in 6.4 liter containers and two plants were in 14.2 liter containers. Irrigation Zone G was a heterogeneous mix of plants and container sizes. Table 1.1 summarizes the plant species and sizes in each section.

[5] Different methods of error reporting were used in each paper.

Table 1.1 Section locations, plant varieties, and container sizes monitored by sensors.

Section name	Zone	Row	Section	Container size (trade #)	Bucket volume (liters)	Genus, species, and variety
D5N	D	5	3	2	6.4	*Rhododendron* 'P.J.M.' Hybrids (*R. minus Mich x Caroliniana x R. dauricum L.*)
D5S	D	5	5	2	6.4	*Rhododendron* 'P.J.M.'
D7N	D	7	3	5	14.2	*Rhododendron* 'P.J.M.'
D7S	D	7	5	5	14.2	*Rhododendron* 'P.J.M.'
G6	G	6	5	3	9.6	*Spiraea japonica L.* 'Bumalda'
G9N[†]	G	9	1	5	14.0	*Salix integra Thunb.*
G9N[‡]	G	9	4	2	6.4	*Potentilla fruticosa L.*
G11S	G	11	4	2	6.1	*Wiegela florida (*Bunge.*) A. DC.*
G16	G	16	2	2	6.4	*Physocarpus opulifolius (L.) Maxim.*

[†] 22 July to 12 August [‡] 12 August to 16 September

1.2.9 Irrigation

The irrigation sprinklers were Rain Bird model 30H (Rain Bird Sales, Inc., Azusa, Calif.) with 3/16" nozzle size. The system operated at nominal pressures of 3.85 kg · cm^{-2} in row D1 to 4.62 kg · cm^{-2} in D9 and 3.5 kg · cm^{-2} in G4, 4.2 kg · cm^{-2} in G10, and 4.48 kg · cm^{-2} in G16. The pressures in these irrigation zones change from row to row because they are situated on a gently sloping, west-facing hill. The nozzles were spaced 12.2 m by 18.3 m and had an overlapping spray pattern as seen in Figure 1.4.

A uniformity evaluation provided by Rain Bird Sales (Appendix C – "Rain Bird Uniformity Evaluation") gives a distribution uniformity of 65% using the sugar-growers uniformity equation and a Christiansen Uniformity Coefficient of 79% (both numbers found using a pressure of 3.5 kg · cm^{-2}). The mean irrigation rate was estimated to be 0.714 cm · hr^{-1} based on the uniformity

evaluation (Appendix C), but data collected on 16 September (presented in chapter 2) showed a mean rate of 0.89 cm · hr^{-1}.

Except when exceptionally hot or cool, the plants were irrigated once per day for approximately two hours with the runoff captured and recycled. Data collected and presented in section 1.3.2 – 'Saturation Analysis' showed that the average irrigation times were 105 minutes in Zone D, and 134 minutes in Zone G.

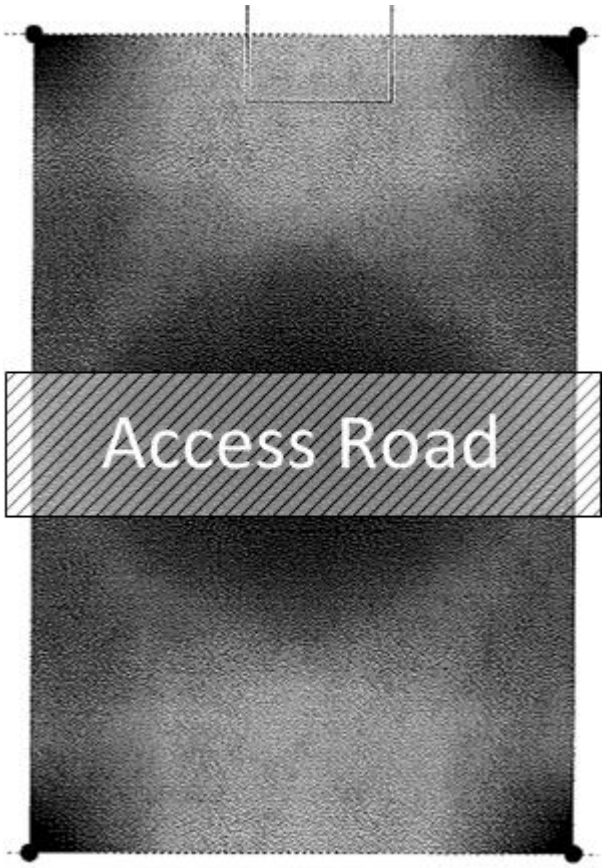

Figure 1.4 Predicted water distribution between the boundaries of four Rain Bird sprinklers (12.2 m by 18.3 m). Darker areas represent more water. The base figure is from Rain Bird Sales Inc, and the access road is added for illustration.

1.2.10 Growing substrate

Both substrates were composed mostly of Douglas fir (Pseudotsuga menziesii) bark with sphagnum peat and Slo-6 pumice. Each also had an addition of a fertilizer mix of an APEX slow release fertilizer (Simplot Turf and Horticulture, Lathrop, Calif.), gypsum, dolomite 10, dolomite 65, and Nitraform slow release fertilizer (Agrium U.S. Inc., Denver, Colo.). The *rhododendron* mix was used in the homogenous zone. The shrub mix was used in the heterogeneous zone. Table 1.2 lists the composition of each substrate and the fertilizer mix in each.

Table 1.2 List of the composition of each substrate mix.

Substrate Material	*'P.J.M.'* mix	Shrub mix
Douglas fir bark (1.9cm -)	70%	70%
Sphagnum Peat	10%	15%
Slo-6 Pumice	20%	15%
APEX 20-8-8[†]	56.7kg	NA
APEX 18-6-11[‡]	NA	45.4 kg
Nitraform	6.8kg	6.8kg
Gypsum	6.8kg	6.8kg
Dolomite 10	6.8kg	6.8kg
Dolomite 65	6.8kg	6.8kg

[†]12 month slow release [‡]8 month slow release

Table 1.3 Summary of substrate physical properties.

Substrate Physical Property		*'P.J.M'* mix	Shrub Mix
Total Porosity	**(% vol.)**	89	89
Air Space	**(% vol.)**	38	41
Container capacity	**(% vol.)**	51	48
Estimated Available Water	**(% vol.)**	30	32
Estimated Unavailable Water	**(% vol.)**	21	16
Dry Bulk Density	**($g \cdot cm^{-3}$)**	0.22	0.20
Bulk Density at Container Capacity	**($g \cdot cm^{-3}$)**	0.73	0.68

The physical properties of the two substrate mixtures were analyzed at Oregon State University North Willamette Research and Extension Center (NWREC) using 7.6 cm cores (four samples each) and a porometer. Two corer tools were used. Both were cylindrical aluminum corers – one had a volume of 350 cm^3 (7.6 cm height x 7.6 cm diameter), and the other had a volume of 110 cm^3, (2.5 cm height x 7.6 cm diameter). Total porosity (TP), container capacity (CC), available water capacity (AW), and air filled porosity (AS) were determined using the NCSU Porometer™ as described by Fonteno and Bilderback (1993). Unavailable water (UW), water held in the substrate at greater than 1.5 MPa, was determined with the 110 cm^3 cores via a procedure developed by Milks et al. (1989). Bulk density (D_b) was determined using oven dried (110°C) substrate in the 347.5 cm^3 volume cores. The results are shown in Table 1.3.

1.2.11 Saturation

The porosity of the substrate was very high at 0.89 (Table 1.3); this is due to the course texture of the substrate yielding many large voids. For comparison, loamy soil has an approximate porosity of 0.47 (Selker et. al., 1999). To be truly saturated, every pore and void in the substrate must be completely filled, but the high porosity and void space of the nursery substrate allowed water to drain more quickly than the substrate was able to be filled leaving it with unfilled voids. Pores are usually considered to be small, but voids are many times larger than pores. As readily available pores and voids filled to capacity, the additional irrigation passed completely through the substrate and drained out of the bottom of the container. When the drainage rate equaled the irrigation rate, the container was said to be at field container capacity[6] and was considered the field saturation point.

Sammons and Struve defined saturation to be that point during an irrigation cycle when the weight of the lysimeter (plant and substrate in a monitored container) does not change for twenty continuous seconds (Sammons and Struve, 2008). Beeson (2006) considered the field saturation point to have been reached once the weight did not gain more than 10 grams over 10 minutes. This is also referred to as the differential method of determining saturation.

Because the network used for this study was factory set to take one measurement every fifteen minutes, a modification of the less strict Beeson method was used. The irrigation system was expected to deliver water at a mean rate of 0.71 $cm \cdot hr^{-1}$ based on the Rain Bird Sales estimate (Appendix C). Table 1.4 summarizes the volumetric irrigation rate predicted to be

[6] This is different from true container capacity in that the tiniest micropores will not have been filled. Filling the tiniest micropores is only possible when the container is completely immersed in water and left to saturate for a long period of time. Also, the larger macropores (or voids) will not have enough surface tension to counteract gravitational force to hold the water in them. This is also called effective saturation.

received by each size of container and the rate at which field saturation is considered to occur for both weight and VWC. The setpoint of saturation was chosen to be the reported water content at which the rate of mass increase in the container was less than 47% of the mean application rate. This was computed from sequential fifteen minute readings and sought to identify the target of a well-watered condition, as reported by each sensor. Note that the setpoint was selected while the container and plant were still increasing in mass and not when the change was zero or negative. If the rate was allowed to fall to zero, the plant and container would be at near-saturation which would result in considerable post-irrigation drainage. It can then be said that the goal is to reach a functional field capacity saturation, a water content to which the container will not drain a great deal after irrigation is halted. Figure 1.5 shows an example of an ideal diurnal cycle of irrigation, drainage, and evapotranspiration with the key features labeled.

Table 1.4 Expected irrigation delivery rates and setpoints of saturation for different sized containers. The last column is volumetric soil moisture content converted to the equal amount of water based on container volumes in Table 1.1.

Container size	Diameter (cm)	Expected irrigation rate ($cm^3 \cdot min^{-1}$)	Rate at weight saturation ($g \cdot min^{-1}$)	Rate at VWC saturation ($cm^3 \cdot cm^{-3} \cdot min^{-1}$)
#2	21.5	4.3	2.0	0.0002
#3	25.0	5.8	2.7	0.0002
#5	33.8	7.9	3.7	0.0002

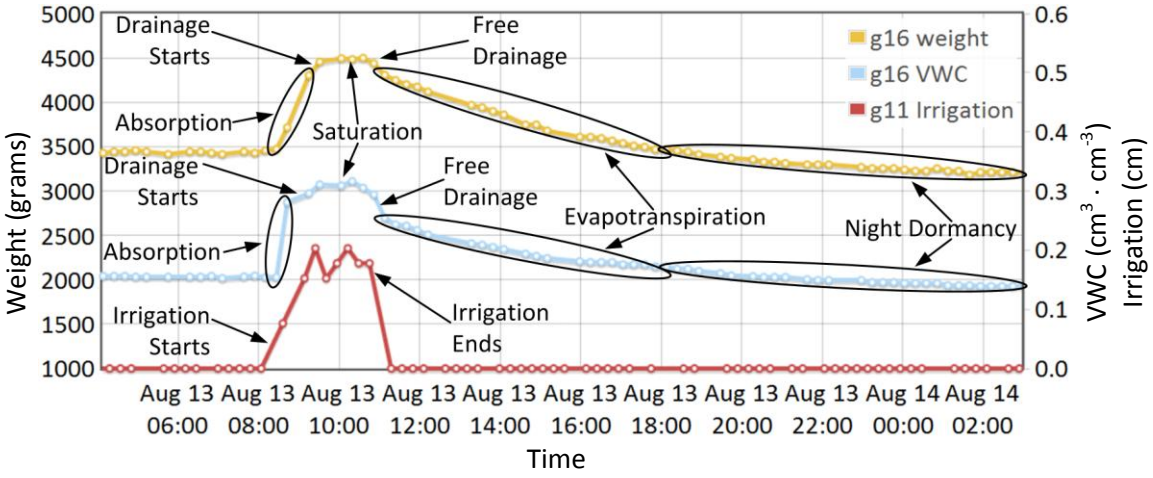

Figure 1.5 An example of an ideal irrigation, drainage, and evapotranspiration cycle labeled with key features. Weight (left axis, gold, grams) is the top line, VWC (right axis, blue, $cm^3 \cdot cm^{-3}$) is the middle line, and irrigation is shown along the bottom for irrigation timing reference (right axis, red, centimeters). The irrigation rate appears to increase slowly at the beginning of the irrigation cycle, but this is due to the nature of the sensor network. Because the network sends data only once every fifteen minutes, accumulated data, such as irrigation and rainfall, do not have accurate start and end times. This irrigation cycle began at approximately 08:25; because only about half of the data cycle was during the irrigation period, only about half of the average irrigation amount during a full data cycle was recorded. Because the final irrigation point is recorded at the mean of the others, we know that the irrigation cycle ended very near to when this point was recorded at 10:45. The data used in this figure also are used in Figure 1.8.

1.3 Results and Discussion

1.3.1 Daily trends

The daily trends in weight and VWC of the monitored plants followed each other very closely, as is seen in an example data set from Row D5 shown in Figure 1.6. As was expected, the weight and VWC increase when the irrigation occurs, slowly decrease throughout the day, and are mostly flat during the night. What becomes very evident in Figure 1.6 is that between 11 and 15 August, the containers were slowly drying out based on the decrease in the daily maximum and minimum in both weight and VWC. The container at D5N had a cumulative underirrigation of 540 ml (assuming 1 gram = 1 ml of water) based on minimum weight, while the container at D5S had a cumulative underirrigation of 750 ml. However, the plant at D5N received (based on daily maximum weight minus previous minimum weight) cumulatively 820 ml more water than the plant at D5S during the same time period. If plant D5S is consistently receiving less water than plant D5N, that would partially explain the lighter weight in D5S in that D5S might be less developed than D5N.

From Figure 1.6 shows that one part of the ideal irrigation cycle, saturation point, was never reached during this time period. Figure 1.7, zooming in on only 12 and 13 August, show that the capacitance probes indicated saturation, but the load cells did not. The weight of D5S looks like it might have reached a saturation value, but it is unlikely given the downward trend of minimum weight over the following few days and that irrigation was turned off at about the same time. The likely explanation is that the maximum weight occurred between measurement times and the weight had already started to decrease due to free drainage. Free drainage can still occur even though the substrate has not reached container capacity.

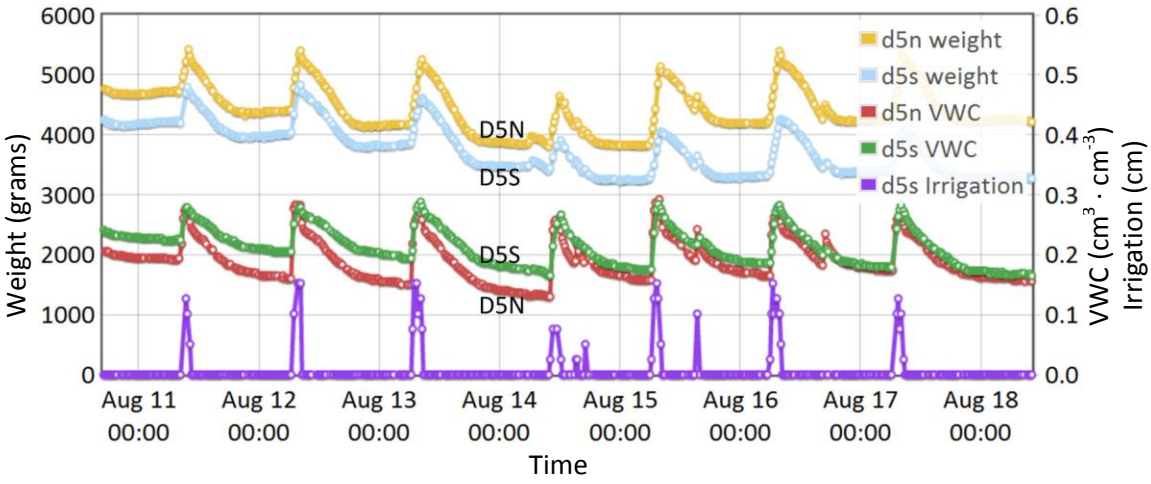

Figure 1.6 Weight (left axis, gold and blue, top two lines, grams) and VWC (right axis, red and green, middle two lines, $cm^3 \cdot cm^{-3}$) in row D5 over a seven day period. Irrigation is shown for timing reference (right axis, purple, bottom line, centimeters).

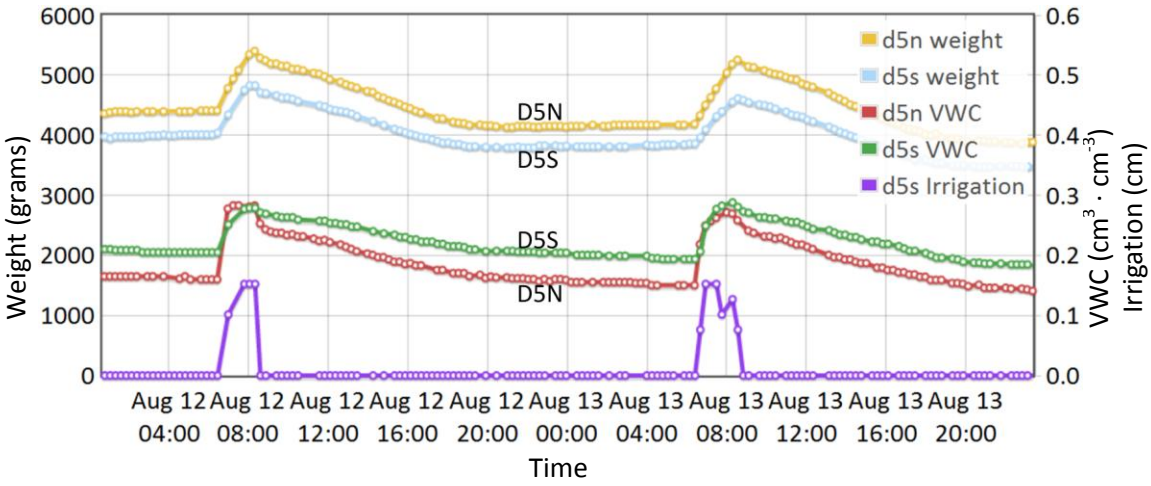

Figure 1.7 Weight (left axis, gold and blue, top two lines, grams) and VWC (right axis, red and green, middle two lines, $cm^3 \cdot cm^{-3}$). Two day period of row D5. Irrigation is shown for timing reference (right axis, purple, bottom line, centimeters).

Figure 1.8 shows the heterogeneous zone (Zone G) during the same 2-day window as Figure 1.7[7]. The same general daily trends were followed by the containers in Zone G as in Zone D. However, due to the longer irrigation length of Zone G, all plants showed an indication in

[7] Section G9 was not included due to network error and subsequent data loss during this time period.

saturation by weight. All capacitance sensors showed saturation values in both days, but the time of saturation was always well before the weight showed saturation. Also, as in Zone D between 11 and 14 August, the daily minimums are decreasing (Figure 1.9), but because the plants are allowed to saturate, the maximums are staying level (within 50 ml of water) with no downward trend.

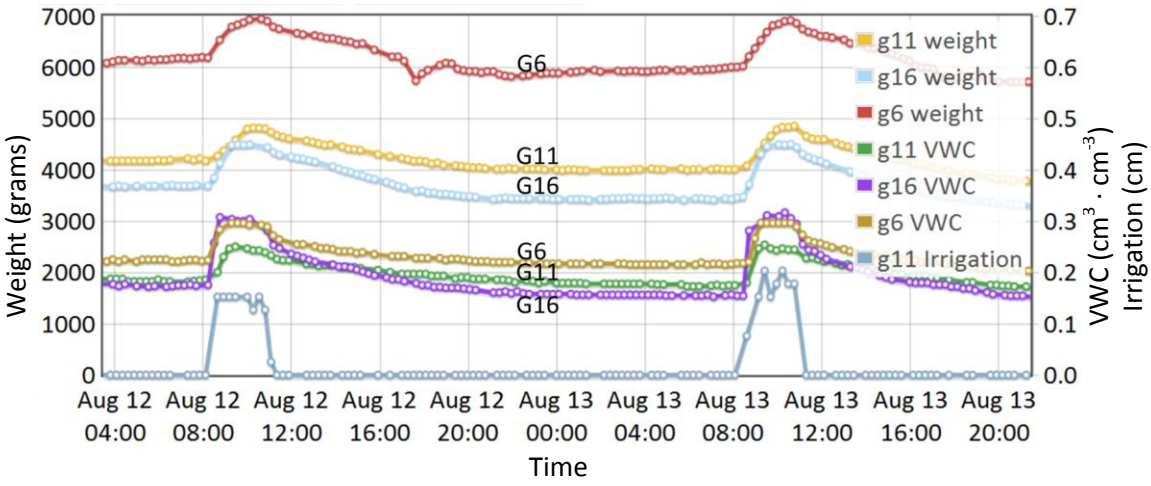

Figure 1.8 Two day period of Zone G. Weight (left axis; gold, blue and red; top three lines; grams) and VWC (right axis; green, purple and dark yellow; middle three lines; $cm^3 \cdot cm^{-3}$). Irrigation is shown for irrigation timing reference (right axis, dark blue, bottom line, centimeters). G9 was omitted due to data loss. G16 from 13 August is also shown in Figure 1.5.

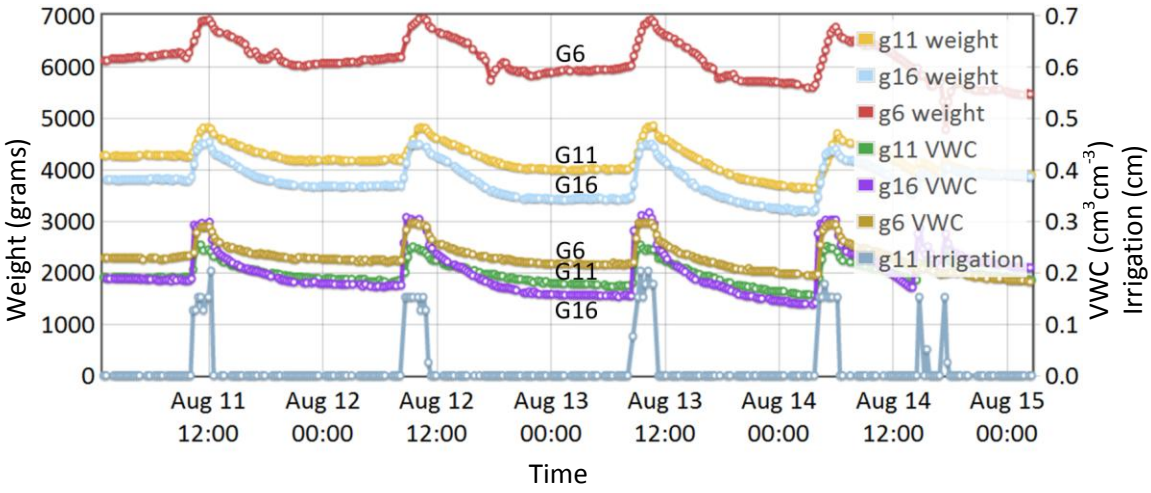

Figure 1.9 Four day period of Zone G. Weight (left axis; gold, blue and red; top three lines; grams) and VWC (right axis, green, purple and dark yellow, middle three lines, $cm^3 \cdot cm^{-3}$). Irrigation is shown for irrigation timing reference (right axis, dark blue, bottom line, centimeters). G9 was omitted due to data loss. G16 from 13 August is also shown in Figure 1.5. Figure 1.8 shows 12 and 13 August.

1.3.2 Saturation analysis

Between 27 July and 15 September, there were 34 well-characterized recorded irrigation events in Zone D (homogenous) and 26 events in Zone G (heterogeneous). Zone D had an average irrigation time of 105 minutes, and Zone G had an average irrigation time of 134 minutes. Zone G was irrigated longer to accommodate the multiple varieties and sizes of plants with varying irrigation requirements.

Figures 1.10 and 1.11 compare the time to saturation of each sensor pair in each zone for those irrigation events where both sensors recorded a saturation point. If the sensors had saturated at approximately the same time during each irrigation event, the data points would cluster around a 45 degree line. However, in both irrigation zones the data are widely distributed with the majority falling in the upper left portions of Figures 1.10 and 1.11 indicating that more time is necessary to reach gravimetric saturation than VWC saturation when

measured at a shallow depth in the substrate. Given that Zone G was irrigated, on average, a half an hour longer than Zone D, it is not surprising that there were more paired saturation events in Zone G than in Zone D. Of the 20 saturation pairs in Zone D, 14 were from the load cell saturating first, 5 from equal saturation time, and 1 from the capacitance sensor saturating first (70%, 25%, 5% respectively). Of the 53 saturation pairs in zone G, 33 were from the load cell saturating first, 14 from equal saturation time, and 6 from the capacitance sensor saturating first (62%, 26%, 11% respectively). When examining the R-squared value of each irrigation zone (Figures 1.10 and 1.11), it was found that there was very little correlation between the two sensors in time to saturate (when combined in groups by zone, Zone D had an R-squared value of 0.14 and Zone G had a value of 0.45). Section G9 had the highest R-squared value for an individual section at 0.87. From these data, it is inferred that other variables, such as individual plant characteristics, meteorological conditions, and sensor installation, are more relevant to determining when each sensor will record saturation values.

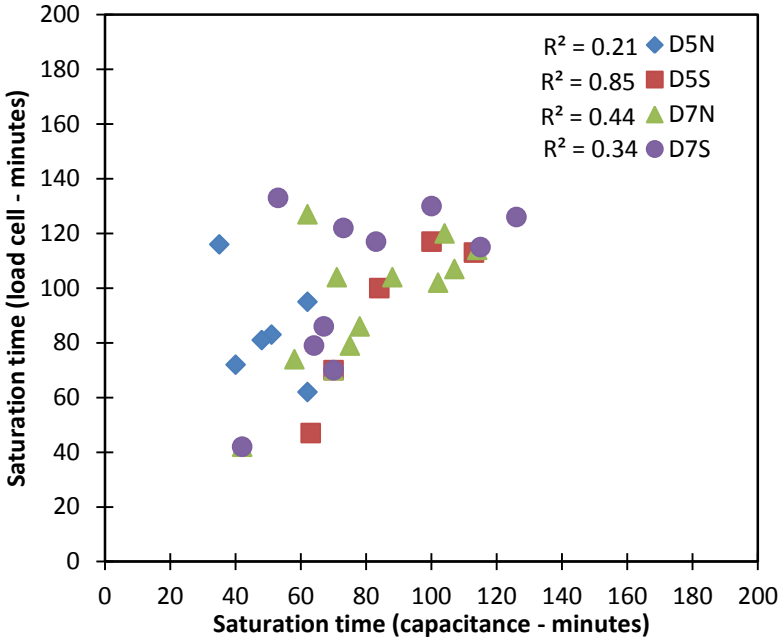

Figure 1.10 Comparison of times of saturation in Zone D between the load cell and capacitance (VWC) sensor broken out by section.

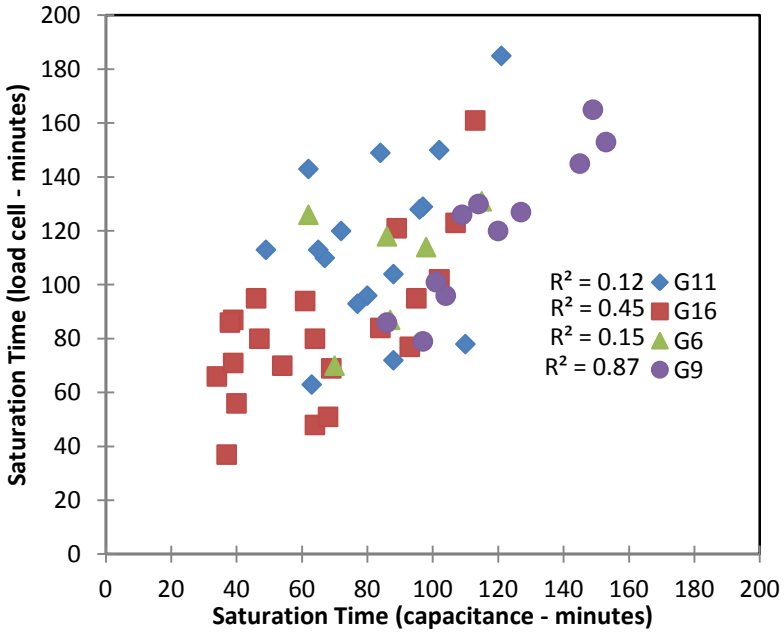

Figure 1.11 Comparison of times of saturation in zone G between the load cell and capacitance (VWC) sensor broken out by section.

Water movement and retention in coarse substrate is difficult to accurately model and conceptualize, but our hypothesis is that the substrate became slightly hydrophobic when dried causing water to initially pool near the surface. A nearly positive pressure head was then needed to initiate water movement through the top of the substrate. In time, the nearly saturated wetting front advanced and allowed movement to the bottom layers of substrate, and ultimately drainage. At the same time, as water finds preferential flow paths to the bottom of the container, a second wetting front will start at the bottom and move toward the top. In this conceptualization, the substrate water retention characteristics were changing in time as the substrate transitioned from dry-hydrophobic to wet hydrophilic. (Figure 1.12)

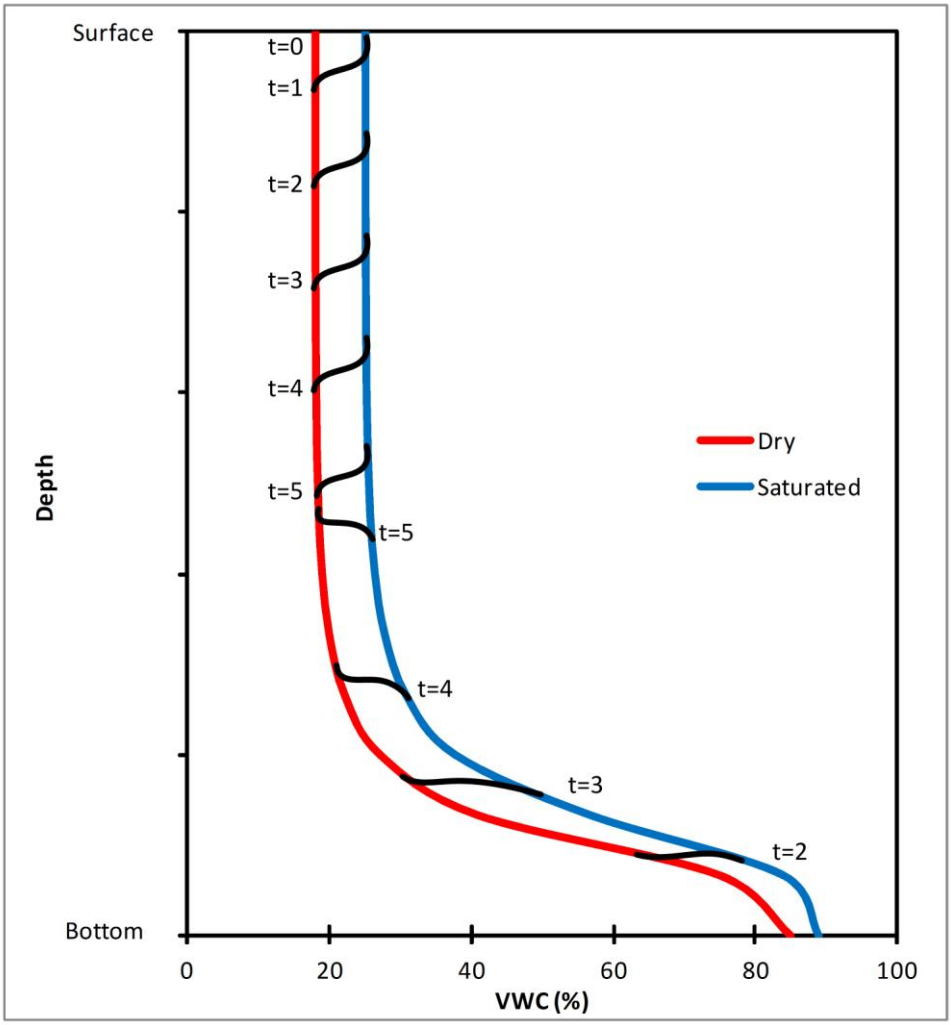

Figure 1.12 An idealized conceptualization of the soil moisture retention curve throughout a container of substrate composed mostly of bark at both dry and saturated levels of VWC with a wetting front shown. The wetting front will initially start at the top of the substrate, and as the water finds preferential paths to the bottom, start saturating from the bottom up until it meets in the middle of the container. The blue curve (saturated) is representative of the field saturated state.

1.3.3 Sensor resolution and report time intervals

It was observed that the capacitive sensor sometimes did not increase for two or more reporting periods (each period is about 16 minutes), but the general trend of the soil moisture

still exhibited the desired increase pattern (as demonstrated in Figure 1.13). This was due to the low resolution of the sensor. Because VWC reached near-saturation levels quicker than weight, the differential method of detecting saturation is insufficient for automation purposes. Small increases to the VWC near the surface of the substrate can be indicative of larger increases further down. Since the capacitance sensor is only capable of sampling a small portion of the substrate, these small changes are very important to monitor. Given the desired rate of increase at saturation to be 0.0002 $cm^3 \cdot cm^{-3} \cdot min^{-1}$ and the maximum resolution of 0.0038 $cm^3 \cdot cm^{-3} \cdot bit^{-1}$, a minimum of 19 minutes between report times would have been sufficient. To decrease the time between sensor readings to 10 minutes (a more reasonable time for active management), the maximum resolution of the sensor would need to decrease to 0.0020 $cm^3 \cdot cm^{-3} \cdot bit^{-1}$. Similarly, the load cell could report at a minimum of 9 minutes given its maximum resolution of 17.83 $g \cdot bit^{-1}$ and desired rate of increase at saturation of 2 $g \cdot min^{-1}$.

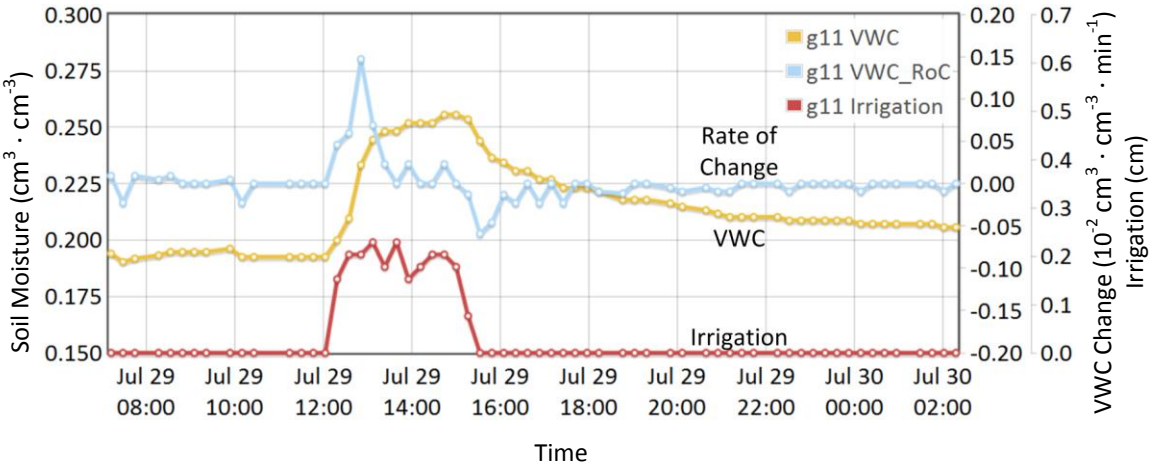

Figure 1.13 Volumetric water content (left axis, gold, $cm^3 \cdot cm^{-3}$) and VWC change (right axis, blue, 10^{-2} $cm^3 \cdot cm^{-3} \cdot min^{-1}$). One day period of section G11. Irrigation is shown for irrigation timing reference (far right axis, red, centimeters).

1.4 Conclusions

Each sensor has its advantages and disadvantages. The load cell provides an integrated measurement and is less susceptible to report sudden fluctuations. The capacitance sensor measures a targeted (or discrete) volume of the substrate, and, in theory, the maximum and minimum VWC values do not fluctuate as the plant grows. Both sensors require some care during installation. The load cell should be near-level, requires more calibration than the capacitance sensor, and is easily susceptible to damage from overload (being stepped on). The capacitance sensor must be installed so as to prevent both preferential flow and the entrapment of water on the sensor blades. Critically, the resolution of the capacitance sensor was not small enough to provide the fine detail needed in an automated irrigation system utilizing a real-time decision making process and it was susceptible to sudden spikes to saturation during irrigation. Additionally, if the goal is to thoroughly saturate all levels of the substrate, then it is clear that the capacitance based sensors are inadequate for the task of determining saturation. This is demonstrated by the fact that the capacitance sensors almost always reported saturation first, yet the load cells continued to report increases of mass (ie – water) followed by relatively little free gravity drainage. Therefore, the additional irrigation was being retained by the substrate and available for use by the plant even after the capacitance sensor had reported saturation.

But both sensors provide valuable information to a nursery manager concerning field saturation and plant water deficits. Even if the sensors are not calibrated to their best accuracy, trends are still plainly evident, and the manager can easily adjust the daily irrigation schedule based on them and basic meteorological data. In a purely automated system, it is recommended that the cutoff point of irrigation be time-based and not real-time value based. It would

probably be sufficient to use the volumetric water content value or weight value at the start of the irrigation cycle to determine the length of irrigation time. Because the load cells were more reliable in sensor readings, a weight indicating field container capacity could be used as a marker for ending an irrigation cycle. It is still abundantly clear that a seasoned nursery manager will be required to operate an automated system at its full potential.

1.5 Literature Cited

Abraham, N., P.S. Hema, E.K. Saritha, and S. Subramannian. 2000. Irrigation automation based on soil electrical conductivity and leaf temperature. Agric. Water Management 45:145–157.

Andreen, W.L. 2011. Water law and the search for sustainability: a comparative analysis. Water Resources Planning and Management. R. Quentin Grafton, Karen Hussey. Cambridge University Press.

Atland, J.E., J.S. Owen Jr., and M.Z. Gabriel. 2011. Influence of pumice and plant roots on substrate physical properties over time. HortTechnology 21(5):554-557.

Beeson, Jr., R.C. 2006. Relationship of plant growth and actual evapotranspiration to irrigation frequency based on managed allowable deficits for container nursery stock. J. Amer. Soc. Hort. Sci. 131:140–148.

Beeson, Jr, R.C. 2007. Determining plant-available water of woody ornamentals in containers in situ during production. HortScience 42:1700-1704.

Beeson, Jr., R.C., M.A. Arnold, T.E. Bilderback, B. Bolusky, S. Chandler, H.M. Gramling, J.D. Lea-Cox, J.R. harris, P.J. klinger, H.M. Mathers, J.M. Ruter, and T.H. Yeager. 2004. Strategic vision of container nursery irrigation in the next ten years. J. Environ. Hort. 22(2):113-155.

Bogena, H.R., Huisman, J.A., Oberdörster, C., and Vereecken, H. 2007. Evaluation of a low-cost soil water content sensor for wireless network applications. J. Hydrol 344:32-42.

Cobos, D. 2008. Decagon Devices Application Note. http://www.decagon.com/assets/Uploads/EC-5-Volume-of-Sensitivity.pdf. Accessed 20 April 2011.

Decagon Application Note. 2011. 13392-03: Calibration equations for the ECH_2O EC-5, ECH_2O-TE and 5TE sensors.

Decagon Devices. 2011. EC-5 Small Volume Soil Moisture Sensor. Specifications. http://www.decagon.com/products/sensors/soil-moisture-sensors/ec-5-soil-moisture-small-area-of-influence/. Accessed 18 October 2011.

Earl, H.J. 2003. A precise gravimetric method for simulating drought stress in pot experiments. Crop Sci. 43: 1868-1873.

Ferrari, G. (ed.). Sensor Networks: Where Theory Meets Practice. Heidelberg, Germany: Springer, 2010.

Fonteno, W.C. and T.E. Bilderback. 1993. Impact of hydrogel on physical properties of coarse-structured horticultural substrates. J. Amer. Soc. Hort. Sci. 118(2):217-222.

Gardiner, D.T. and Miller, R.W. 2004. Soils in our environment. Prentice Hall: Upper Saddle River, NJ. 2004.

Kizito, F., Campbell, C.S., Campbell, G.S., Cobos, D.R., Teare, B.L., Carter, B., Hopmans, J.W. 2008. Frequency, electrical conductivity and temperature analysis of a low-cost capacitance soil moisture sensor. J. Hydrology 352: 367-378.

Lea-Cox, J.D., Black, S., Ristvey, A., and Ross, D.S. 2008. Towards precision scheduling of water and nutrient applications, utilizing a wireless sensor network on an ornamental tree farm. Proc. Southern Nursery Assoc. Res. Conf. 53:553-558.

Lea-Cox, J.D., Ristvey, A.G., and Kantor, G.F. 2009. Wireless water management. Amer. Nurseryman. Jan 2009:44-47.

Milks, R.R., W.C. Fonteno, and R.A. Larson. 1989. Hydrology of horticultural substrates: II. Predicting physical properties of media in containers. J. Amer. Soc. Hort. Sci. 114(1):53-56.

Murray, J.D., Lea-Cox, J.D. and Ross, D.S. 2004. Time Domain Reflectometry Accurately Monitors and Controls Irrigation Water Applications. Acta Hort. 633:75-82.

Owen, Jr., J.S., Warren, S.L., Bilderback, T.E. 2007. A gravimetric approach to real-time monitoring of substrate wetness in container-grown nursery crops. Acta Hort 819: 317-324.

Parsons and Bandaranayake 2009. Performance of a new capacitance soil moisture probe in a sandy soil. Soil Sci. Soc. Am. J. 73.

Prehn, A. 2008. A gravimetric approach to real-time monitoring of substrate water content in container-grown nursery crops. North Carolina State Univ., Raleigh, M.S.

Rodriguez, F.R., 2009. Calibrating capacitance sensors to estimate water content, matric potential, and electrical conductivity in soilless substrates. University of Maryland, College Park, M.S.

Rosenbaum, U., J.A. Huisman, a. Weuthen, H. Vereecken, H.R. Bogena. 2010. Sensor-to-sensor variability of the ECH20 EC-5, TE, and 5TE sensors in dielectric liquids. Vadose Zone J. 9:181-186.

Sakaki, T., A. Limsuwat, K. M. Smits, and T. H. Illangasekare. 2008. Empirical two-point α-mixing model for calibrating the ECH2O EC-5 soil moisture sensor in sands, *Water Resour. Res.*, *44*, W00D08.

Sammons, Jonathan D. and Daniel K. Struve. 2008. Monitoring effective container capacity: A method for reducing over-irrigation in container production systems. J. Environ. Hort. 26(1):19-23.

Selker, J.S., C.K. Keller, and J.T. McCord. 1999. Vadose zone processes. Lewis Publishers, Boca Raton, FL.

Warsaw, A.L., R.T. Fernandez, B.M. Cregg and J.A. Andresen. 2009. Container-grown ornamental plant growth and water runoff volume and nutrient content under four irrigation treatments. HortScience 44:1573-1580.

Welsh, D.F. and J.M. Zajicek. 1993. A model for irrigation scheduling in container-grown nursery crops utilizing management allowed deficit (MAD). J. Environ. Hort. 11:115–118.

Chapter 2

Irrigation Distribution and Canopy Interaction

2.0 Abstract

As ornamental container nurseries face increased pressure to reduce irrigation, many are looking to automated solutions to increase their water application efficiency. An important factor in determining irrigation needs is to have an accurate understanding of the irrigation distribution. This study was conducted on-site at a commercial container nursery to determine the irrigation distribution, the effect on container weight, and the impact of canopy type and size on irrigation efficiency. It was found that the irrigation pattern conformed to the expected pattern, container weights did not conform to the irrigation pattern, and canopy height had a larger impact on leaching fraction than canopy width.

2.1 Introduction

2.1.1 Background

Population increases and in-stream water protection (Andreen, 2011) are putting pressure on water supplies causing nursery managers to grow increasingly concerned about the future of their own water supplies (Beeson et al., 2004). Beeson et al. emphasized that in coming years the limiting factor of production at most nurseries will be water availability. In Oregon, as in all Western States, water withdrawals from above ground sources are prioritized by seniority, with the oldest rights given priority when seasonal water availability decreases during July and August (OWRD 2009). If a nursery is unable to obtain a water right with enough seniority to guarantee a supply of surface water during the dry, summer months, the options are to convert a portion of their land to a reservoir or to obtain permits for wells; both options are more expensive, and the reservoir will take potential production land.[8]

A top priority of any nursery manager is to ensure that each plant receives enough water to prevent water-related stress. But because of non-uniform irrigation distribution, nursery managers often irrigate for the needs of a plant in the driest area of the irrigation zone causing plants in wetter areas to receive much more water than necessary. In addition, to ensure proper re-wetting of the substrate and to prevent the media from becoming

[8] Water allocation by seniority is called the Prior Appropriation Principle and is most common in the western United States. East of the Mississippi River, the riparian doctrine is most common. Under the riparian doctrine, a landowner with water flowing adjacent to or through the property may use as much water as needed. Regardless of the water right doctrine in place, the threat of reduced water access is causing a renewed look at irrigation efficiency in the agricultural and nursery industries (Beeson et al. 2004).

hydrophobic, Yeager et al. (2007) recommend a leaching fraction[9] (LF) of 0.10 to 0.15. However, as evidenced from leaching rates presented below, it is probably common that most nurseries exhibit much higher leaching fractions.

2.1.2 Scope and goals of this work

The goal of this experiment was to determine the spatial variability of the system taking into account crop characteristics such as weight, plant size, and plant species. The spatial variability was to be used to determine the number of plants to monitor in order to make sound management decisions.

[9] Leaching fraction is the fraction of applied water that leached through the container. LF = Volume leached through container/Total volume applied to container

2.2 Materials and Methods

2.2.1 Site description

The research site was at Bailey Nurseries, Inc (BNI, 45.3584N 123.2137W, Figure 2.1) located near Yamhill, Oregon. The climate is temperate Mediterranean, and the study time period coincided with the warm, dry summer. The study area focused on two zones of irrigation,

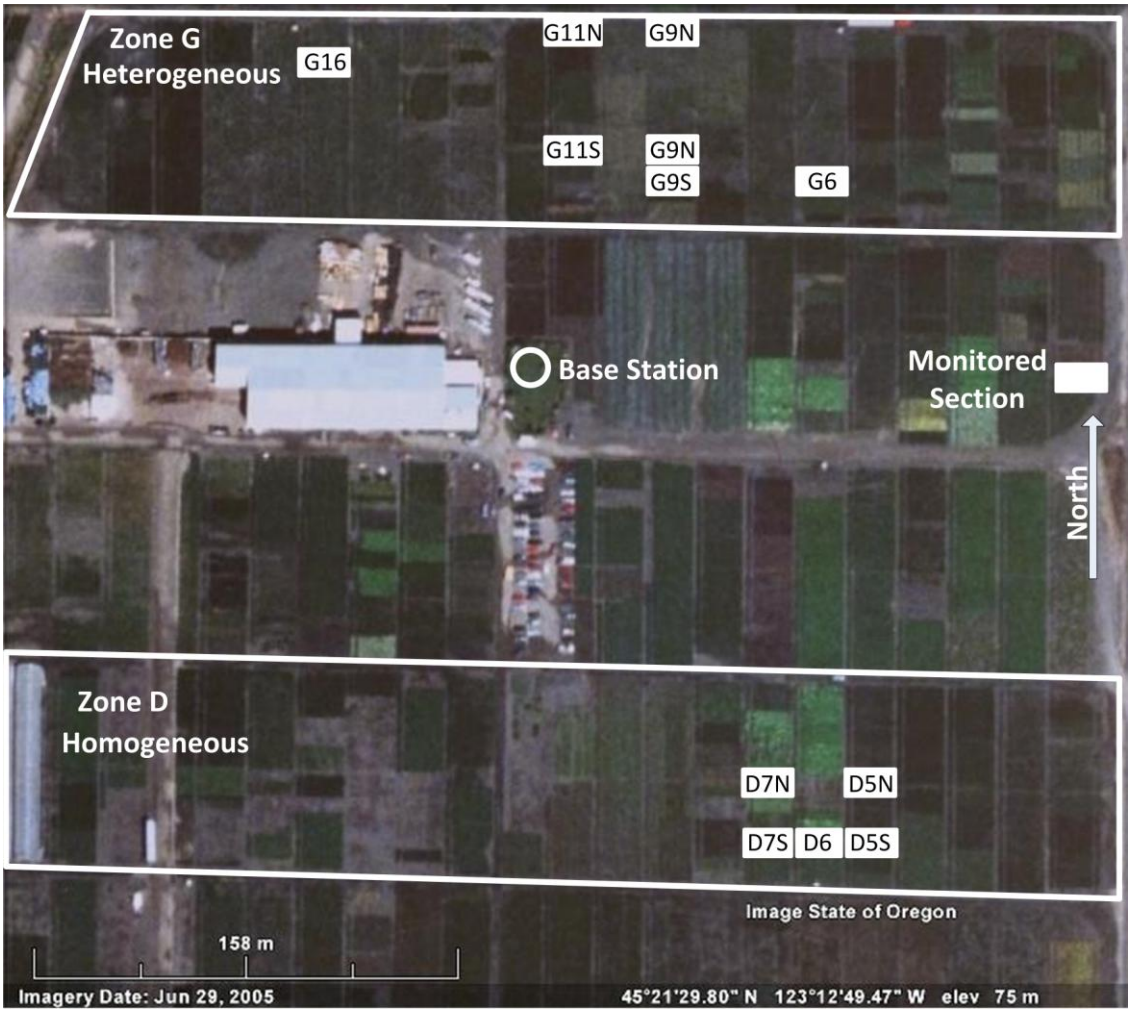

Figure 2.1 Satellite view of the study site showing irrigation zones, monitored sections, and Base Station location. Monitored sections are the small, white rectangles with their names overlaid onto them. Two sections are labeled G9N due to a change midway through the experiment. (Satellite view courtesy of Google Earth.)

one with 3 species of plants in a single genus and in 5 sizes (homogeneous zone, Zone D, 446 m by 74 m, approx. 3.2 ha) and the other with 18 genus, 30 species, 75 varieties, and 5 sizes (heterogeneous zone, Zone G, 389 m by 74 m, approx. 2.8 ha). Each zone is further divided into uniformly sized rows (14.5 m by 74 m, approx. 1100 m^2), and each row into uniform sections between the overhead sprinklers (14.5 m by 14.0 m, approx. 200 m^2). For the purpose of this study, a section marked D7 section 3 will mean the third section from the north, seventh row from the east, in irrigation zone D.

2.2.2 Container properties

Containers were made of polypropylene of black, white, or cream color. Sizes monitored were trade sizes #2, #3, and #5 (with volumes of 6.1, 9.6, and 14.2 liters, respectively). The containers sat on a slightly inclined bed of coarse gravel overlying a moisture barrier for water capture and recycling.

2.2.3 Plant species

Irrigation Zone D was a species homogeneous mix of *Rhododendron 'P.J.M.' Hybrids (R. minus Michx. Caroliniana x R. dauricum L.)* in five sizes. Sections monitored in Zone D contained three sizes of containers (6.5 L, 9.6 L, and 14.2 L). Irrigation Zone G was a heterogeneous mix of plants and container sizes. Table 1.1 summarizes the plant species and sizes in each section.

Table 2.1 Section locations, plant varieties, and container sizes monitored for weight manually. D7N had two sizes of plants.

Section name	Zone	Row	Section	Container size (trade #)	Bucket volume (liters)	Genus, species, and variety
D5N	D	5	3	2	6.4	*Rhododendron* 'P.J.M.' Hybrids (*R. minus Mich x Caroliniana x R. dauricum L.*)
D5S	D	5	5	2	6.4	*Rhododendron* 'P.J.M.'
D7N	D	7	3	5	14.2	*Rhododendron* 'P.J.M.'
D7S	D	7	5	5	14.2	*Rhododendron* 'P.J.M.'
G6	G	6	5	3	9.6	*Spiraea japonica L.* 'Bumalda'
G9N[†]	G	9	1	5	14.0	*Salix integra Thunb.*
G9N[‡]	G	9	4	2	6.4	*Potentilla fruticosa L.*
G11S	G	11	4	2	6.1	*Wiegela florida (*Bunge.*) A. DC.*
G16	G	16	2	2	6.4	*Physocarpus opulifolius (L.) Maxim.*

[†]22 July to 12 August [‡] 12 August to 16 September

2.2.4 Growing substrate

Both substrates were composed mostly of Douglas fir (*Pseudotsuga menziesii*) bark with sphagnum peat and Slo-6 pumice. Each also had an addition of a fertilizer mix of an APEX slow release fertilizer (Simplot Turf and Horticulture, Lathrop, Calif.), gypsum, dolomite 10, dolomite 65, and Nitroform slow release fertilizer (Agrium U.S. Inc., Denver, Colo.). The *rhododendron* mix

Table 2.2 List of the composition of each substrate mix.

Substrate Material	*'P.J.M.'* mix	Shrub mix
Douglas fir bark (1.9cm -)	70%	70%
Sphagnum Peat	10%	15%
Slo-6 Pumice	20%	15%
APEX 20-8-8[†]	56.7kg	NA
APEX 18-6-11[‡]	NA	45.4 kg
Nitraform	6.8kg	6.8kg
Gypsum	6.8kg	6.8kg
Dolomite 10	6.8kg	6.8kg
Dolomite 65	6.8kg	6.8kg

[†]12 month slow release [‡]8 month slow release

was used in the homogonous zone. The shrub mix was used in the heterogeneous zone. Table 2.2 lists the composition of each substrate and the fertilizer mix in each.

The physical properties of the two substrate mixtures were analyzed at Oregon State University North Willamette Research and Extension Center (NWREC) using 7.6 cm cores (four samples each) and a porometer. Two corer tools were used. Both were cylindrical aluminum corers – one had a volume of 350 cm^3 (7.6 cm height x 7.6 cm diameter), and the other had a volume of 110 cm^3, (2.5 cm height x 7.6 cm diameter). Total porosity (TP), container capacity (CC), available water capacity (AW), and air filled porosity (AS) were determined using the NCSU Porometer™ as described by Fonteno and Bilderback (1993). Unavailable water (UW), water held in the substrate at greater than 1.5 MPa, was determined with the 110 cm^3 cores via a procedure developed by Milks et al. (1989). Bulk density (D_b) was determined using oven dried (110°C) substrate in the 347.5 cm^3 volume cores. The results are shown in Table 2.3.

Table 2.3 Summary of substrate physical properties.

Substrate Physical Property		***'P.J.M'* mix**	**Shrub Mix**
Total Porosity	**(% vol.)**	89	89
Air Space	**(% vol.)**	38	41
Container capacity	**(% vol.)**	51	48
Estimated Available Water	**(% vol.)**	30	32
Estimated Unavailable Water	**(% vol.)**	21	16
Dry Bulk Density	**($g \cdot cm^{-3}$)**	0.22	0.20
Bulk Density at Container Capacity	**($g \cdot cm^{-3}$)**	0.73	0.68

2.2.5 Observation dates and schedule

The plants in each monitored section were weighed on 22 July, 05 August, 19 August, and 02 September 2010. On each field day, one section was also monitored for leaching fractions. The fifth and sixth field days, 15 and 16 September, 2010, were used to monitor a

widely distributed and semi-randomized selection of plants so that canopy interference could be avoided. Catch-cans and leaching fraction buckets were also used. This is described more fully in the section 2.2.7 – Canopy Interaction Analysis.

2.2.6 Procedure methodology

When weighing plants, a scale (51XW and CD-33, Ohaus Corp., Parsippany, New Jersey) was set up in the back of a vehicle for convenient transport, access, and shelter from wind. Each time the vehicle was moved, a known weight was recorded for calibration; if the scale differed by more than 20 grams from the known weight, the scale was leveled until this standard was achieved. The recorded weights of the plants were then adjusted by the percentage difference of the known weight to its recorded weight.

Each field weighing day the plants were measured before and after irrigation in the morning, generally before noon. Irrigation sets lasted approximately two hours after which the pots of soil were considered to be saturated. After irrigation, the plants were left for a minimum of 30 minutes before weighing started on the first section to allow maximum free-gravity drainage to occur. During weighing, efforts were made to keep each plant and pot level while transporting to the scale so as to avoid additional draining.

To find the leaching fraction of a plant, the plant and container were nested inside a similarly sized container to capture the leachate. An empty container of equal top area was placed adjacent to the monitored plant to capture the expected amount of irrigation for that monitored plant. The leaching fraction was then found using Equation 2.1. The summary of sections monitored for leaching fraction is in Table 2.4. Water application efficiency is commonly

defined as 1 minus leaching fraction; however, this does not account for canopy interception efficiency.

$$leaching\ fraction = \frac{leachate\ volume\ from\ plant}{volume\ in\ empty\ bucket} \qquad \textbf{Equation 2.1}$$

Table 2.4 Summary of sections used for leaching fraction analysis.

Field Date	Section	Species	Size (Trade)
22 July	D5S	*Rhododendron 'P.J.M.'*	2
05 August	G9S	*Potentilla fr.*	2
19 August	G16	*Physocarpus op.*	2
02 September	G16	*Physocarpus op.*	2

2.2.7 Canopy interaction analysis

On the last two field days (15 and 16 September) a canopy interaction analysis was performed on five different types and sizes of plants (*physocarpus op* pruned, *physocarpus op* unpruned, *rhododendron PJM* #2, *rhododendron PJM* #3, and *spiraea x bum*). Four rows of each species and size (total twenty rows) with six plants in each row (total 24 plants of each species and size) were placed in irrigation zone F row 9 in a pseudo-randomized pattern on a square grid with spacing of 2.44 m. In between each plant row and midway between each plant a small collection cup was placed on top of an upturned plant container to collect irrigation volumes at the approximate level of the substrate surface. Figure 2.2 is a picture showing a few rows for illustration.

Instead of using an empty container of equal size to collect water during irrigation to find the leaching fraction of each plant, the small collection cups were used instead. An ordinary

Kriging method was used to find the estimated irrigation rate at each plant location and the results used to find the estimated irrigation volume based on container diameter.

Figure 2.2 Picture of the spacing of plants on 15 and 16 September. Note the rows of plants are single species and size and the collection cups are spaced between rows of plants.

The goal of this experiment was to find an indication as to the effect an individual canopy size and type has on capturing irrigation and to also provide a check on the irrigation pattern compared to the predicted spray pattern in figure 2.3. This is why the plants were spaced far enough apart to avoid canopy interference from one another and the collection cups.

The prediction was that the canopy type of *physocarpus* was a collector, or funnel type of canopy. The *spiraea* was predicted to be a shedder, or umbrella type of canopy. The *rhododendron* was expected to be neutral. These predictions were based on general observations made through the experiment period.

Because the area of interest was the effect of the canopy on leaching fraction, all of the plants were started at saturation. To achieve this, the plants were irrigated early in the morning. Immediately before the experiment started, the plants were irrigated again for 30 minutes and

then allowed to rest for 30 minutes to allow for immediate drainage. The plants were then placed in leaching buckets, irrigated for an additional hour, and allowed to rest for 30 minutes before measuring the leaching amounts. On the first day, 15 September, a light rain started during the measuring time, possibly skewing the results. Therefore, the results of 16 September will be analyzed and presented. Both days were cool and heavily clouded with relatively low evaporation and plant activity.

2.2.8 Irrigation

The irrigation sprinklers were Rain Bird model 30H (Rain Bird Sales, Inc., Azusa, Calif.) with 3/16" nozzle size. The system operated at nominal pressures of 3.85 kg · cm^{-2} in row D1 to 4.62 kg · cm^{-2} in D9 and 3.5 kg · cm^{-2} in G4, 4.2 kg · cm^{-2} in G10, and 4.48 kg · cm^{-2} in G16. The pressures in these irrigation zones change from row to row because they are situated on a gently sloping, west-facing hill. The nozzles were spaced 12.2 m by 18.3 m and had an overlapping spray pattern as seen in Figure 2.3.

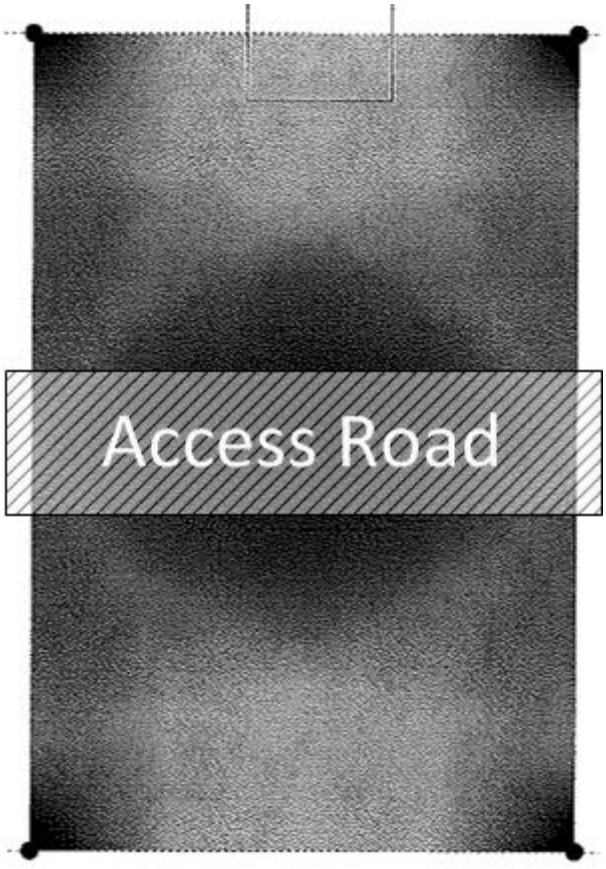

Figure 2.3 Predicted water distribution between the boundaries of four Rain Bird sprinklers (12.2 m by 18.3 m). Darker areas represent more water. The base figure is from Rain Bird Sales Inc, and the access road is added for illustration.

A uniformity evaluation provided by Rain Bird Sales (Appendix C – "Rain Bird Uniformity Evaluation") gives a distribution uniformity of 65% using the sugar-growers uniformity equation and a Christiansen Uniformity Coefficient of 79% (both numbers found using a pressure of 3.5 kg $\cdot$ cm^{-2}). The mean irrigation rate was estimated to be 0.714 cm $\cdot$ hr^{-1} based on the uniformity evaluation (Appendix C), but data collected on 16 September (presented in section 2.3.2 – "Results of Irrigation Distribution") showed a mean rate of 0.89 cm $\cdot$ hr^{-1}.

Except when exceptionally hot or cool, the plants were irrigated once per day for approximately two hours with the runoff captured and recycled. Data collected and presented in section 1.3.2 – 'Saturation Analysis' showed that the average irrigation times were 105 minutes in Zone D, and 134 minutes in Zone G.

2.3 Results and Discussion

2.3.1 Results of manual weighing

Comparing the coefficients of variation (C.V.) of the weights of the containers before and after irrigation, eighty percent of the sections showed a decrease in variation (Figure 2.4). The R-squared value was 0.63, which demonstrates that the pre and post-irrigation weight variations are not tightly linked. The highest C.V. of a single section was 0.12.

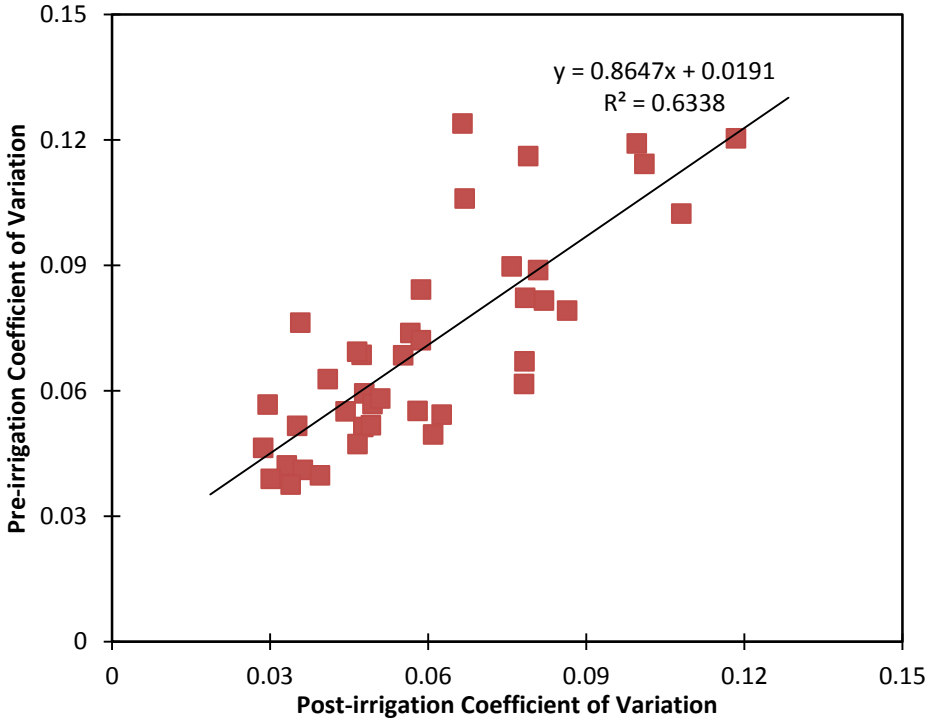

Figure 2.4 Comparison of coefficient of variation in container masses before and after irrigation.

Table 2.5 Summary of means of coefficients of variation grouped by various categories.

Category	Pre-irrigation C.V.	Post-irrigation C.V.	Water Net Gain C.V.
All Sections	0.071	0.060	0.29
Zone G	0.064	0.054	0.33
Zone D	0.081	0.068	0.24
22 July	0.069	0.061	0.24
19 Aug	0.073	0.054	0.41
02 Sept	0.074	0.070	0.28
05 Aug	0.067	0.053	0.25
Size 2	0.063	0.053	0.28
Size 3	0.097	0.087	0.32
Size 5	0.066	0.052	0.30
Salix	0.038	0.032	0.22
Potentilla	0.051	0.051	0.34
Physocarpus	0.055	0.041	0.36
Wiegela	0.070	0.053	0.29
Rhododendron	0.081	0.068	0.24
Spiraea	0.093	0.085	0.42

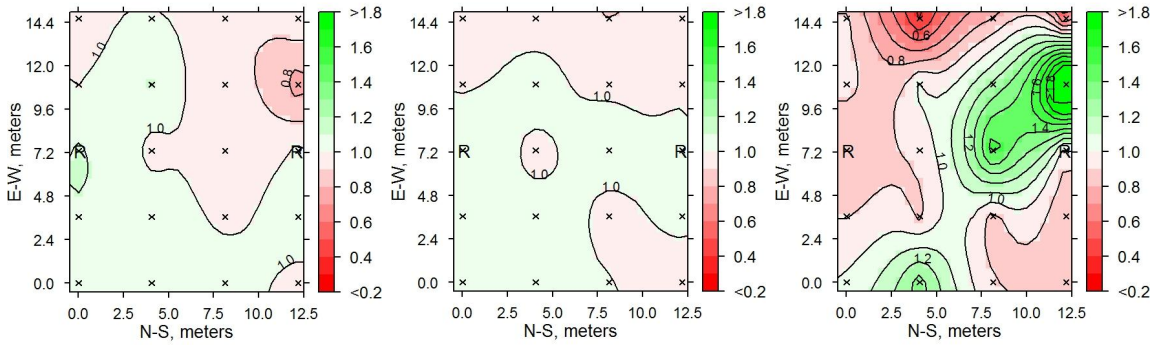

Figures 2.5a-c Maps of plant and container weight (normalized to mean weight) before and after irrigation and the net water gain (left to right) of section G16 on 02 September. Each 'R' represents an irrigation riser and each 'x' is a monitored plant. All plant weight maps are found in Appendix D – "Manual Weighing Data". This date and section is shown for illustrative purposes and does not represent all weighing data. The darker shades indicate areas where the weight was further from the mean weight.

Figures 2.5a-c show an illustrative example of the data collected from the manual weighing of plants before and after irrigation and the net gain in weight (all normalized to the mean weight). Assuming that 1 gram is equal to 1 ml of water, the net gain can be viewed as the net volume of water retained by the plants and substrate. Due to the variety of plant species and sizes, the data shown in Figures 2.5a-c should not be considered representative of the entire data set. The full data set can be found in Appendix D – "Manual Weighing Data." This particular figure demonstrates that should a container not be irrigated for a day, one irrigation cycle is capable of bringing the weight of the container and plant (a proxy for water content in the container) back to near-mean. Prior to irrigation the normalized weights of the containers were relatively uniform with a coefficient of variation of 0.084 which fell to 0.059 after irrigation. This may be seen by considering the container in the upper right corner of Figures 2.5a-c which had a normalized weight of 0.74 prior to irrigation, increasing to 0.99 after irrigation. Of course, these containers were irrigated beyond their container capacity (as seen from the leachate discussion in the next section) on a daily basis, so the barrier to re-attaining container capacity was relatively low.

2.3.2 Results of leaching fraction

Leaching fraction buckets were initially deployed to determine if the containers were receiving enough irrigation to saturate the substrate (indicated by the presence of leachate). During the first four field days, a total of 69 leaching fraction buckets were monitored with 63 (91.3%) presenting leachate after a normal two-hour irrigation cycle. This indicated a two-hour irrigation cycle was adequate to start water movement through the containers, but as chapter 1 showed, it does not necessarily indicate a fully saturated substrate.

Table 2.6 Leaching fraction data from the first four field days.

Date	Section	Plant species	Irrigation duration (minutes)	# monitored buckets	# buckets leaching	Average leachate (max-min) (ml)	Average Leaching Fraction
22 July	D5S	*PJM*	122	12	9	123 (0-500)	0.27
05 Aug	G9S	*Potentilla*	122	18	16	214 (0-600)	0.39
19 Aug	G16	*Physo.*	120	19	19	1376 (475-2550)	3.4
02 Sept	G16	*Physo.*	135	20	19	1308 (0-4925)	2.5

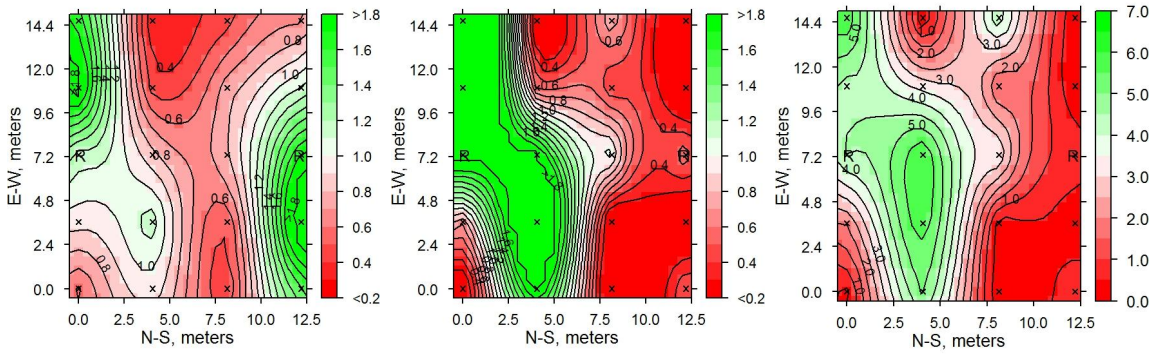

Figures 2.6a-c Maps of catchcan and leachate volumes (normalized to mean) and the leaching fraction map (left to right) of section G16 on 02 September. The 'R' is an irrigation riser. The 'x' is a monitored plant. The three left rows of plants leached much more water than the far right row. Darker shades in a and b represent data further from the mean. Darker shades in "C" represent higher and lower leaching fractions. The three left rows had much larger canopies (unpruned) than the far right row. All leaching fraction maps are found in Appendix E – "Leaching Fractions." This date is shown for illustrative purposes and does not represent all leaching fraction data.

Although the main purpose of the leaching fraction data was to have an indication of the water application efficiency, a surprising feature appeared in the data concerning canopy effects. On 19 August and 02 September section G16 was monitored for leaching fraction; it was found that the mean leaching fraction was greater than one on both days (3.4 and 2.5

respectively). This implied that the canopy captured more water than an empty bucket, effectively capturing water that would otherwise have been lost to the empty spaces between containers and channeling the water to the substrate (a funnel type canopy). Initial observations from these two days also allowed for comparison between pruned and unpruned plants because one row of plants on each day was pruned while the others were left unpruned. A typical unpruned plant had a canopy about 80 cm above the top of the container while a pruned plant had a canopy of half that at about 40 cm.

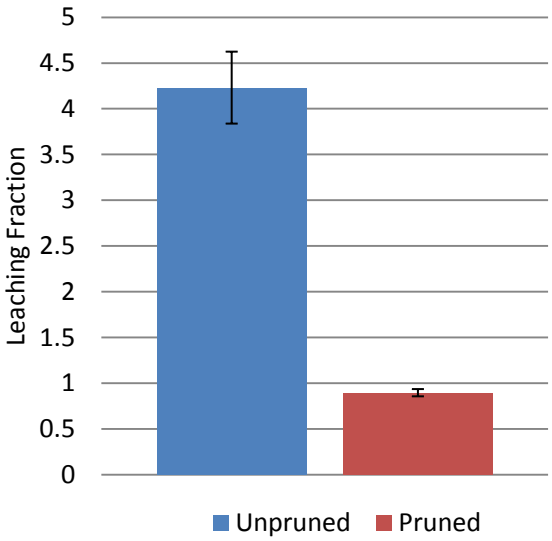

Figure 2.7 Mean leaching fraction of G16 on 19 August with standard error bars.

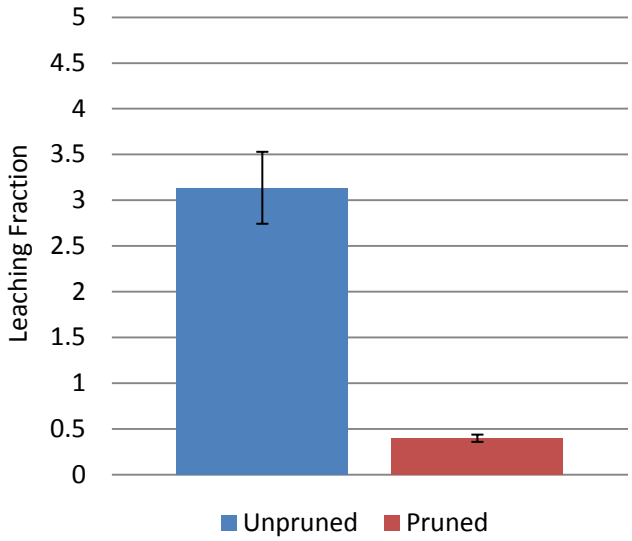

Figure 2.8 Mean leaching fraction of G16 on 02 September with standard error bars.

On both days, the leaching fraction of unpruned plants was more than 370% of pruned plants. These results highlight the importance of canopy maintenance to ensure even and adequate irrigation. Since the soil water holding capacity was seen to be the key determinant of post-irrigation retained water, the more than two-fold rate of water capture with full canopy suggests that the irrigation duration should have been gradually reduced as the plant canopies grew taller. However, reducing the irrigation time to accommodate this one species in a heterogeneous irrigation zone would have caused other species to receive too little irrigation. Thus plant species, canopy type, and canopy size are important factors when choosing a "control plant" for irrigation monitoring in a heterogeneous irrigation zone.

2.3.3 Canopy interaction analysis

The irrigation distribution in a mostly empty row during a period of low wind was found to have similarities to the Rain Bird Sales prediction for this system (Figure 2.3). Overlaying the

Rain Bird Sales figure onto the observed irrigation map with the top two corners of Figure 2.3 aligning with two irrigation risers in Figure 2.9, it can be seen that the expected and observed irrigation patterns are visually similar, with higher volumes near the risers and in the center of four risers and lower volumes between any two risers. The irrigation distribution fluctuated ±32% from the mean (over two standard deviations, or 95% of the samples). The distribution uniformity was 81%, which is better than the Rain Bird Sales estimate of 65%. The summary of leaching fractions by plant type is presented in Table 2.7.

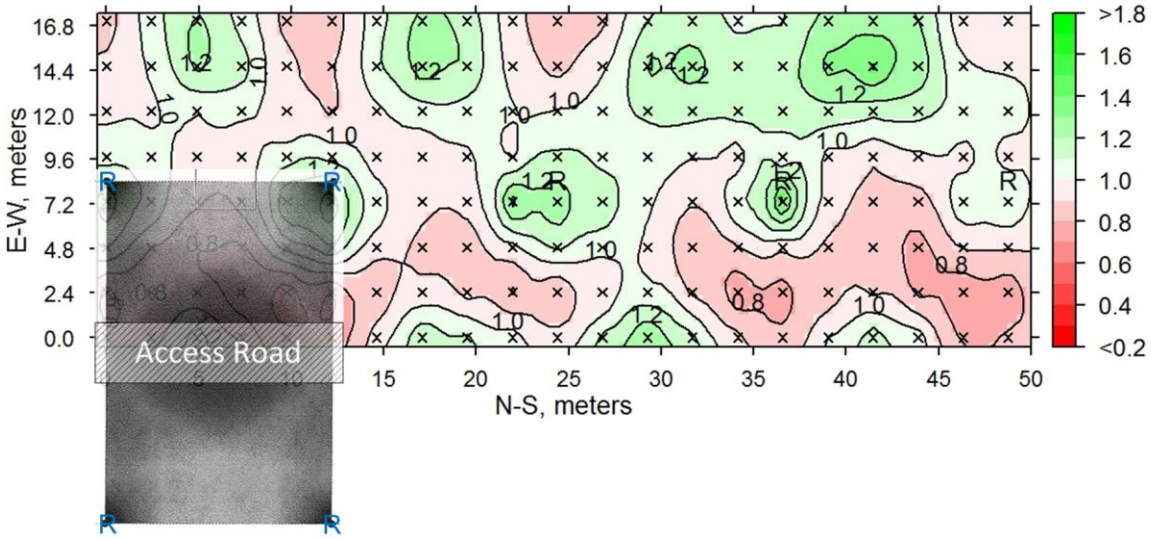

Figure 2.9 Normalized irrigation distribution in row F9 on 16 Sept. Each 'R' is an irrigation riser; each 'x' is a catch-can cup. The Rain Bird Sales irrigation density prediction from Figure 2.3 is overlaid to scale with a slight transparency to provide a comparison between measured and predicted values.

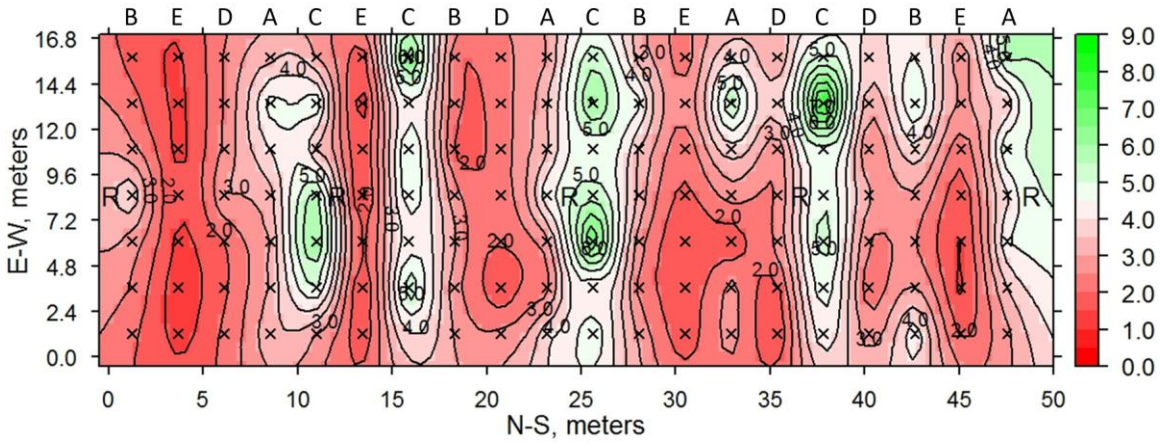

Figure 2.10 Leaching fractions in row F9 on 16 September. Each 'x' is a monitored plant; each 'R' is an irrigation riser. Each letter A, B, C, D, and E above each row corresponds to a plant type in Table 2.6.

Table 2.7 Results of leaching fraction canopy interaction experiment. Each plant and size listed below was represented by four E-W rows of plants as seen in Figure 2.10.

Species and size	Row label in Figure 2.10	Mean Leaching Fraction	Leaching Fraction Standard Deviation	Mean Canopy Height (cm)	Canopy Height Standard Deviation (cm)
Rhododendron PJM #2	A	3.6	0.98	61	6.2
Rhododendron PJM #3	B	3.0	0.89	53	4.9
Physocarpus unpruned	C	5.1	1.2	85	7.3
Physocarpus pruned	D	2.5	0.55	39	4.7
Spiraea	E	1.7	0.45	44	4.1
All plants		3.2	1.4	56	17

Comparing leaching fraction between plants with the tallest canopy height (unpruned Physocarpus) to those with the shortest height (pruned Physocarpus) in Table 2.8, canopy height is a major determinate in a plant's leaching fraction (P = 0.063). The correlation between canopy height and leaching fraction is stronger (R-squared = 0.58) than that of the canopy width.

Table 2.8 Correlation between leaching fraction and canopy dimensions.

Dimension Type	R-squared value
Height	0.58
Largest Width	0.40
Smallest Width	0.42

2.4 Summary

If the performance of this irrigation system is indicative of the performance of similar irrigation systems, then any system's predicted irrigation pattern can be used as a helpful guide when choosing a plant to monitor. The plant chosen should be in the middle of a small area that receives approximately the same amount of water so that if the wind blows the irrigation one way or another, the sensor readings will be minimally affected. It should also be in an area of the irrigation pattern that is expected to receive less than average irrigation (between two irrigation risers); this should decrease the amount of effort required to determine the required irrigation duration in order to ensure that almost all of the plants receive adequate irrigation. Using just this one plant and the expected irrigation rate at its location as a guide, one can determine the irrigation length necessary to bring the entire section to saturation. An aspect of plant maintenance that was discovered by this study was the importance of a well maintained canopy. As the canopy was left to grow in the *physocarpus*, the leaching fraction doubled ($P < 0.003$)

2.5 Literature Cited

Andreen, W.L. 2011. Water law and the search for sustainability: a comparative analysis. Water Resources Planning and Management. R. Quentin Grafton, Karen Hussey. Cambridge University Press.

Beeson, Jr., R.C., M.A. Arnold, T.E. Bilderback, B. Bolusky, S. Chandler, H.M. Gramling, J.D. Lea-Cox, J.R. Harris, P.J. Klinger, H.M. Mathers, J.M. Ruter, and T.H. Yeager. 2004. Strategic vision of container nursery irrigation in the next ten years. J. Environ. Hort. 22(2):113-155.

Oregon Water Resources Department (OWRD). 2009. *Water Rights in Oregon*.

Yeager, T., D. Fare, J. Lea-Cox, J. Ruter, T. Bilderback, C. Gilliam, A. Niemiera, K. Tilt, S. Warren, R. Wright, and T. Whitwell. 2007. Best management practices: guide for producing nursery crops. 2nd ed. Southern Nursery Assn., Atlanta, Georgia.

Chapter 3

Wireless Network Performance

3.0 Abstract

As ornamental container nurseries face increased pressure to reduce irrigation, many are looking to automated solutions to increase their water application efficiency. Due to the necessary wide distribution of sensors at a container nursery, a wireless network is easier, and most-likely cheaper to implement than a hard-wired sensor network. A wireless network also allows for more flexibility in sensor location. When choosing a wireless network, a matter of critical importance is the network reliability. This study examined the reliability of a mesh-style wireless network used as part of a larger study at a container nursery. The findings indicate that this network must improve its reliability in order to be used as a real-time control for an automated irrigation system. On the other hand, the system was sufficient for calculation of irrigation set-time and monitoring net irrigation application and evaporative consumption.

3.1 Introduction

Recent technological advancements in wireless data transmission, environmental sensors, solar power supplies, and decreasing hardware costs have made it possible to remotely monitor agricultural crops from the convenience of an office. This paper examines the use of a wireless soil water content measurement system at an ornamental container nursery in Yamhill, Oregon, USA (Bailey Nurseries Inc.).

Several studies have utilized customized wireless networks to transmit sensor data to a computer (Cayanan et al., 2008; Lea-Cox et al., 2010). Some of those studies were in controlled laboratory environments (Cayanan et al., 2008), some used commercial greenhouse operations (Lea-Cox et al., 2010), and some used active field sites (Cardell-Oliver et al., 2005); however, few have used real-time sensor data on wireless networks to make active irrigation management decisions.

Cayanan et al. (2008) used a non-commercial wireless transmitter ("Poseidon" Wireless Module) developed at the University of Guelph in conjunction with a custom Matlab PC interface. The Matlab program sent data requests to the wireless modules every twenty minutes. The system controlled water delivery via drip irrigation lines based on volumetric water content (VWC) of the coconut coir substrate using Decagon Devices ECH$_2$O-TE sensors. The U. of Guelph system was able to be configured to accommodate many different irrigation schemes; however, the Matlab software utilized was not conventional and could be difficult to teach to users with limited computer skills. It also relied on non-rechargeable batteries with a lifetime of approximately two weeks requiring the user to replace the batteries in each wireless module many times during the course of the growing season.

Lea-Cox et al. (2010) utilized a non-commercial wireless system developed by Carnegie Mellon Robotics Institute (Lea-Cox, Ristvey et al., 2008) with probes from Decagon Devices at a commercial cut-flower greenhouse operation. The battery and solar powered wireless nodes recorded every five minutes the average of the data obtained over the preceding one-minute.

Both Cayanan et al. and Lea-Cox et al. used non-commercial products in their studies. The study herein evaluates commercially-available, network products in a commercial, open-air, container nursery. The objective of this study was to use a system currently available to commercial nursery operators and to test its performance as a soil moisture-monitoring tool.

3.2 Materials and methods

The experiment consisted of eight data-collection nodes (eKo Node 2120, Memsic Corporation, Andover, Mass.) communicating wirelessly with a single solar-powered base station (BaseStation, PureSense Environmental, Inc., Fresno, Calif.). The BaseStation collected the data from the eKo Nodes and transmitted them over a cellular modem to the PureSense servers in California, which then posted the data to a webpage for viewing.

Each solar powered eKo Node was capable of monitoring up to four instruments, but for this study only two instruments were monitored per node – a load cell (15kg RL1042, Rice Lake Weighing Systems, Rice Lake, Wisc.) and a volumetric soil moisture sensor (EC-5, Decagon Devices, Inc., Pullman, Wash.). Two eKo Nodes also monitored a weather station (ES2000v6, Memsic Corporation, Andover, Mass.), one in each irrigation zone, that collected wind speed and direction, irrigation and rainfall, temperature, relative humidity, solar radiation, UV radiation, and barometric pressure. Figure 3.1 shows a simplified network diagram of the system. One of the advantages of the eKo Nodes over similar devices was their capability to communicate to the BaseStation via another node; if a node was too far from the BaseStation to communicate

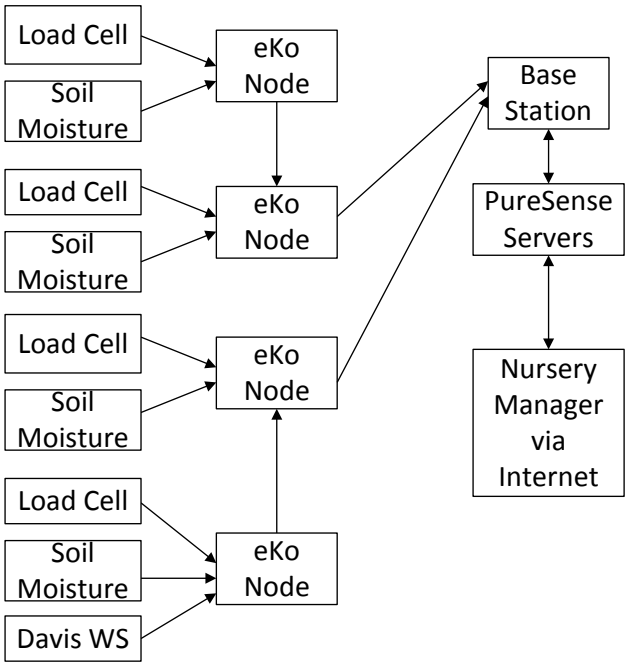

Figure 3.1 Simplified network representations showing possible transmit paths.

with it directly, the node could pass its data to a nearby node that was able to communicate with the BaseStation. This ability, called mesh networking (Ferrari, 2010), enabled the network to extend far from the BaseStation by utilizing intermediary nodes.

The network collected data over a period of nine weeks (18 July 2010 to 21 September 2010) during the active production season for the nursery. Under normal operation the nodes were designed to communicate with the BaseStation every fifteen minutes to transmit sensor data. Each transmission was considered a data point for the purposes of this chapter. Upon network startup, each node went through an initialization mode during which it transmitted once per minute for 60 minutes. Periods of initialization were not considered normal operation and are excluded from the results.

3.3 Results and discussion

Between 21 July and 24 August, 2010, at any given time, at least one of the eight nodes was not transmitting properly. However, a firmware update provided by PureSense on 24 August to the BaseStation corrected most of these transmission problems. Therefore, the network reliability analysis presented below will focus only on the dates between 24 and 28 August, 02 to 09 September, and 13 to 21 September. Missing dates are due to power losses at the BaseStation.

During the period between 24 August and 21 September when the BaseStation was operational, the system collected 10,353 data points out of the expected 13,766, a transmission reliability of 75.2 percent. The performance was better than the 63.8 percent rate reported by Cardell-Oliver et al. (2005) on their custom wireless network, but illustrated that wireless communication with this system is still far from the reliability needed to be used in an active-control implementation. Figure 3.2 shows the data points aggregated by how many minutes elapsed between successive data points (rounded to the nearest 15 minutes); note that this is a log scale on the vertical axis. The majority of data (81%) were received as expected (approximately 15 minutes), but a significant minority of data points (19%) were received after 20 minutes. It can be inferred from Figure 3.2 that occasionally the system fails to record data at the BaseStation at the expected time, thus decreasing data density and sample size available to the nursery manager to make irrigation management decisions. Most often, this was an anomaly and the system recorded the next data point as expected. However, a small percentage of the time (3.8%) the system missed two consecutive data points.

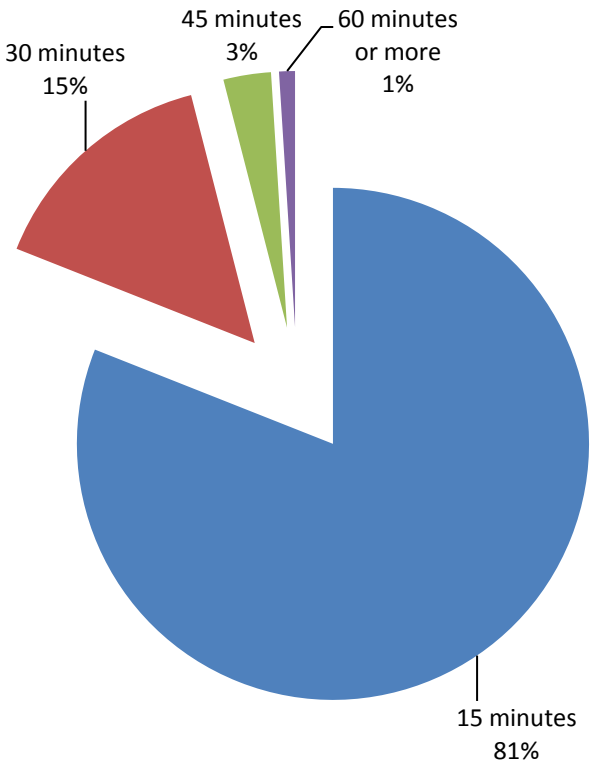

Figure 3.2 The portion of data points received aggregated by minutes elapsed between successive data points.

One of the problems with the network was losing power at the BaseStation. This could have been a problem with poor siting; the BaseStation was placed in a location that was shaded in the afternoon by a two story building. Since it wasn't receiving full sun all day long, it could have had difficulty properly recharging the battery. This could have been resolved with a larger solar panel combined with a larger-capacity battery, or improved siting. Thus, though important to the performance of the system at this demonstration site, and a valuable reminder of the importance of tracking battery levels in time, this is not seen as a fundamental characteristic of this class of applications of wireless sensing.

3.4 Conclusion

3.4.1 Needs of an automated system

In chapter 1 we saw that careful selection and proper installation of sensors are critical for accurate measurements. In chapter 2 we saw that identifying a representative specimen must also be addressed with care to ensure proper irrigation of the entire section. And in chapter 3 we saw that a network system that occasionally misses a scheduled sensor reading may make real-time control sufficiently unreliable as to be unacceptable. Clearly these issues must be seen as system design constraints in the application of this technology, as we discuss below.

A completely automated irrigation system needs the following:

1) Sufficient data density to maximize water application efficiency (WAE). A shorter reporting interval would allow for greater control over the irrigation cycle and higher utilization of water, even moving into controlled soil-moisture deficits for desired biological effects such as flowering or dormancy. Also, as discussed in chapter 1, sensor resolution is an important factor in determining the effectiveness of reducing the reporting time interval. If the reporting time is reduced below the time needed for the sensor reading to increase one bit (sensor resolution divided by effective irrigation rate), then the field node would be sending unnecessary data to the BaseStation. Alternatively, a system could be designed to take field measurements at short intervals, but only transmit to the BaseStation on a sensor change; this is called a reactive system, such as one used by Cardell-Oliver et al.

(2005). However, using irrigation rate and estimated canopy interception, a decent estimate of the effective irrigation rate could be made in lieu of data density.

2) Network transmission reliability to prevent data loss. If the end of an irrigation cycle depends on measured values, transmission reliability is critical. An irrigation system that reduces its dependency on data transmission would be a more robust option (i.e. – timer fail-safes).
3) Redundancy to ensure a representative sample. An accurate irrigation map showing the expected irrigation distribution could suffice for the extra sensors. Extra sensors are expensive and could lead to worse network performance (by having too many devices on the network) and overwhelm the nursery manager with too much data.
4) Sensor accuracy and proper installation. If the end of an irrigation cycle depends on measured values, sensor accuracy is important, but not necessarily critical. An alternative system could use soil moisture or container-weight values to determine the amount of water needed to bring that container up to field capacity and the effective irrigation rate to determine the time needed to deliver that much water.
5) Robust power management. It will always be that the design of a wireless sensing system must balance energy supply (solar panel output and battery capacity) with energy consumption (dominated by the radio usage).
6) Outputs to control irrigation pumps. Remote operation of the entire irrigation system is the end goal of such an automated system. This can only be accomplished with output relays integrated into the system to control the flow of water.

7) Easy to use data display and control interface. A system such as this is effectively useless if the nursery manager cannot easily access the data and control set-points which in turn control the irrigation.

3.4.2 Current system provisions

The PureSense BaseStation and Memsic eKo Node system monitored in this study provides the following benefits, some of which are solutions for some of the criteria outlined above. PureSense provided both an easy-to-use website and a custom computer application (not shown) for monitoring environmental and soil water conditions. The eKo Nodes and PureSense BaseStation used solar-recharged batteries making them maintenance free throughout the growing season. The eKo Node wireless mesh network allowed for widespread distribution of sensors without the expense of burying communication cables. Because the sensors used only a short cable to connect with the eKo Node, the sensors and eKo Nodes could be easily moved to monitor a different section. The system provided a reliable estimate of the plant status in the hour prior to irrigation (with 99% probability). Further, with over 80% reliability, we could expect to obtain the weight within 15 minutes of the end of irrigation, and with 98% probability the weight an hour after irrigation. It is the opinion of the author that fifteen minutes between sensor readings with 80% reliability is sufficient to monitor soil moisture during draw-down.

These data allowed us to:

1) Reliably determine when container saturation achieved a threshold value,

2) Verify that the full water holding capacity of the system was achieved after an irrigation cycle.

These data would be sufficient to:

1) Determine when to start irrigation
2) Compute an irrigation time duration sufficient to achieve field saturation
3) Verify that the plants obtained field saturation.

Furthermore, in most instances (over 80% of the cases) the data would allow observation of over-irrigation as evidenced by plateau in weight during the final period of the irrigation set and a significant drop in weight immediately following the end of irrigation (drainage to field capacity). These data would be very valuable to irrigation management even without automation.

Therefore it is still possible to employ this system to manage irrigation. We know that successive irrigation sets follow very similar patterns, so knowledge of the degree of depletion prior to irrigation, as well as having a history of the relationship between irrigation duration and net water accumulation, may be sufficient information to schedule the duration for each irrigation event as computed prior to onset of water application. Thus, while satisfying all of the characteristics of an ideal monitoring system, the benefits, robustness, and economy of using a one-size-fits-all approach may yet provide sufficient functionality to improve irrigation performance using a product which is currently available on the market.

3.4.3 Current system limitations

The system does have some limitations which must be taken into account in developing a successful irrigation control system based on this approach to monitoring. We now see important limitations presented by the unchangeable reporting intervals (15 minutes); power limitations of the eKo Nodes (a partial reason for unchangeable reporting intervals); limited selection of sensors; lack of any output relays for control of external systems; and most importantly, the unexplained loss of over twenty percent of data, even after all other sources of error were addressed. It is the opinion of the author that 15 minutes between sensor readings with 80% reliability is not sufficient to actively control irrigation (also called process control). For this a shorter interval of perhaps 5 or 10 minutes, and at least 95% reliability would seem prudent so as to not apply water needlessly due to lack of accurate and current data; however, reporting at intervals shorter than the ability of the irrigation rate to increase a sensor measurement would be a fruitless in terms of data captured. Though 15 minute reporting may have been a good choice for many applications, here we see that this system has not been designed with the requirements of active irrigation control as an objective.

3.4.4 Comparison of current system to other systems and suggestions for improvement

Compared to many other soil moisture monitoring systems, the current system showed areas of distinct advantages. Most other solutions require changing batteries periodically or providing electricity at the sensor site; both would be costly (in wiring and/or maintenance effort), and could cause such systems to have failures which would be unacceptable in a production nursery environment. However, missing one in five readings should be cause for more serious thought about the implementation of the current system to control irrigation.

While we anticipate that such reliability will improve, it should be noted that the basic system employed here (eKo Nodes) has been on the market under the Crossbow brand name for over a decade, so a transformative improvement in this basic functionality seems unlikely. An automated irrigation system that relies on the current system should have built in time restraints to prevent over-watering. To ensure redundancy a second pair of sensors should be monitored in each section. Since the PureSense BaseStation currently does not have output control, using this system for irrigation automation would require the user to download the data from the PureSense servers every few minutes. In its current implementation, the system of PureSense BaseStation and Memsic eKo Nodes is designed for periodic monitoring and not for active management as would be required by an automated system.

So we see that the current state of the art in wireless distributed sensing for irrigation management has both limitations and real potential. It is expected that many of the limitations will be addressed in the coming years, but even as currently operating, valuable information is obtained with high reliability.

3.5 Literature Cited

Cardell-Oliver, R., Smettem, K., Kranz, M., Mayer, K., 2005. A reactive soil moisture sensor network: design and field evaluation. Inter. J. Distribut. Sensor Networks 12, 149–162.

Cayanan, D. Feliciano, Dixon, M., Zheng, Y. 2008. Development of an automated irrigation system using wireless technology and root zone environment sensors. Acta Hort. 797: 167-172.

Ferrari, G. (ed.). Sensor Networks: Where Theory Meets Practice. Heidelberg, Germany: Springer, 2010.

Lea-Cox, J.D.**,** F. R. Arguedas-Rodriguez, A. G. Ristvey, D. S. Ross and G. Kantor. 2010. Wireless Sensor Networks to Precisely Monitor Substrate Moisture and Electrical Conductivity Dynamics in a Cut-Flower Greenhouse Operation. *Acta Hort*. (Accepted) (GreenSys2009).

Lea-Cox, J.D., Ristvey, A.G., Arguedas-Rodriguez, F., Ross, D.S., and Anhalt, J. 2008. A low-cost multihop wireless sensor network, enabling real-time management of environmental data for the greenhouse and nursery industry. Acta Hort. 801:523-529.

APPENDICES

Appendix A

Calibration of Load Cell Data

A.1 Initial calibration attempts

Between 7/19/2010 12:00:00 and 7/22/2010 09:40:00, a known, unchanging weight (a one-gallon plastic jug filled with dry sand and sealed with a screw-on plastic top) was placed on each load cell. After reviewing the data (Figure A.1), it was immediately evident that a periodic, recurring deviation occurred on a diurnal time-frame.

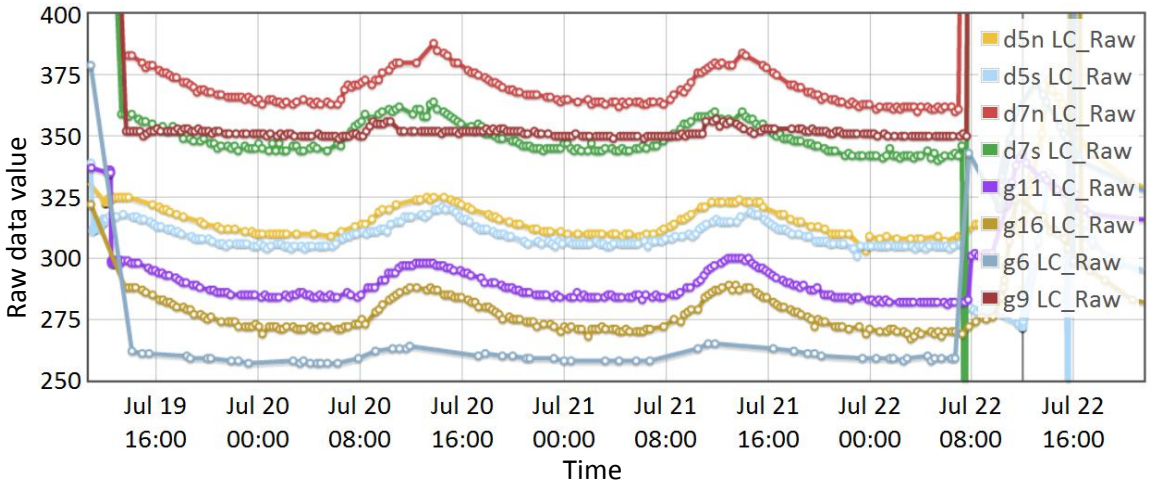

Figure A.1 Raw data of all load cells during the calibration period. The weight on each load cell was constant during this time.

Comparing the load cell data to solar radiation and air temperature from a calibrated meteorological data set from the Forest Grove, Oregon, Agri-Met weather station approximately 22 kilometers NNE from the experiment location in Yamhill, the load cell data appears to correlate better with solar radiation than air temperature. However, a calibration attempt with

radiation only produced a calibrated load cell value with a negative trending slope (Figure A.2). Using both radiation and temperature produced a somewhat better calibrated reading (Figure A.3).

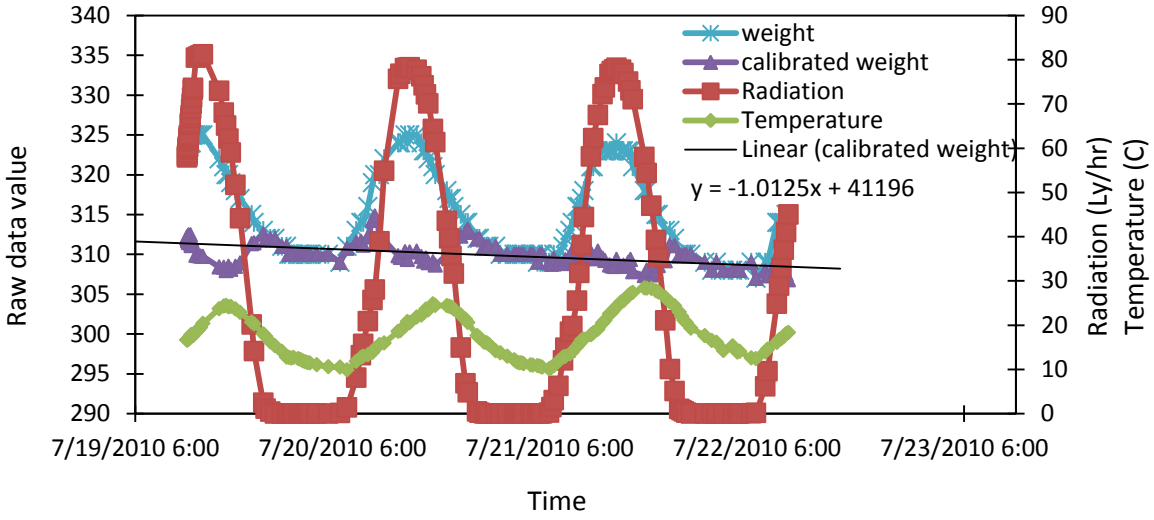

Figure A.2 Raw load cell data of section D5N (blue asterisk) compared to Forest Grove air temperature (Celsius, right axis, green diamond), and solar radiation (Langleys per hour, right axis, red square). Calibrated load cell value (purple triangle) based on radiation only is shown with a linear trend line and equation.

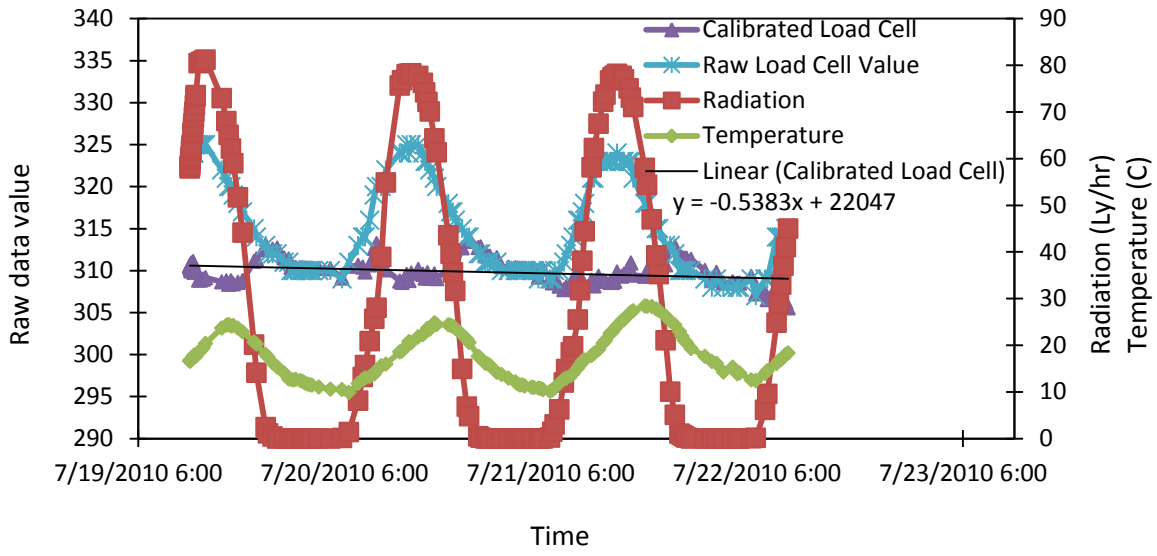

Figure A.3 Raw load cell data of section D5N (blue asterisk) compared to Forest Grove air temperature (Celsius, right axis, green diamond), and solar radiation (Langleys per hour, right axis, red square). Calibrated load cell value (purple triangle) based on radiation and temperature is shown with a linear trend line and equation.

However, when comparing the load cell data with the excitation signal data, it was evident that both values were subject to the same signal variation as seen in Figure A.4.

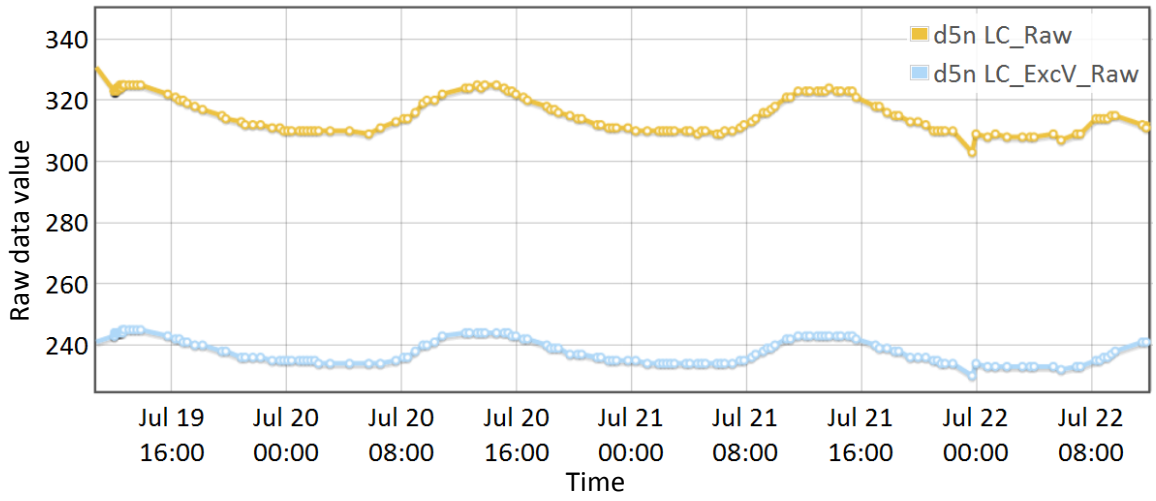

Figure A.4 Raw load cell data from section D5N (LC_Raw, gold, top line) compared to the raw excitation voltage value of the load cell (LC_ExcV_Raw, blue, bottom line). These values are raw and have not been converted to units.

It is instructive at this point to explain how the excitation voltage and subsequent load cell reading are produced. The excitation voltage comes from the unregulated power supply of the batteries of the eKo Node. The voltage of these batteries fluctuates through the day as the solar panels recharge them during the day and as they discharge at night. The load cell outputs a voltage that is directly proportional to the excitation voltage applied to it. As the excitation voltage increases through the daytime, the load cell output also increases in the same proportion. The load cell output is then amplified with an electronic amplification board (ES9100, Memsic Corporation) before being read and digitized by the eKo Node (Memsic Corporation), transmitted to the base station, and finally transferred to the database.

To convert the raw, amplified data from the load cell into real units (grams), one needs to know the excitation voltage and the output voltage as well as the unique output characteristic of the load cell (how much voltage the load cell outputs per unit input voltage at

the maximum capacity of the load cell). Conversely, one can do a two or more point calibration using known weight values. The second method can generally be considered superior to the first because it removes the impact of a possible change in the output characteristic of the load cell since the factory calibration, and it also directly accounts for the amplification of the output signal without needing to know anything specific about the amount amplification. The second method also inherently incorporates the weight of the support plate into the final equation allowing the user to ignore another tedious step of exactly measuring the weight of each support plate.

In the first conversion method (exact knowledge of the system), the fluctuating excitation voltage is directly accounted for in the conversion formula and is not of any consequence. But when using the second conversion method (2-point conversion), the diurnal influence has not been removed from the final product. This can be addressed by normalizing the output with respect to the excitation voltage, or, since the output is directly proportional to the excitation voltage and a two-point conversion is being used, the output can simply be divided by the excitation voltage. Figure A.5 shows the calibrated data of section D5N compared with the uncalibrated data as a typical example of the remaining sections.

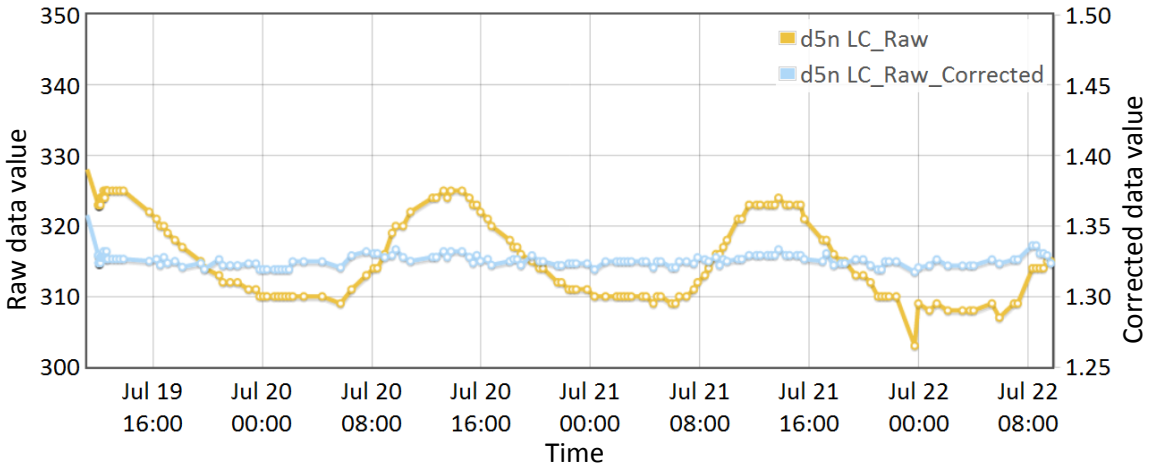

Figure A.5 Raw data from section D5N (LC_Raw, gold, left axis) compared to the corrected data value of the load cell (LC_Raw_Corrected, blue, right axis) during the calibration period. This is a typical pattern seen in the remainder of the sections.

Table A.1 Means and standard deviations before and after calibration attempts.

Section	Non-Calibrated			Calibrated†		
	Mean	Standard Deviation	Slope	Mean	Standard Deviation	Slope
D5N	314.8	5.58	-3.09	314.9	0.83	0.047
D5S	309.6	4.68	-2.19	309.3	1.54	0.39
D7N	369.8	7.12	-2.74	370.1	2.12	-0.46
D7S	349.4	6.16	-2.60	349.5	2.40	-0.19
G6	260.0	2.28	0.22	260.3	1.25	-0.092
G9N	351.4	1.56	-0.22	351.5	1.52	-0.26
G11S	288.4	5.49	-4.08	288.0	1.48	-0.69
G16	276.2	6.19	-1.86	276.2	1.99	-0.43
Mean	315.0	4.88	-2.07	315.0	1.64	-0.21
Standard Deviation	39.2	1.97	1.44	39.3	0.51	0.33

†Values shown are from normalizing the calibrated data to the mean of uncalibrated data for comparison on equal scale.

One possible reason for the trend in slope in each raw data set is that the time series are not three complete diurnal cycles. If exactly three diurnal cycles were observed, it is expected that the slopes would be quite minimal. However, using only two and a half cycles allows for

better critique of the calibration scheme precisely because it accentuates the slope in data and readily shows the improvement due to calibration.

A.2 Corrected Data to Weight Conversion

On 02 September 2010 between 9:00 and 9:30 a two point calibration was done on the load cell in section D5N using two different known weights. First, a weight of 4282.1 g was placed on the load cell and then a second weight was added for a total of 8143.8 g.

Table A.2 Values used to convert raw data values to weight units for the section D5N. The slope (m) and intercept (b) of the final conversion formula are also given.

Section name	Time start	Time 2nd weight	Weight 1 (g)	Weight 2 (g)	Corrected sensor value 1	Corrected sensor value 2	m	b
D5N	9:06	9:17	4282.1	8143.8	1.4422	2.5893	3366.5	-573.1

The weight is then found from the formula:

$$\text{Weight} = \text{calibrated sensor value} * m + b \qquad \textbf{Equation A.1}$$

Table A.3 Summary of the weight conversion values obtained and used to convert the raw data into units of grams. Section G9N is discussed in section A.3 – "Section G9".

Section name	Time start	Time 2nd weight	Weight 1 (g)	Weight 2 (g)	Corrected sensor value 1	Corrected sensor value 2	m	b
D5N	9:06	9:17	4282.1	8143.8	1.4422	2.5893	3366.5	-573.1
D5S	9:30	9:40	4282.1	8143.8	1.4279	2.5611	3407.8	-583.9
D7N	15:01	15:13	4282.1	8143.8	1.7273	2.8678	3386.0	-1566.5
D7S	14:34	14:48	4282.1	8143.8	1.6667	2.8115	3373.3	-1340.1
G6	13:34	13:46	4282.1	8143.8	1.2449	2.3853	3386.3	66.5
G9N[†]	NA	NA	NA	NA	NA	NA	3436.2	-1873.3
G9N[‡]	NA	NA	NA	NA	NA	NA	2316.9	-1787.1
G11S	8:36	8:48	4282.1	8143.8	1.3366	2.4847	3363.6	-213.6
G16	8:10	8:23	4282.1	8143.8	1.2819	2.4219	3387.5	-60.3

[†]22 July to 12 August [‡] 12 August to 16 September

A.3 Calibration of section G9N

This data set was more difficult to convert into actual weight measurements. The standard conversion method using the two known weights on 02 September creates negative values during a period of known zero weight (06-09 August) and during the 3 day temperature calibration. Further investigation revealed that the sensor may have been stressed beyond its mechanical limit at some point between 06-09 August causing the time periods before and after those dates to have different calibration values. The multiple point calibration is shown in the figure and table below and uses the average of manually weighed values from the G9 section before and after watering on 22 July, 05 August, 19 August, and 02 September along with the calibration weight on 22 July and known zero value on 08 August. The values of m and b are obtained from the linear trend lines in the figure. G9A corresponds to the period before the move, and G9B corresponds to the period after the move.

Table A.4 List of values of known weights used in Figure A.6.

Date	Known weight	Sensor value
22 July	3839	350.25
22 July	8910	667.96
22 July	9333	693.46
05 August	8953	734.69
05 August	9591	787.53
08 August	0	130.54
19 August	4257	629.76
19 August	4409	657.09
02 September	3613	579.6
02 September	4268	641.07
02 September	4281.1	662.24
02 September	8143.8	934

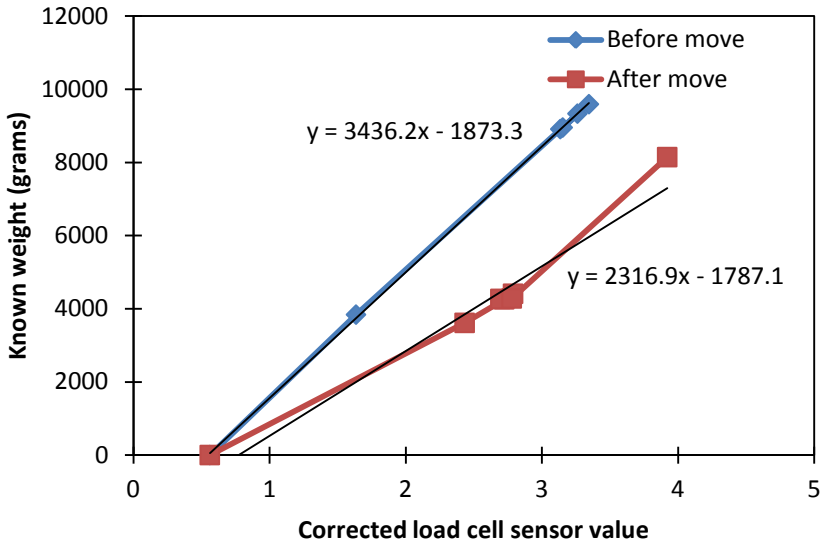

Figure A.6 Comparison of data from G9N before (blue diamond) and after (red square) the load cell was moved. The linear trend is shown for each with their respective formulas.

Appendix B

Sensor Resolution

B.1 Load Cell

The load cells employed bridge resistance circuitry to provide a weight dependent voltage output with a 15 kg rated maximum load. The eight load cells had an average full-scale voltage output (bridge response) of 2.0036 mV · V^{-1} (range 1.9943 to 2.0096 mV · V^{-1}, factory measured)[10]. This output, or signal, was then amplified by the ES9100 board to be within the sensitivity range of the eKo Node. The eKo Node is capable of sensing an analog voltage between 0.0000 mV and 3000.0000 mV with a 10-bit analog to digital resolution, i.e – the range of 0 to 3000 mV is chopped up into 1023 pieces of 2.9326 mV per bit[11].

The goal of amplification was to make the load cell output at full-scale (15 kg) to be as close to 3.0 V as possible without exceeding it. Two different revisions of the ES9100 board were used. In revision 1 boards, the gain (amplification value) was changed with a 274 ohm (±1%) resistor to create a nominal gain of 366.0 V·V^{-1}. Revision 2 boards used a factory-placed gain resistor of 301 ohms (±1%) to provide a gain of 333.2 V·V^{-1}.

[10] If a 15 kg load (full-scale) is placed on a load cell rated at 2.0 mV · V^{-1} and the electric circuit was powered by 1.0 V, a voltage of 2.0 mV should be observed on the output. If powered by 5.0 V, the output should be 10.0 mV.

[11] Another way of looking at this is to say that for every increase of 2.9326 mV, the value shown in the eKo Node increases by 1.

The resolution of the load cells, according to the operational theory, is dependent upon the load cell excitation voltage (ExcV), the unique load cell bridge response (V_{BR}), and the gain resistor (R_G). Following are the steps necessary to find the resolution of the load cell.

The expected load cell output (LC_{OUT}) at maximum load (LC_{MAX}) is found from the formula:

$$LC_{OUT} = ExcV\ (V) * V_{BR}\ (mV/V) \qquad \textbf{Equation B.1}$$

This output is then multiplied by the amplification board according to the gain (G) formula of:

$$G = 1+100000\ (ohm) / R_G\ (ohm) \qquad \textbf{Equation B.2}$$

to get the input at the eKo Node ADC (ADC_{INP}):

$$ADC_{INP} = LC_{OUT}\ (mV) * G \qquad \textbf{Equation B.3}$$

At this point, if using V_{BR} which is at load cell maximum weight (LC_{MAX}), the ADC_{INP} is at the maximum value produced by the load cell and amplification board, which should be slightly below the 3000 mV maximum of the analog to digital converter of the eKo Node. The next step is to find the theoretical weight at 3000 mV (ADC_{MAX}). The load cell should increase its output linearly with weight so a simple linear scalar formula will suffice:

$$ADC_{MAX} = 3000\ (mV) * LC_{MAX}\ (g)/ ADC_{INP}\ (mV) \qquad \textbf{Equation B.4}$$

The resolution is:

$$\text{Resolution} = ADC_{MAX}\ (g) / 1023\ (bits) \qquad \textbf{Equation B.5}$$

Substituting Equations B.1, B.2, B.3, and B.4 into B.5 gives the final resolution:

$$\text{Resolution} = \frac{3000(mV) * LC_{MAX}\ (g)}{1023\ (bits) * ExcV(V) * V_{BR}\left(\frac{mV}{V}\right) * \left(1 + \frac{100000(ohm)}{R_G(ohm)}\right)} \qquad \textbf{Equation B.6}$$

The load cells chosen have a maximum load value (LC_{MAX}) of 15 kg, or 15000 g, the mean bridge response (V_{BR}) was 2.0036 mV · V^{-1}, and the mean gain resistor was 287.5 ohms. Throughout the experiment the mean load cell excitation voltage (ExcV) was 4.150 V. This leads to an overall expected mean resolution of 15.1659 g · bit^{-1}. The excitation voltage had a range of 3.763 to 4.410 V, the bridge response had a range of 1.9943 to 2.0096 mV · V^{-1}, the 100000 ohm resistor had a tolerance of 0.35%, and the gain resistor (R_G) was either 274 ohm or 301 ohm and had a tolerance of 1%. The overall theoretical range of resolution could then be between 13.381 g · bit^{-1} and 17.826 g · bit^{-1}.

B.2 EC-5 VWC Probe

The conversion from the raw EC-5 data uses the following formula:

$$VWC = (1.19 * 1.25 * VWC_{RAW} / ExcV_{RAW}) - 0.401 \qquad \textbf{Equation B.7}$$

where VWC is volumetric water content (cm^3 · cm^{-3}), VWC_{RAW} is the VWC data as recorded by the analog to digital converter in the eKo Node, and $ExcV_{RAW}$ is the excitation voltage as recorded by the analog to digital converter in the eKo Node. (Both RAW values are a number between 0 and 1023 and have units of bits.) Assuming that the excitation voltage raw value

stays at the mean of 400 bits, the resolution of the volumetric soil content is 0.0037 $cm^3 \cdot cm^{-3}$. The minimum and maximum recorded Exc_{RAW} values were 389 and 412, respectively; therefore the resolution of the capacitance probe was in the range of 0.0036 and 0.0038 $cm^3 \cdot cm^{-3}$.

Appendix C

Rain Bird Sales Uniformity Evaluation

C.1 Reproduction of uniformity evaluation data

Rain Bird Sales, Inc.
Uniformity Evaluation

Sprinkler Name	RAIN BIRD	Base Pressure (PSI)	50.0
Sprinkler Model	30H	Riser Height (IN)	30.0
Nozzle Size	3/16" 27°	Set Screw Setting	
Flow Rate (GPM)	N/A	Degree of Arc	360
Date/Time of Test	06/07/88	Mins./Revolution	0.52
Testing Facility	CIT #00088	Record Number	260-P
Comment	Sprinkler provided by: RAIN BIRD		

Distr. Uniformity	65%	Min (In/Hr)	0.167		Spacing
CU (Christiansen)	79%	Mean(In/Hr)	0.281	N/A (Theor.)	Rectangular
Sched Coeff (5%)	1.6	Max (In/Hr)	0.514		40.0' x 60.0'

#1A070 same 27
@ 60psi forecast
CU: 79
DU: 65%
SC: 1.7

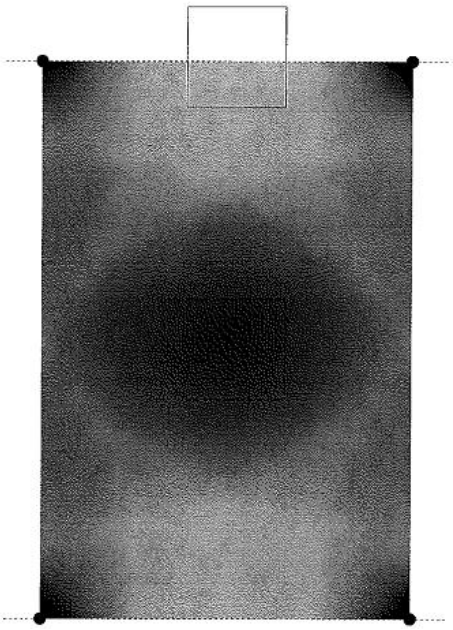

Figure C.1 Reproduction of Rain Bird Sales Inc. uniformity evaluation sheet as transmitted.

Appendix D

Manual Weighing Data

D.1 22 July

For all graphs, the 'R' is the irrigation riser. The small 'x' is a monitored plant. All data is normalized to the mean for that graph.

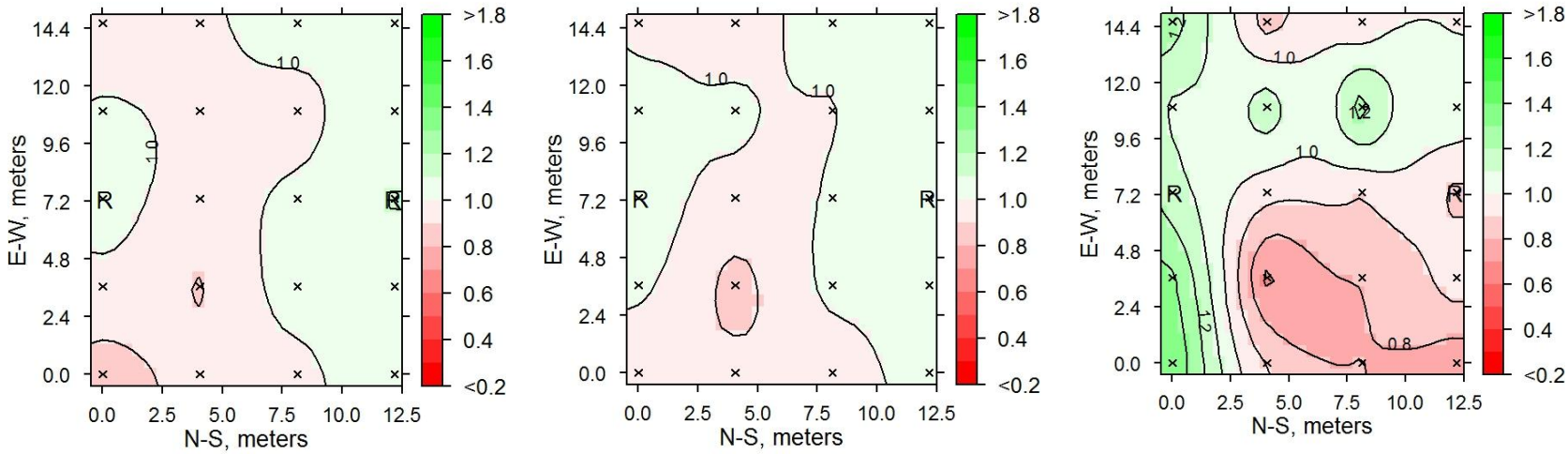

Figures D.1a-c 22 July section D5N masses (left to right) pre and post irrigation and net water gain.

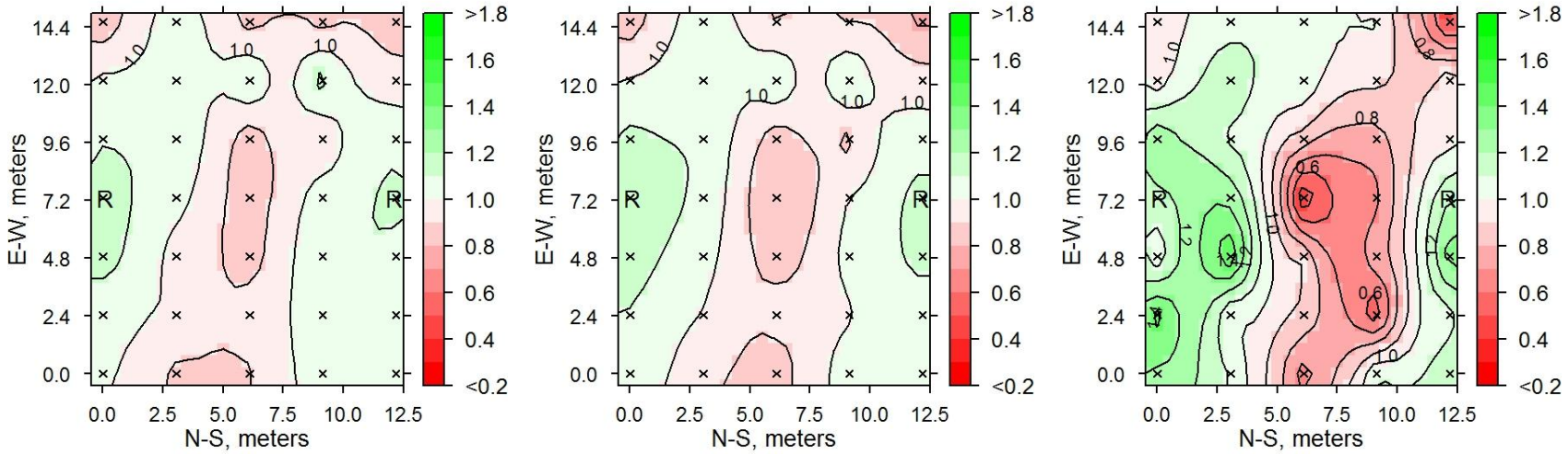

Figures D.2a-c 22 July section D5S masses (left to right) pre and post irrigation and net water gain.

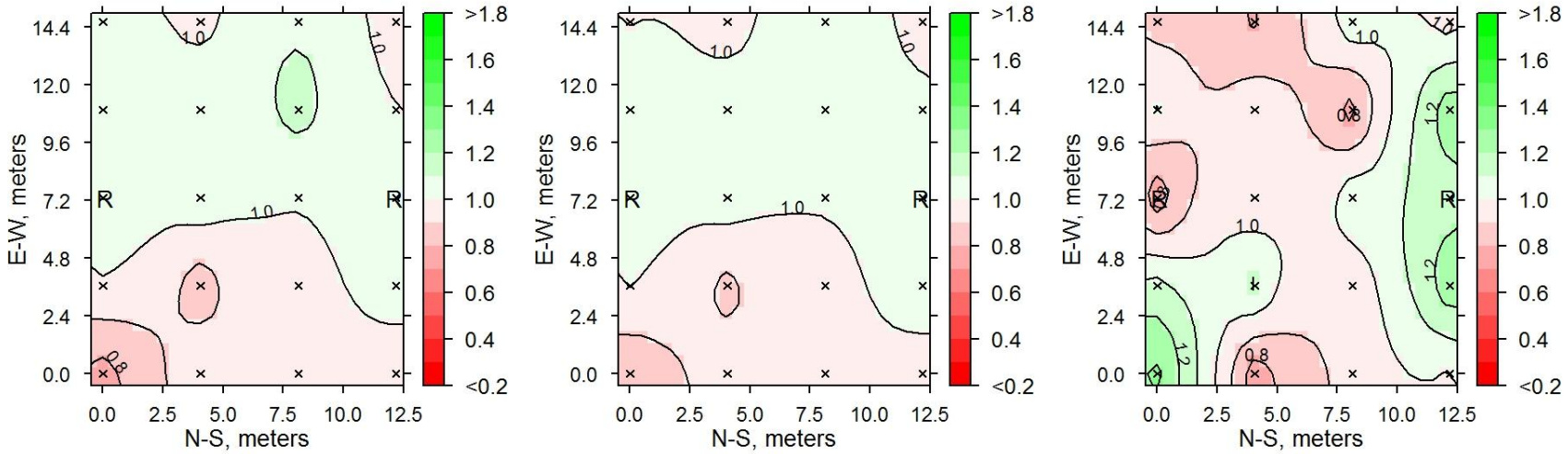

Figures D.3a-c 22 July section D6 masses (left to right) pre and post irrigation and net water gain.

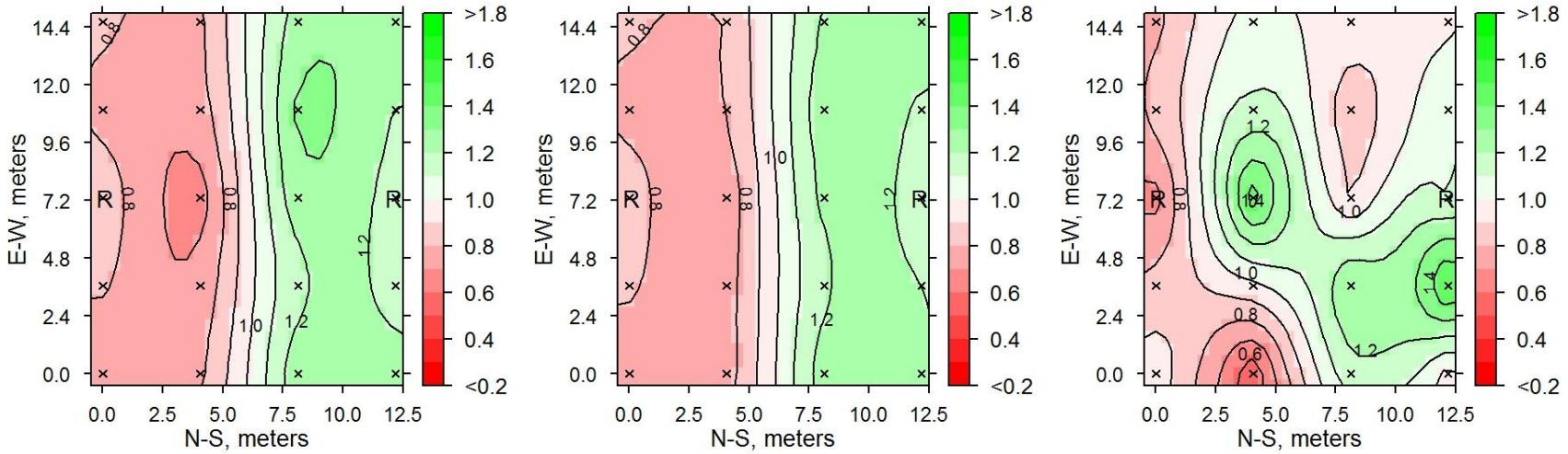

Figures D.4a-c 22 July section D7N masses (left to right) pre and post irrigation and net water gain.

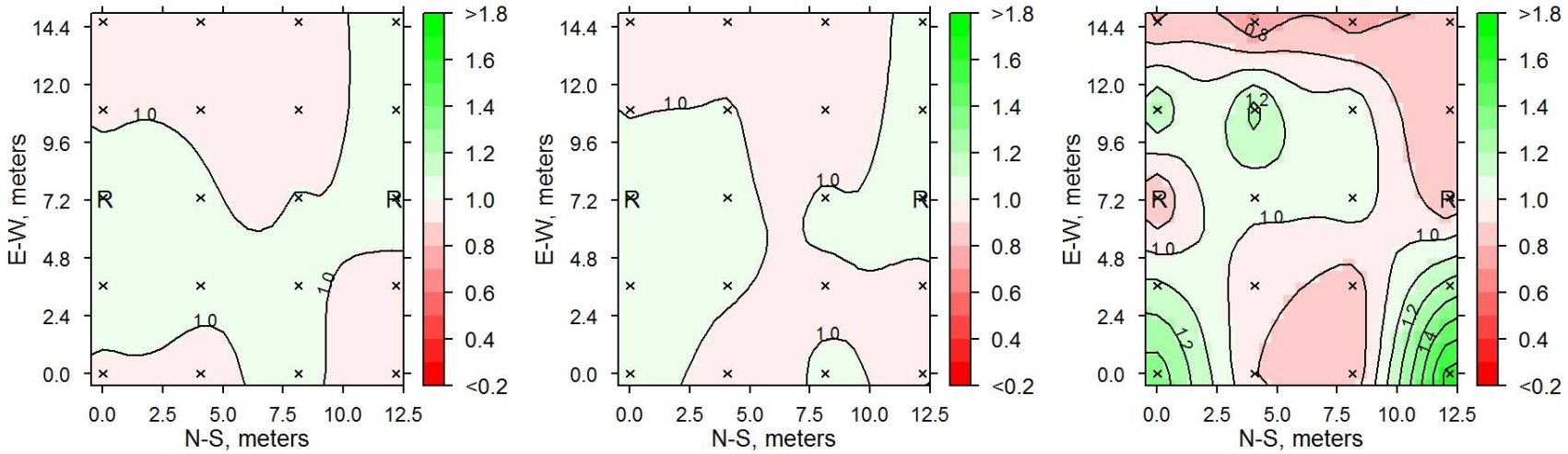

Figures D.5a-c 22 July section D7S masses (left to right) pre and post irrigation and net water gain.

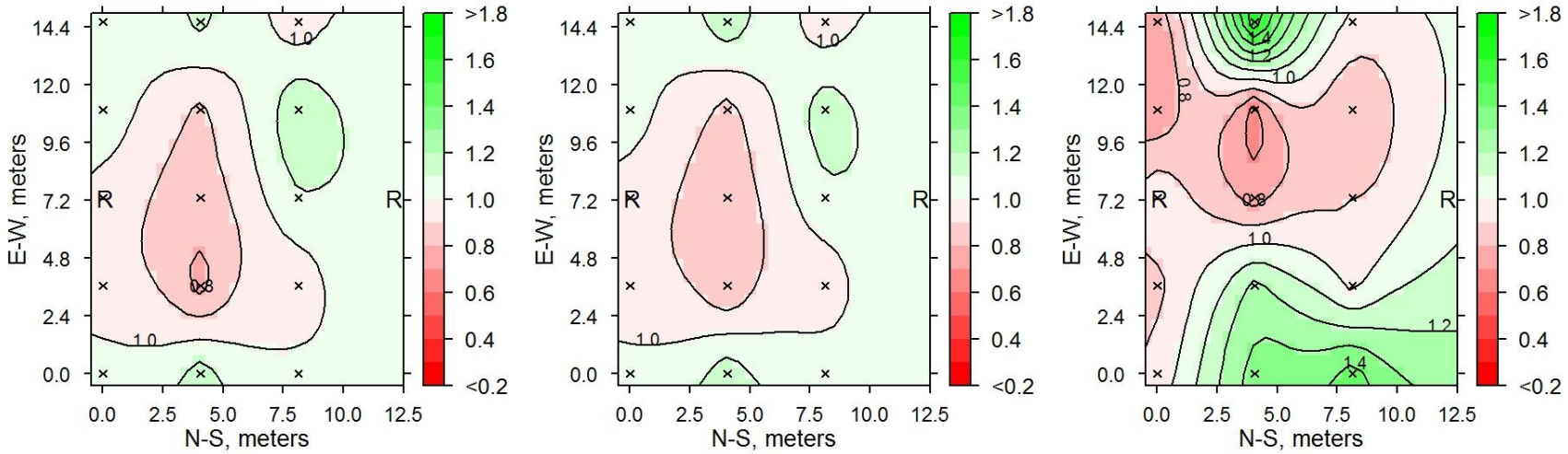

Figures D.6a-c 22 July section G6 masses (left to right) pre and post irrigation and net water gain.

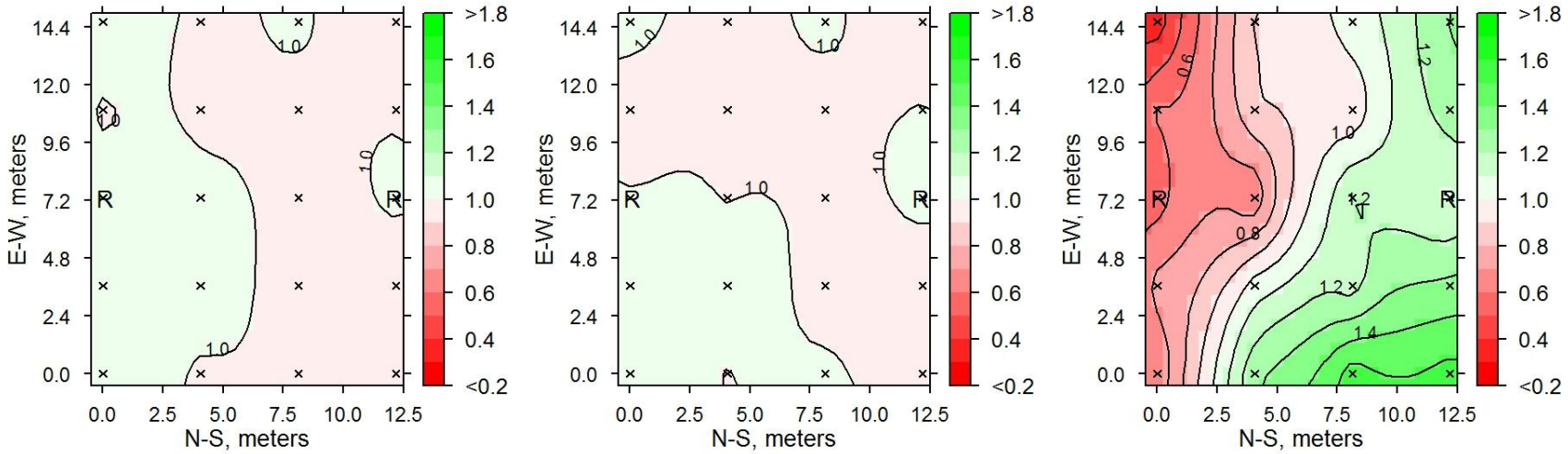

Figures D.7a-c 22 July section G9N masses (left to right) pre and post irrigation and net water gain.

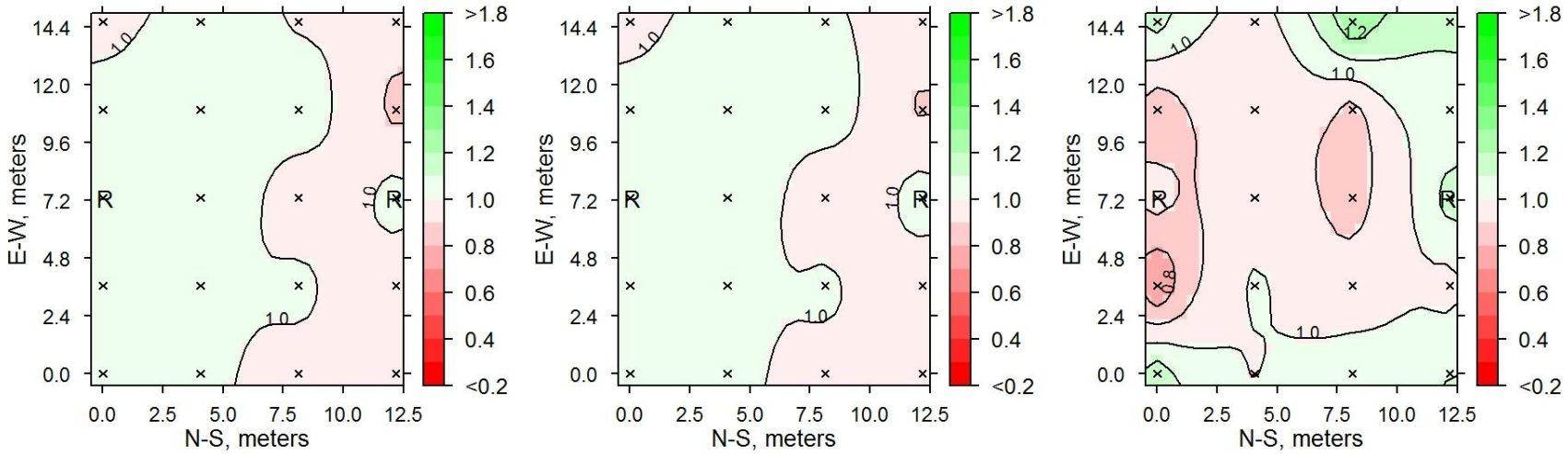

Figures D.8a-c 22 July section G9S masses (left to right) pre and post irrigation and net water gain.

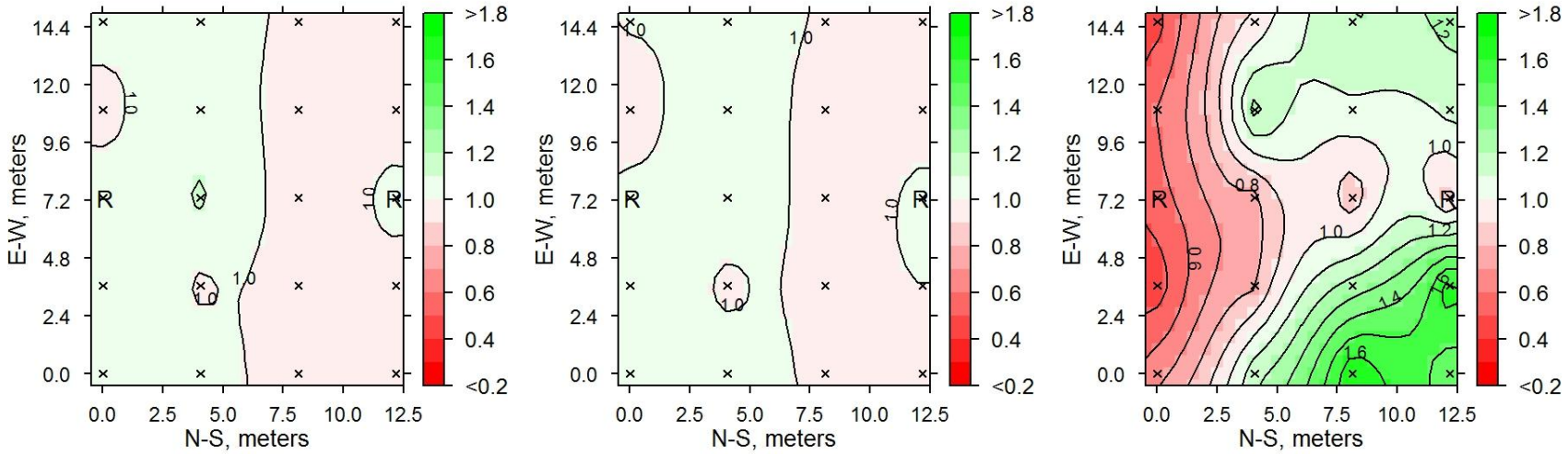

Figures D.9a-c 22 July section G11N masses (left to right) pre and post irrigation and net water gain.

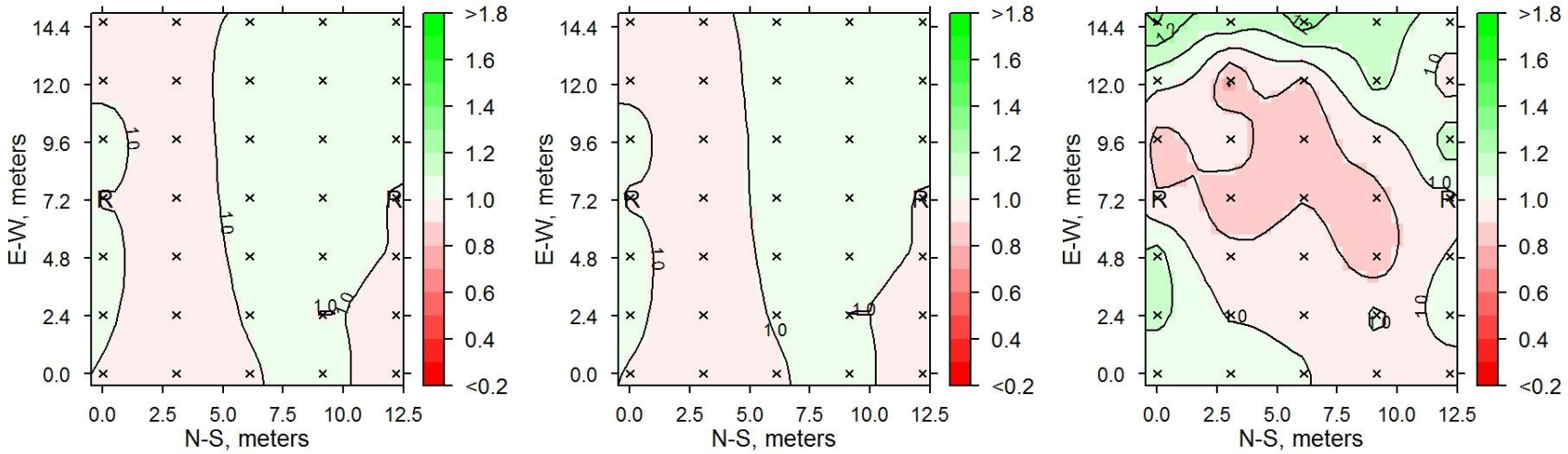

Figures D.10a-c 22 July section G11S masses (left to right) pre and post irrigation and net water gain.

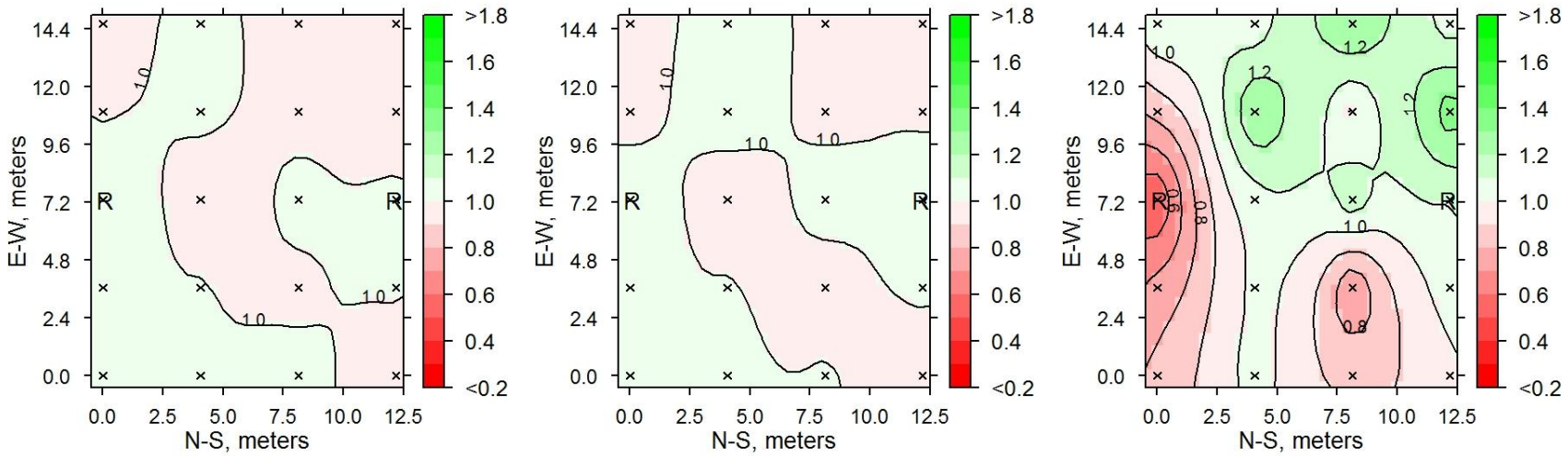

Figures D.11a-c 22 July section G16 masses (left to right) pre and post irrigation and net water gain.

D.2 05 August

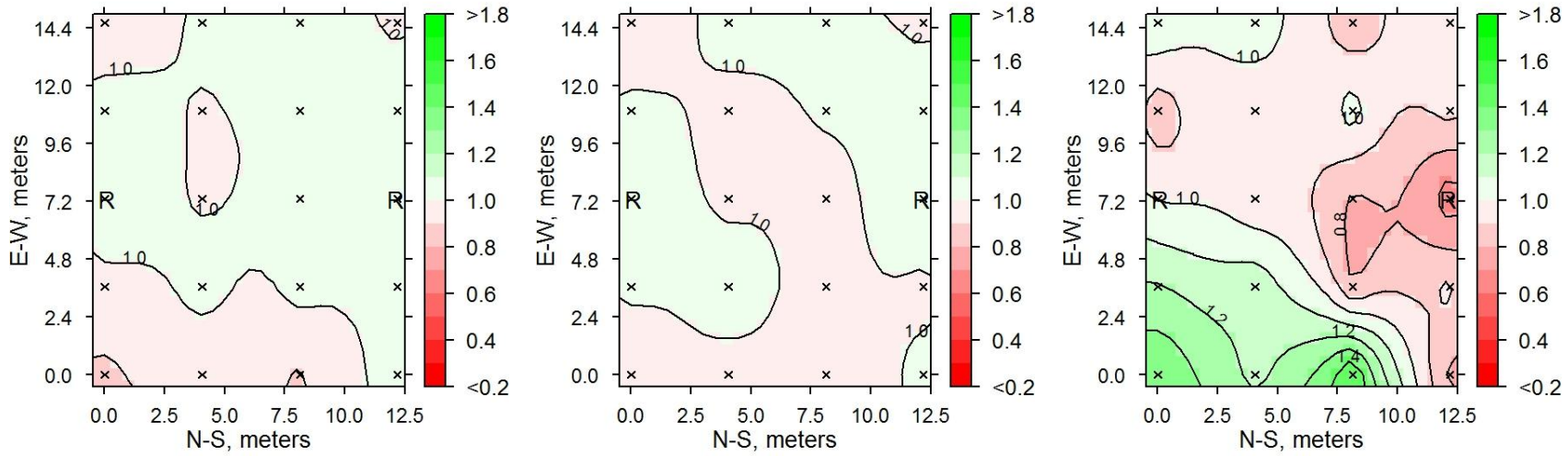

Figures D.12a-c 05 August section D5N masses (left to right) pre and post irrigation and net water gain.

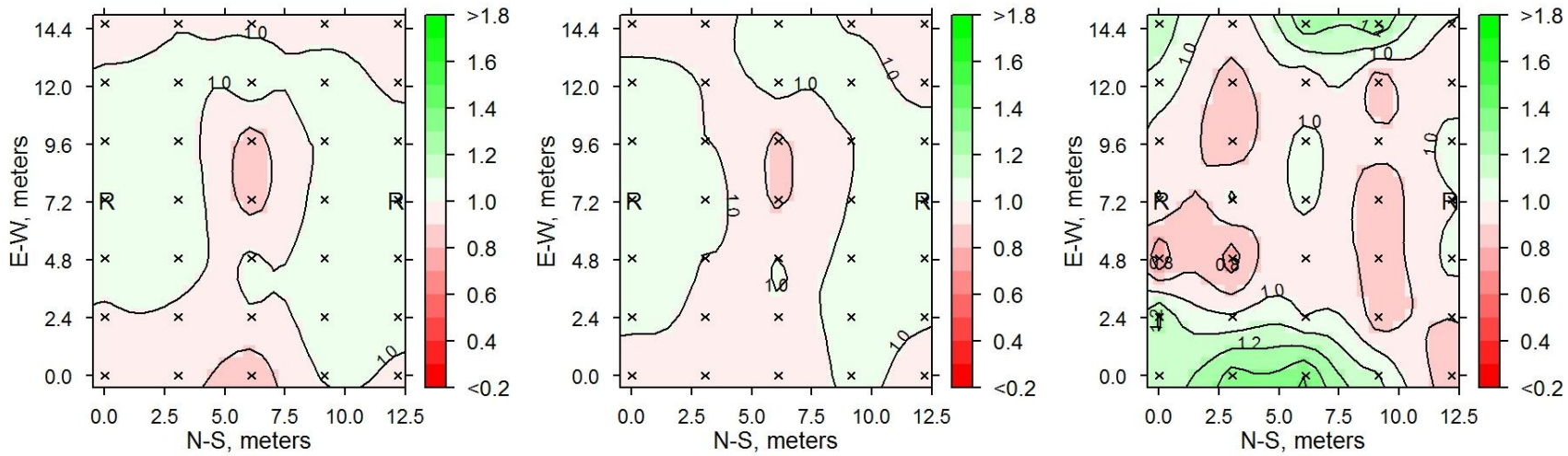

Figures D.13a-c 05 August section D5S masses (left to right) pre and post irrigation and net water gain.

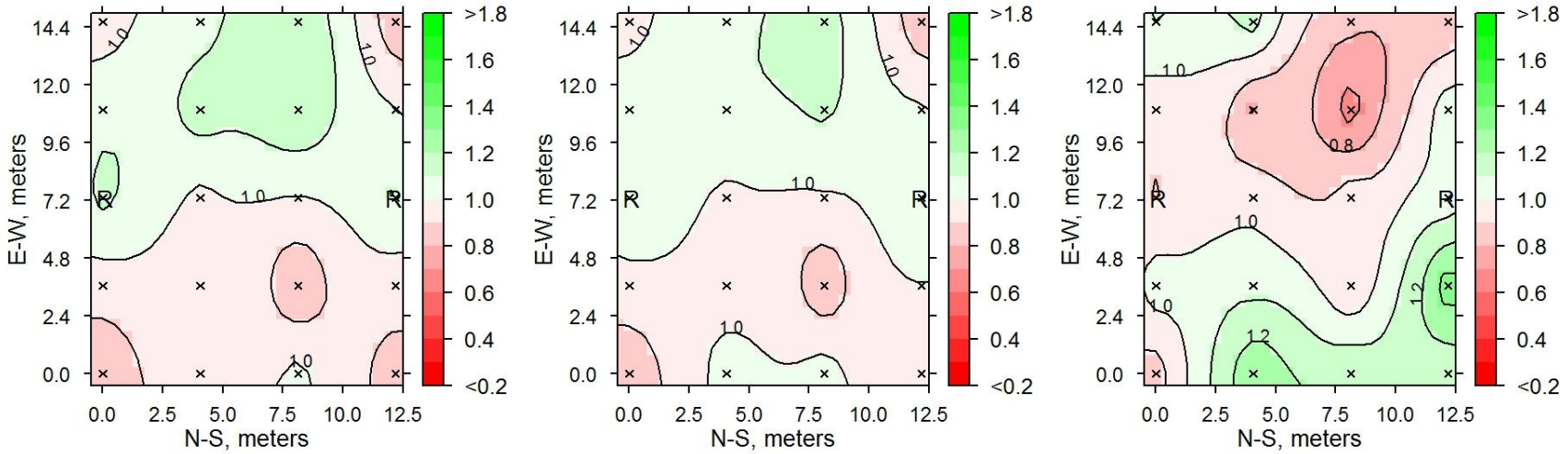

Figures D.14a-c 05 August section D6 masses (left to right) pre and post irrigation and net water gain.

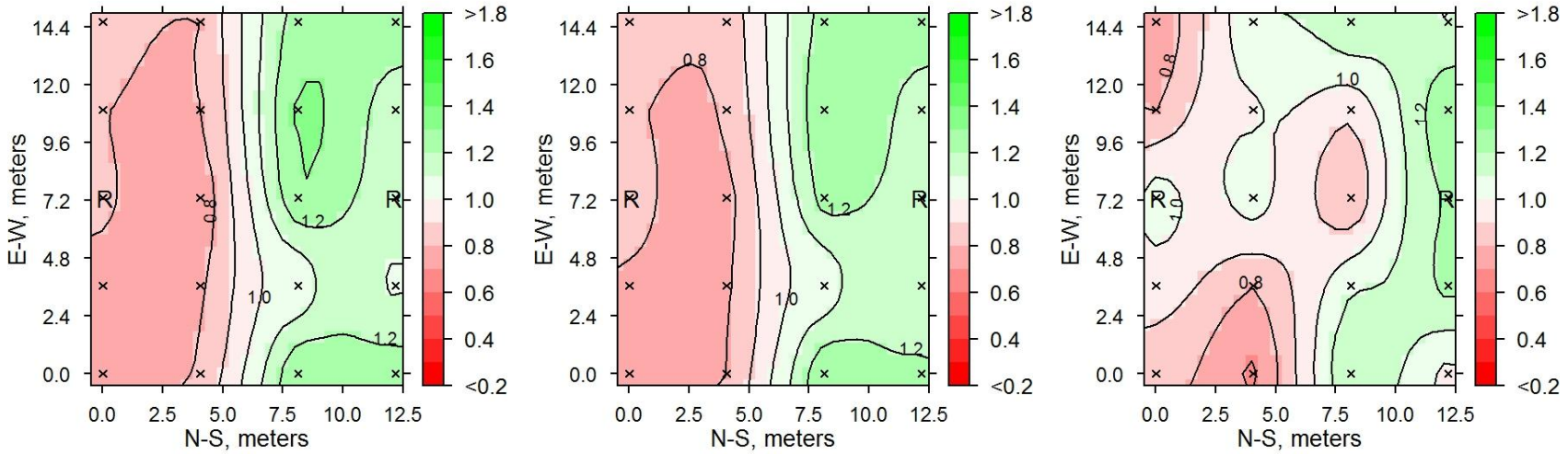

Figures D.15a-c 05 August section D7N masses (left to right) pre and post irrigation and net water gain.

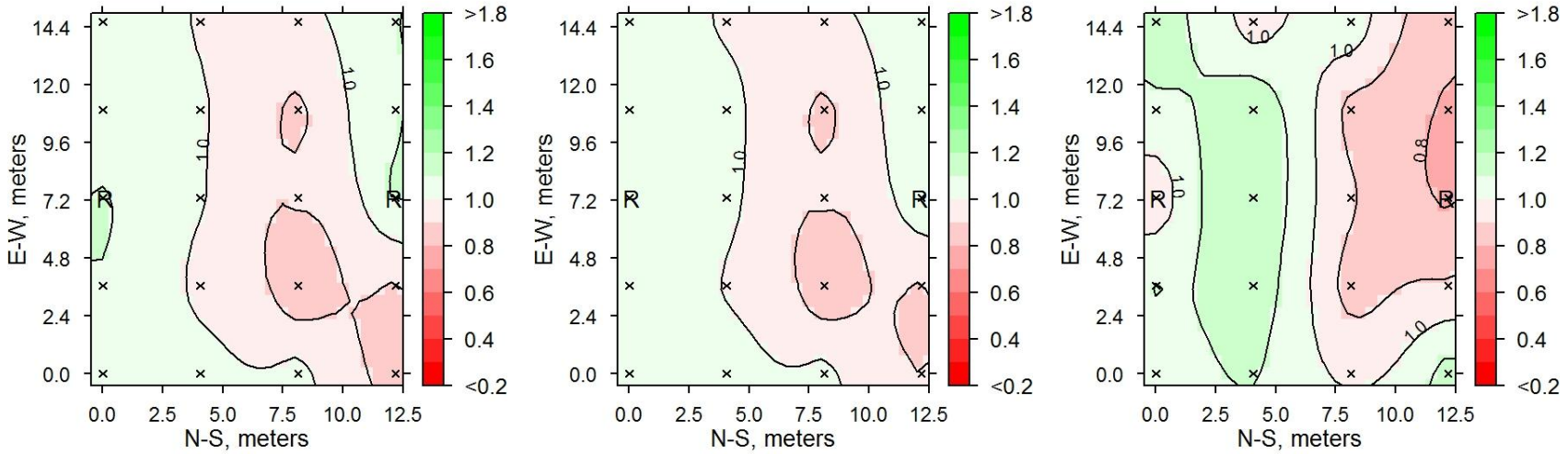

Figures D.16a-c 05 August section D7S masses (left to right) pre and post irrigation and net water gain.

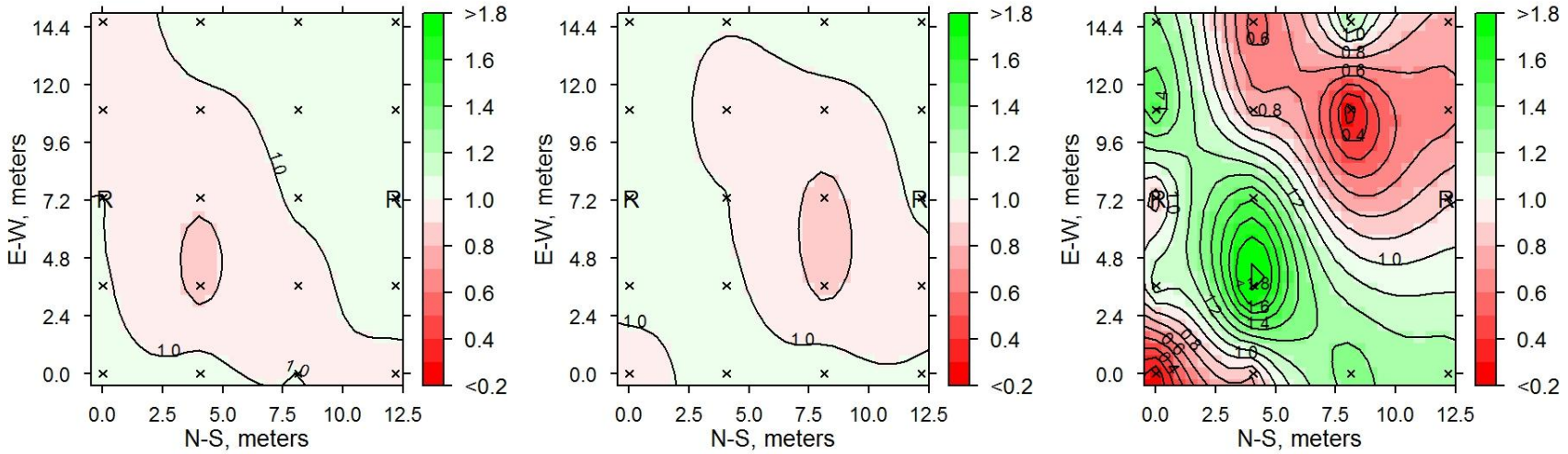

Figures D.17a-c 05 August section G6 masses (left to right) pre and post irrigation and net water gain.

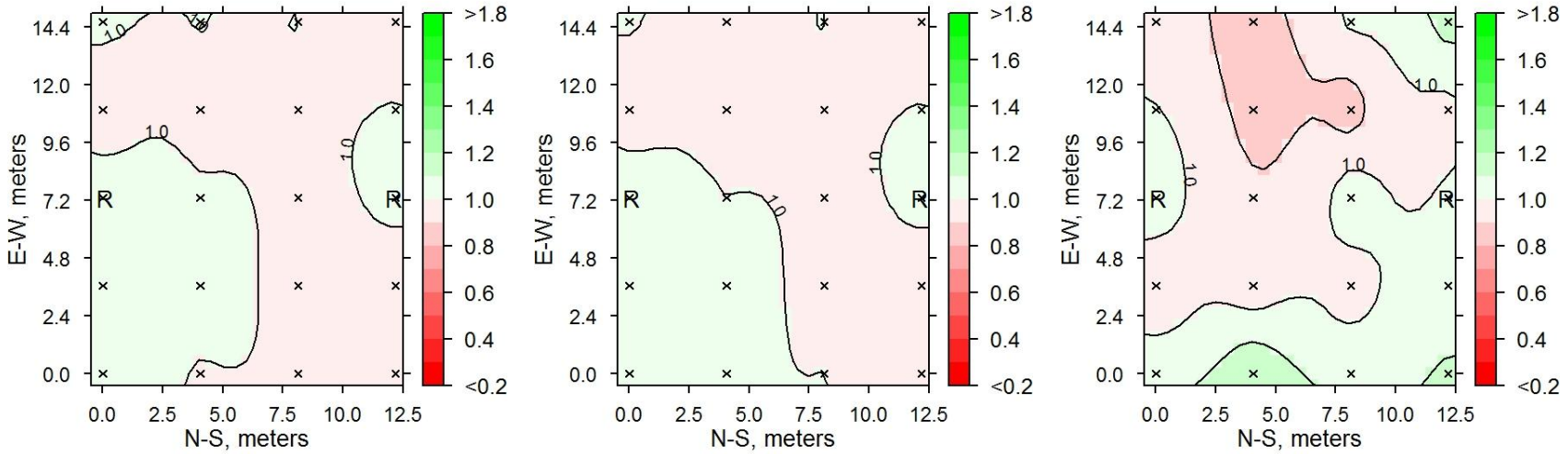

Figures D.18a-c 05 August section G9N masses (left to right) pre and post irrigation and net water gain.

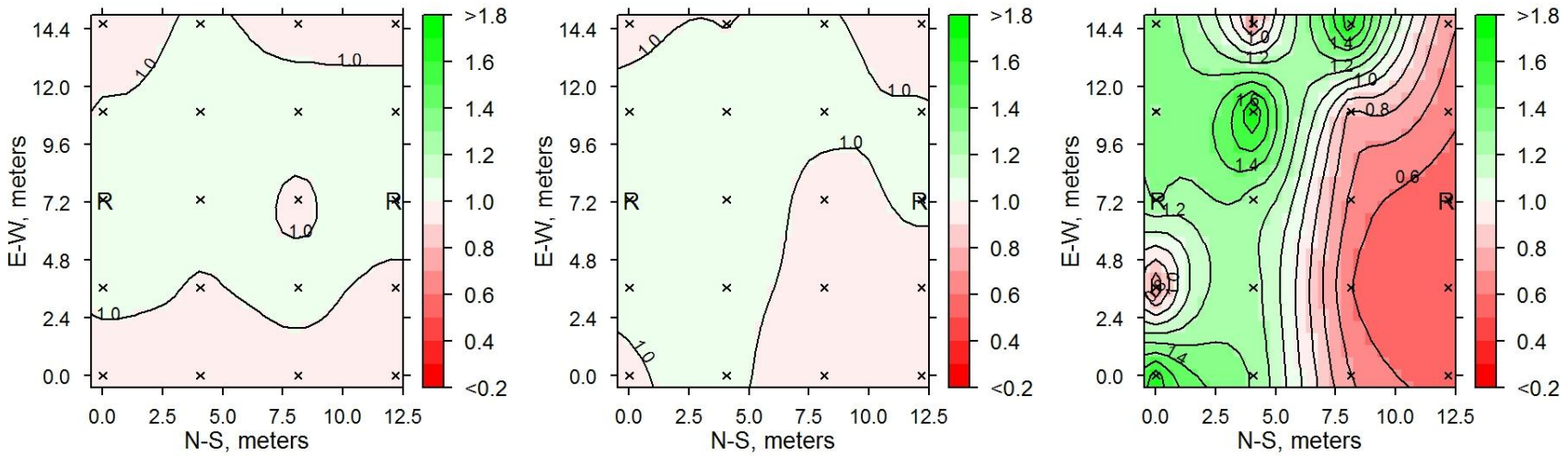

Figures D.19a-c 05 August section G9S masses (left to right) pre and post irrigation and net water gain.

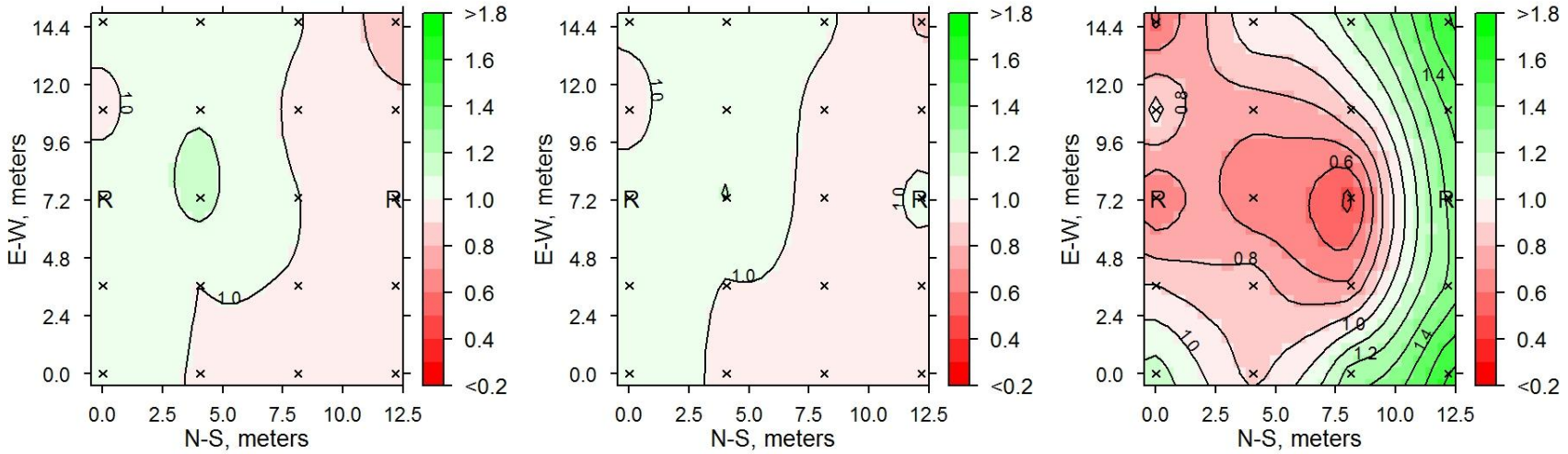

Figures D.20a-c 05 August section G11N masses (left to right) pre and post irrigation and net water gain.

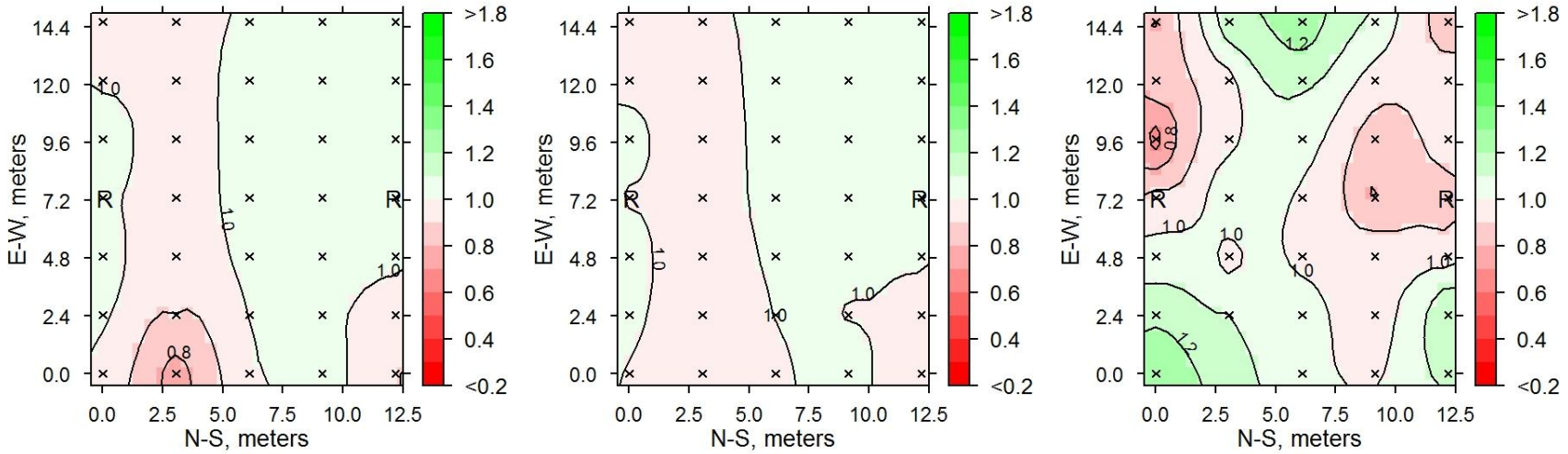

Figures D.21a-c 05 August section G11S masses (left to right) pre and post irrigation and net water gain.

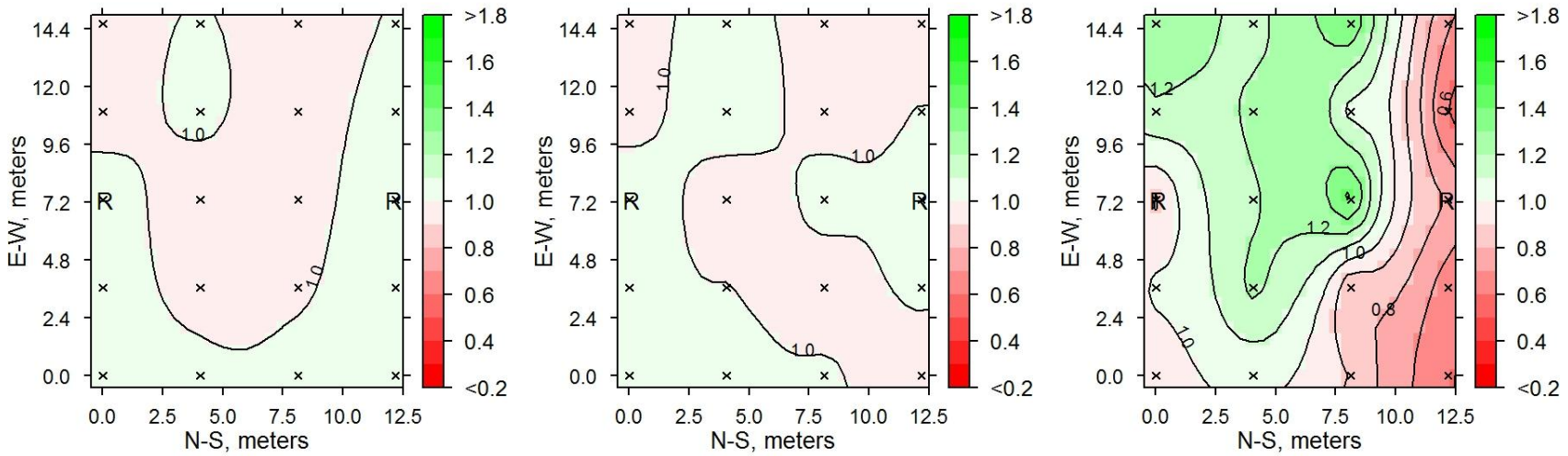

Figures D.22a-c 05 August section G16 masses (left to right) pre and post irrigation and net water gain.

D.3 19 August

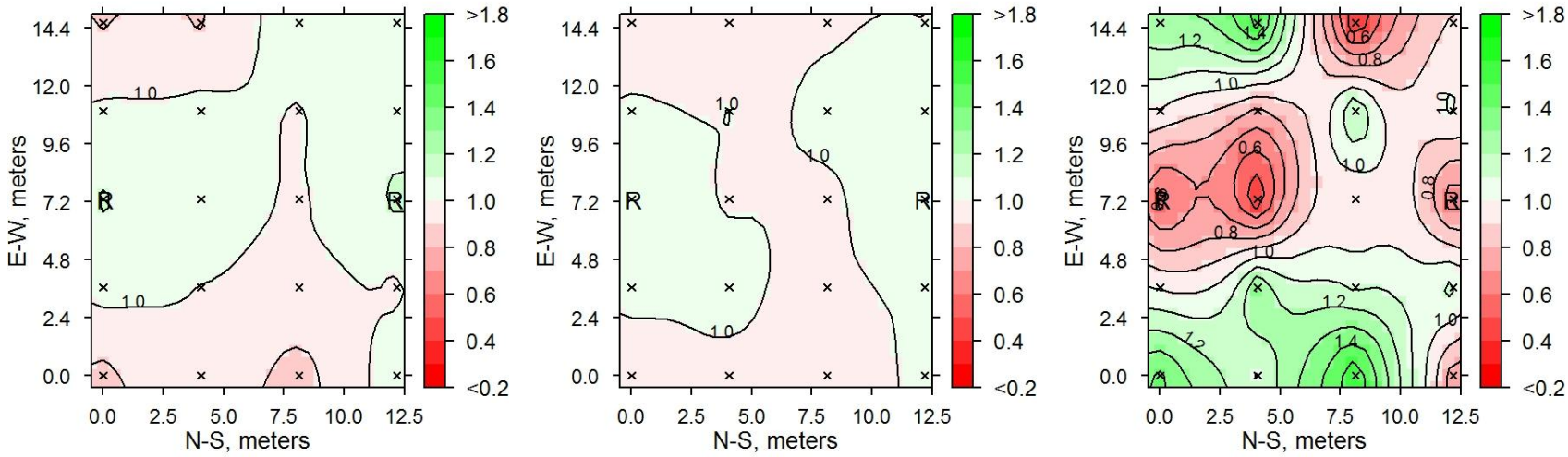

Figures D.23a-c 19 August section D5N masses (left to right) pre and post irrigation and net water gain.

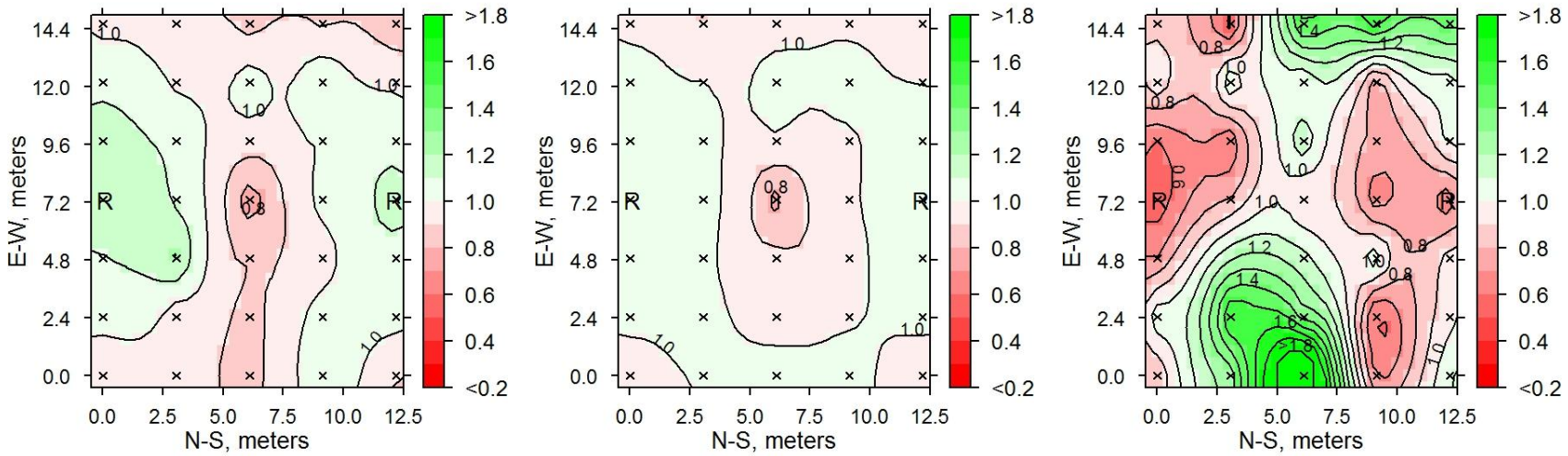

Figures D.24a-c 19 August section D5S masses (left to right) pre and post irrigation and net water gain.

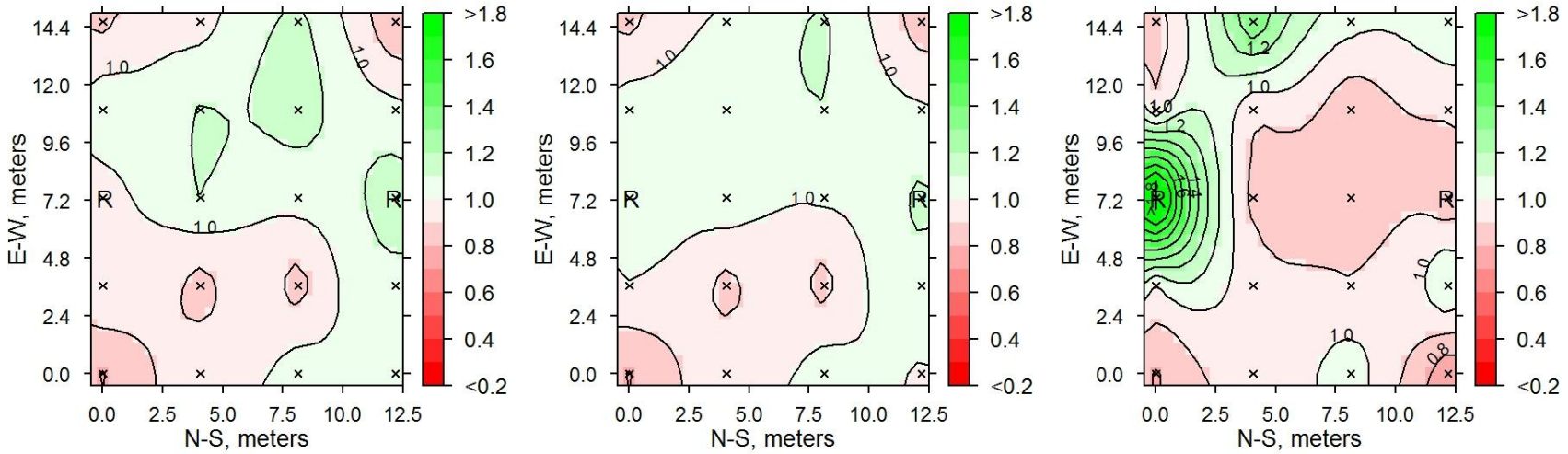

Figures D.25a-c 19 August section D6 masses (left to right) pre and post irrigation and net water gain.

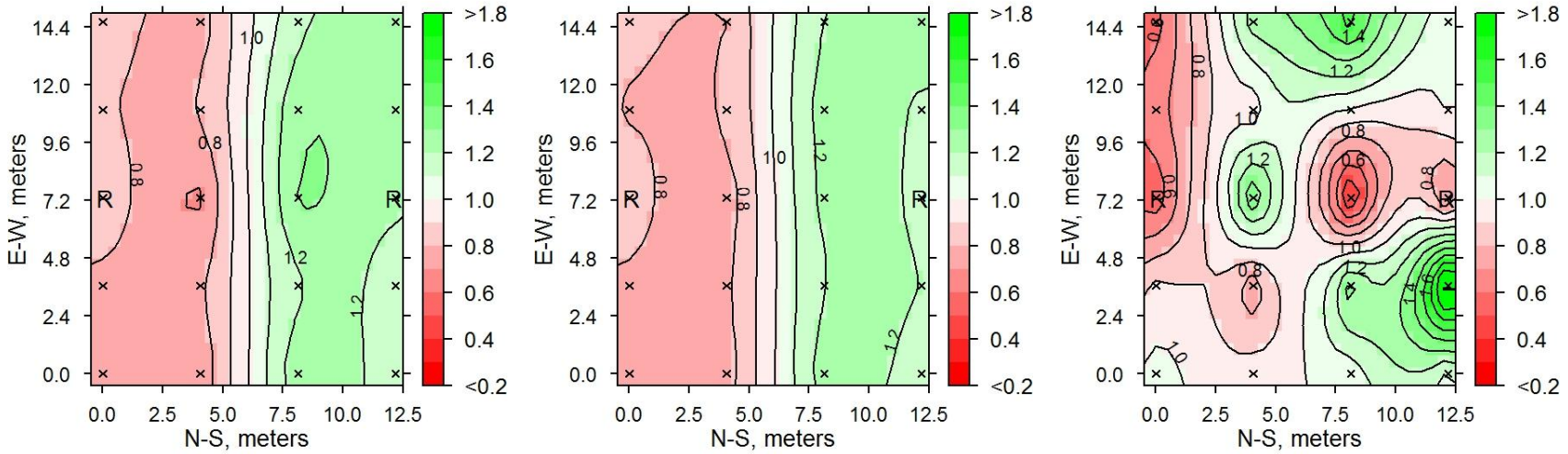

Figures D.26a-c 19 August section D7N masses (left to right) pre and post irrigation and net water gain.

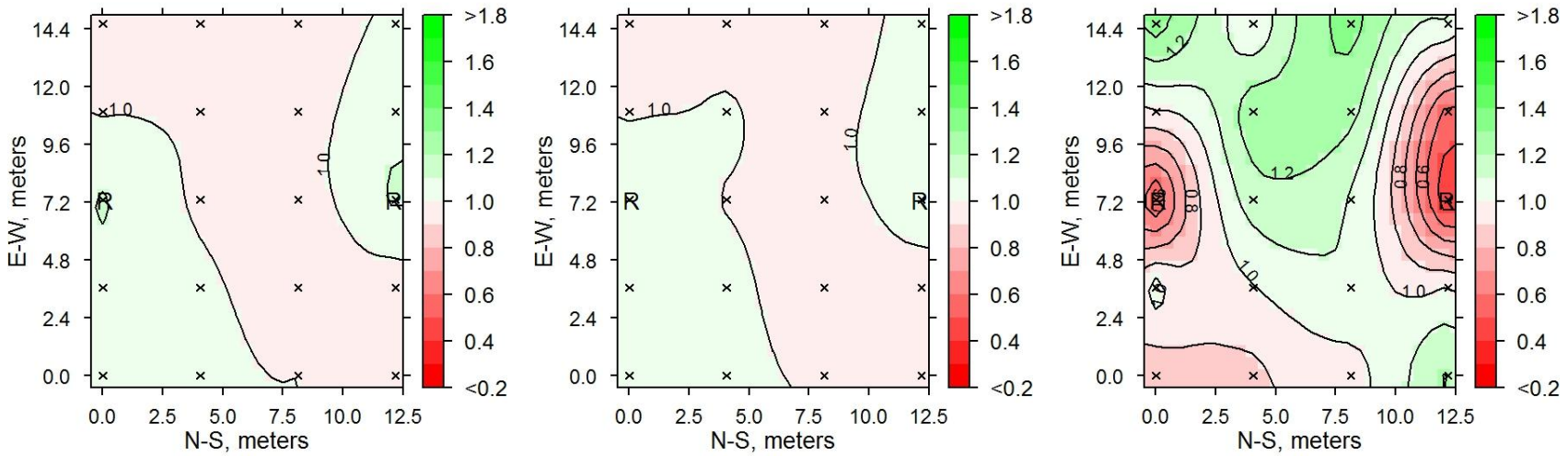

Figures D.27a-c 19 August section D7S masses (left to right) pre and post irrigation and net water gain.

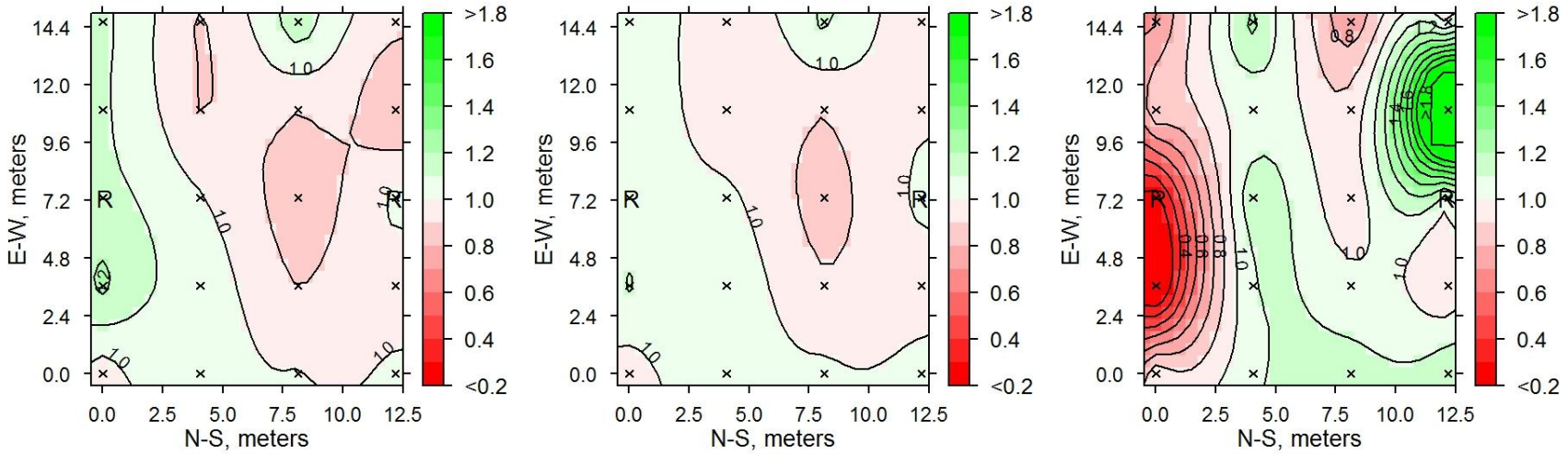

Figures D.28a-c 19 August section G6 masses (left to right) pre and post irrigation and net water gain.

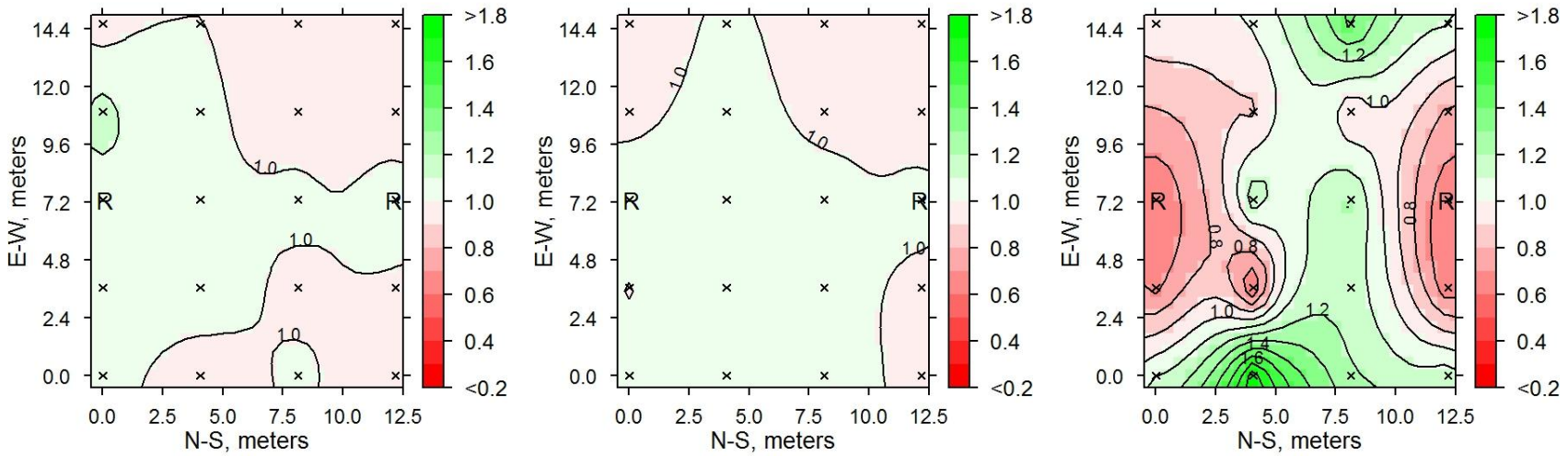

Figures D.29a-c 19 August section G9N masses (left to right) pre and post irrigation and net water gain.

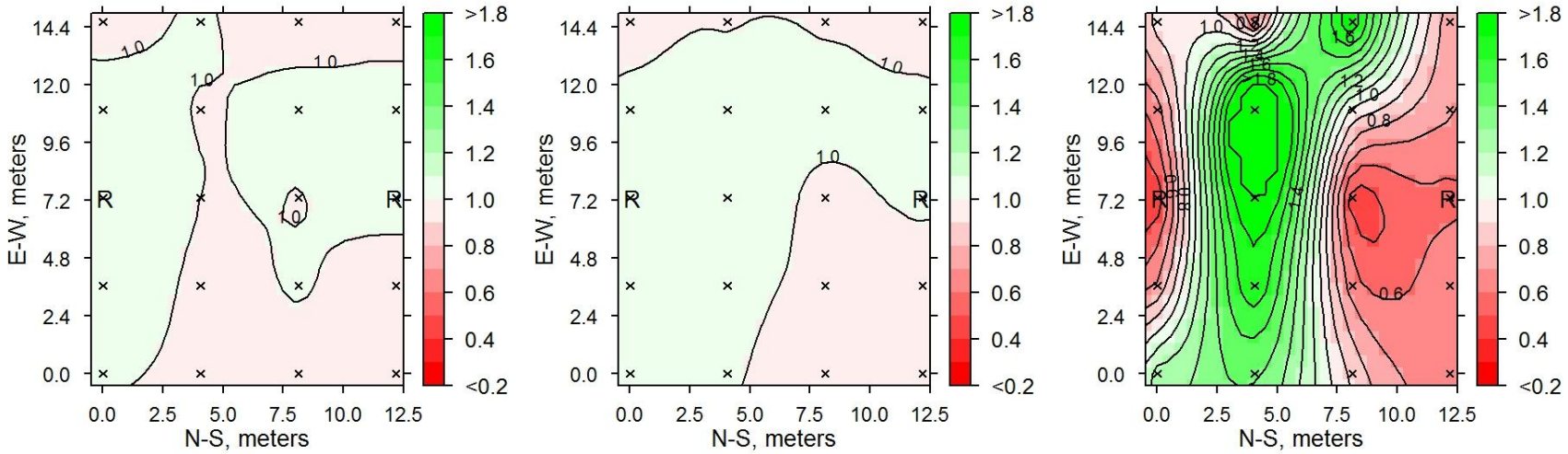

Figures D.30a-c 19 August section G9S masses (left to right) pre and post irrigation and net water gain.

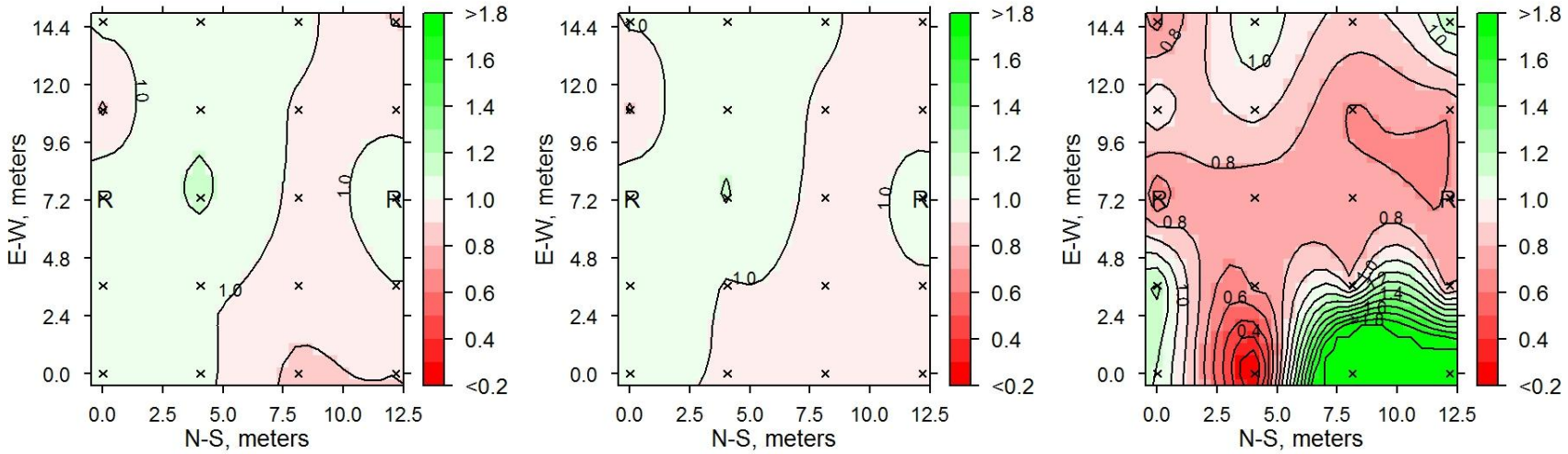

Figures D.31a-c 19 August section G11N masses (left to right) pre and post irrigation and net water gain.

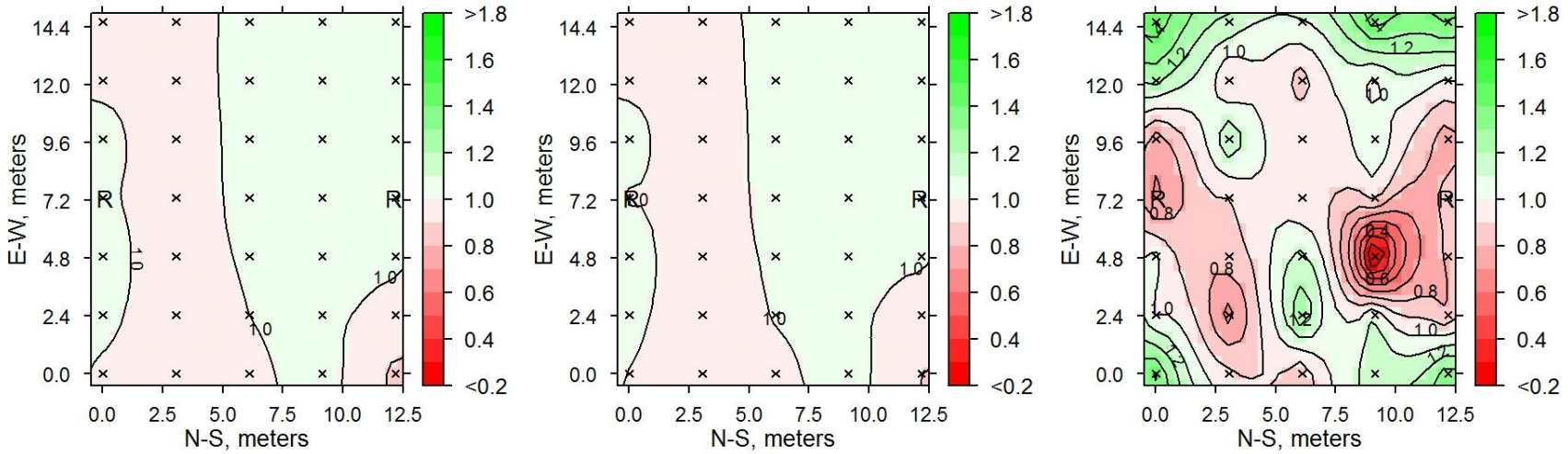

Figures D.32a-c 19 August section G11S masses (left to right) pre and post irrigation and net water gain.

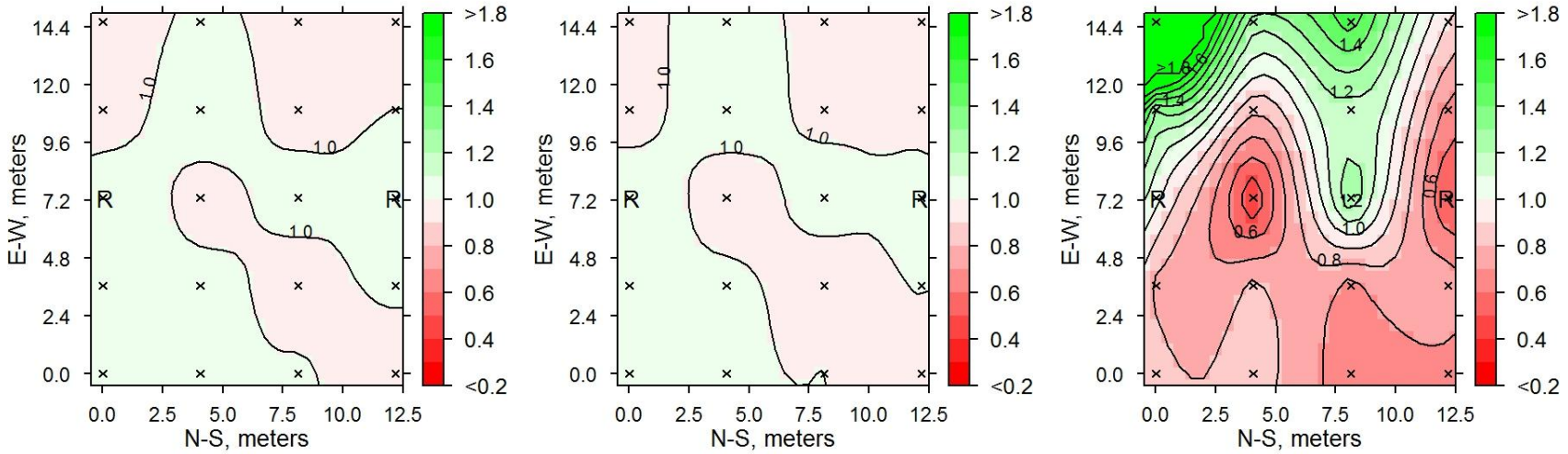

Figures D.33a-c 19 August section G16 masses (left to right) pre and post irrigation and net water gain.

D.4 02 September

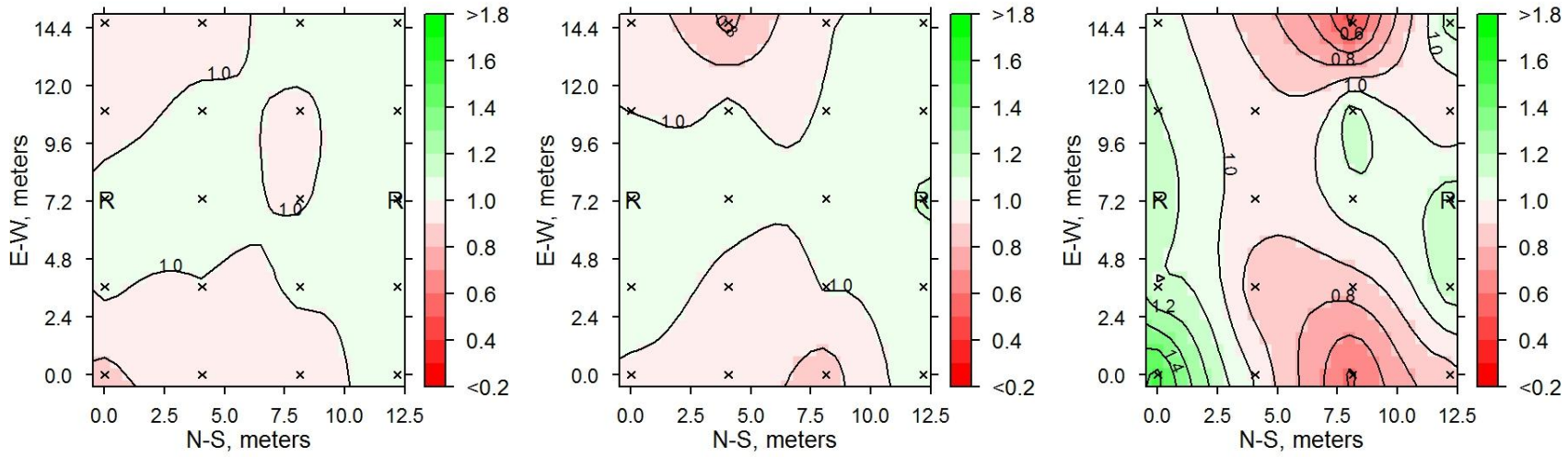

Figures D.34a-c 02 September section D5N masses (left to right) pre and post irrigation and net water gain.

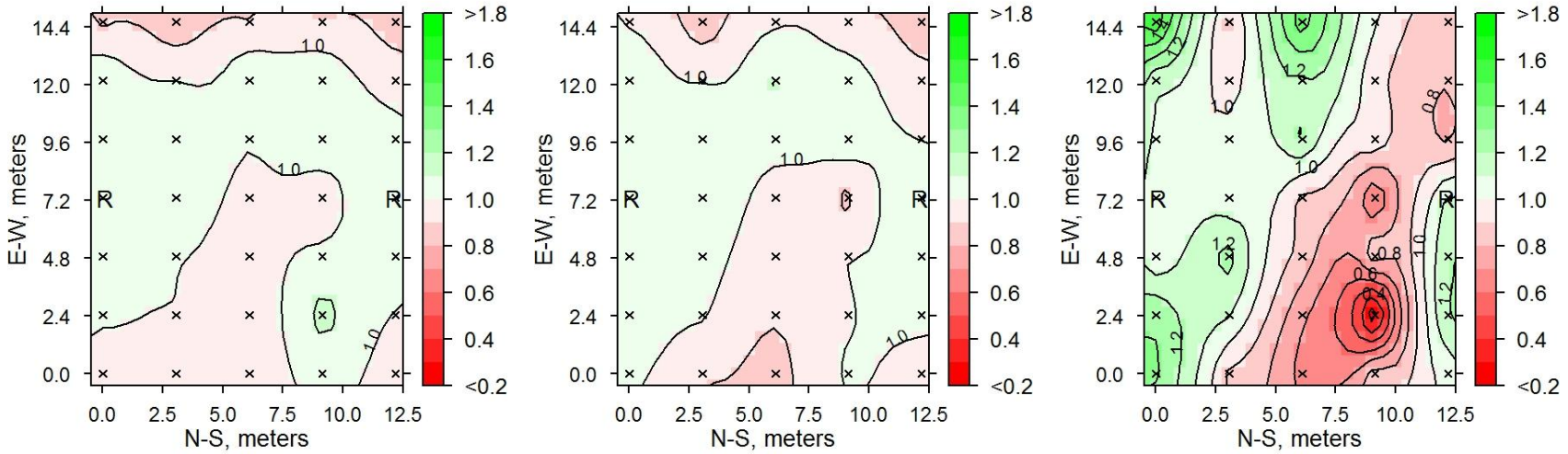

Figures D.35a-c 02 September section D5S masses (left to right) pre and post irrigation and net water gain.

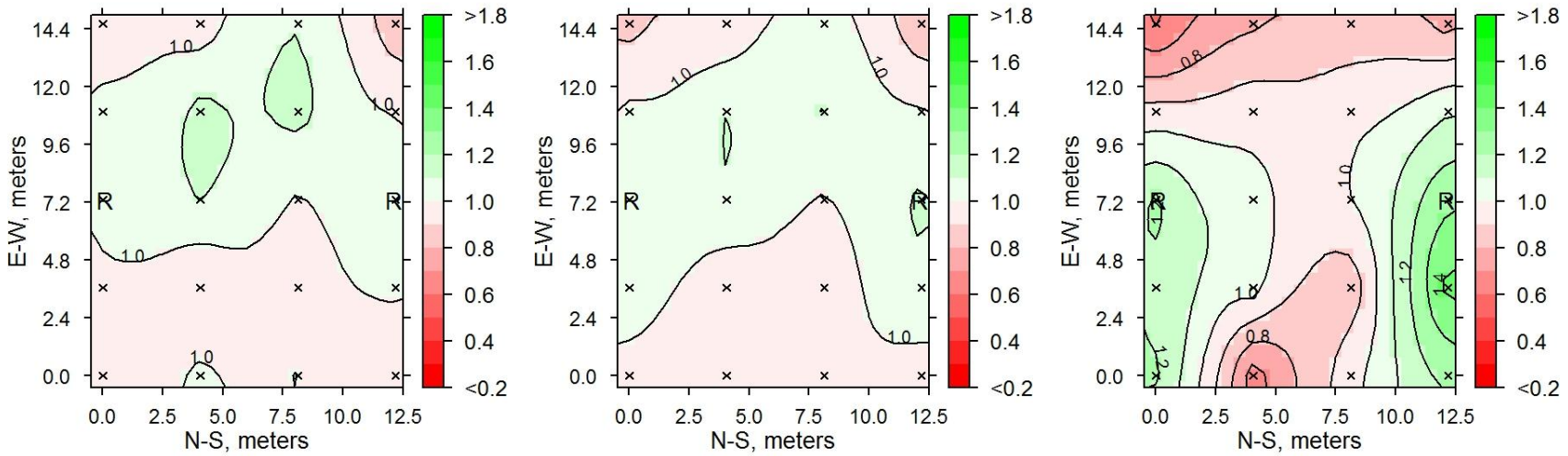

Figures D.36a-c 02 September section D6 masses (left to right) pre and post irrigation and net water gain.

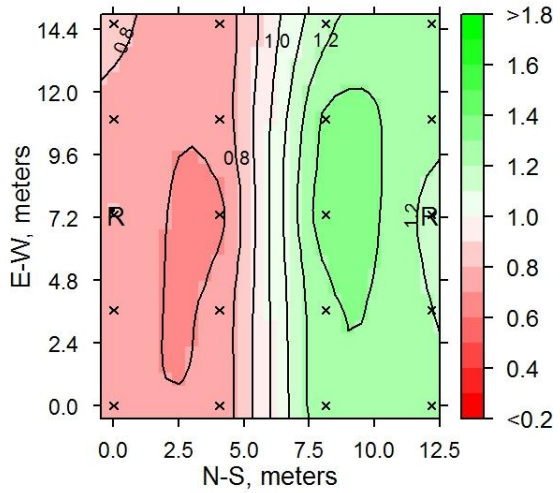

Figures D.37 02 September section D7N masses pre-irrigation. Due to a field error, post-irrigation and net gain measurements are not available.

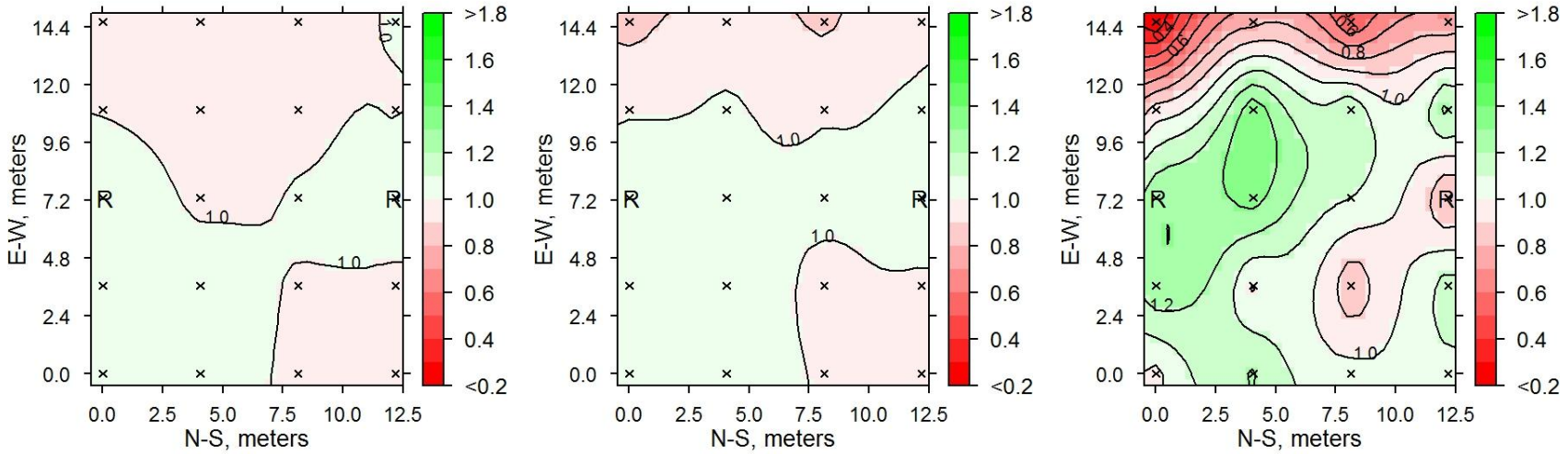

Figures D.38a-c 02 September section D7S masses (left to right) pre and post irrigation and net water gain.

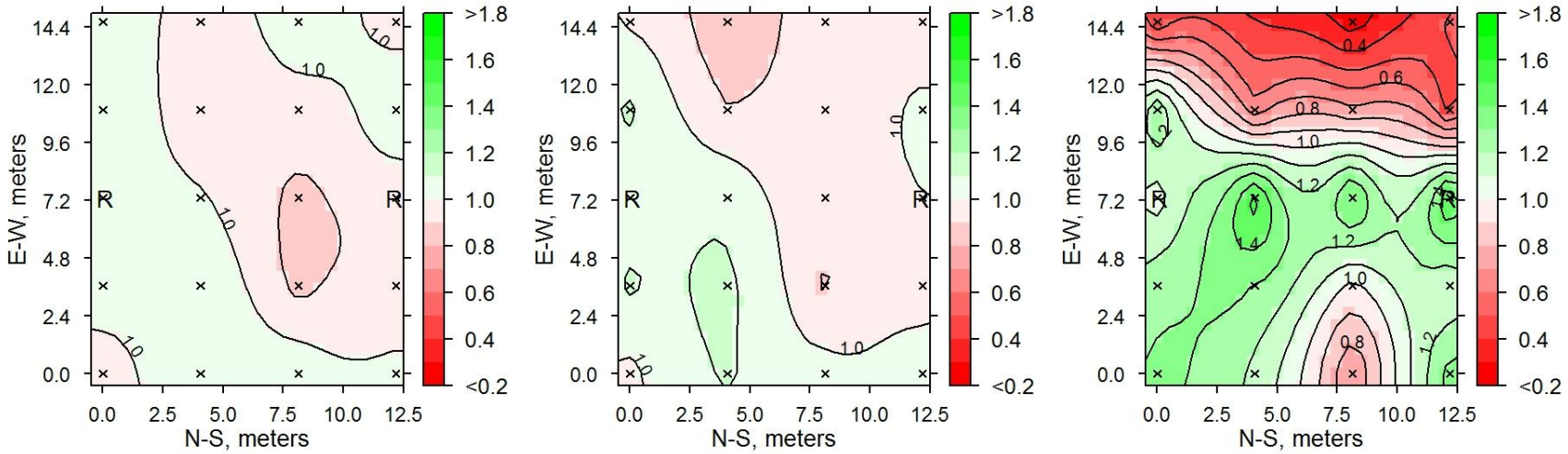

Figures D.39a-c 02 September section G6 masses (left to right) pre and post irrigation and net water gain.

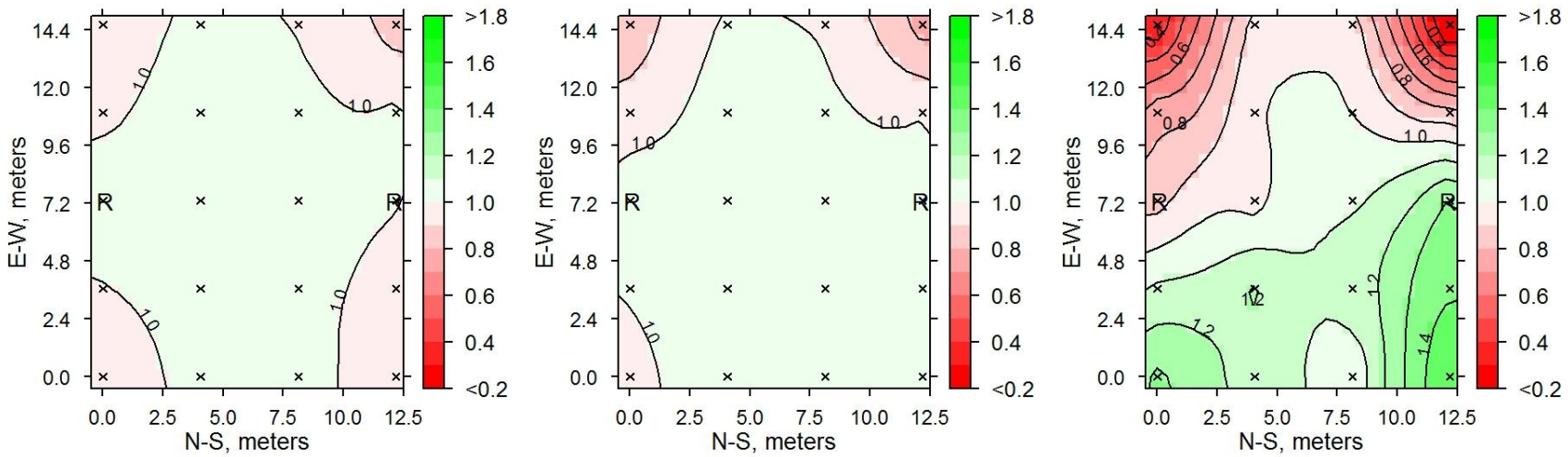

Figures D.40a-c 02 September section G9N masses (left to right) pre and post irrigation and net water gain.

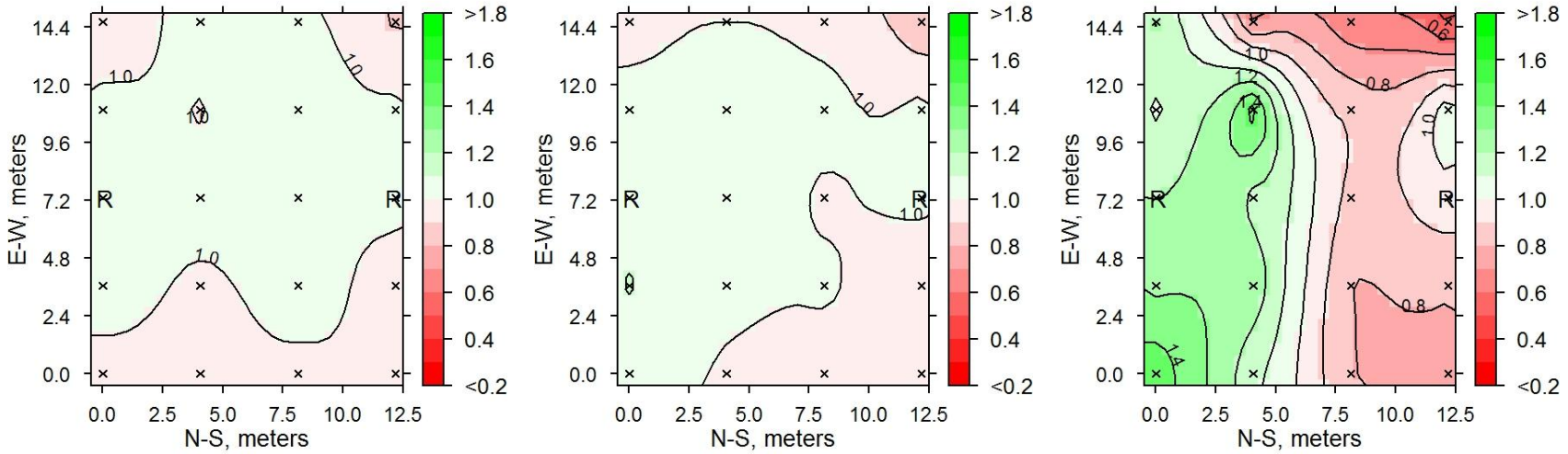

Figures D.41a-c 02 September section G9S masses (left to right) pre and post irrigation and net water gain.

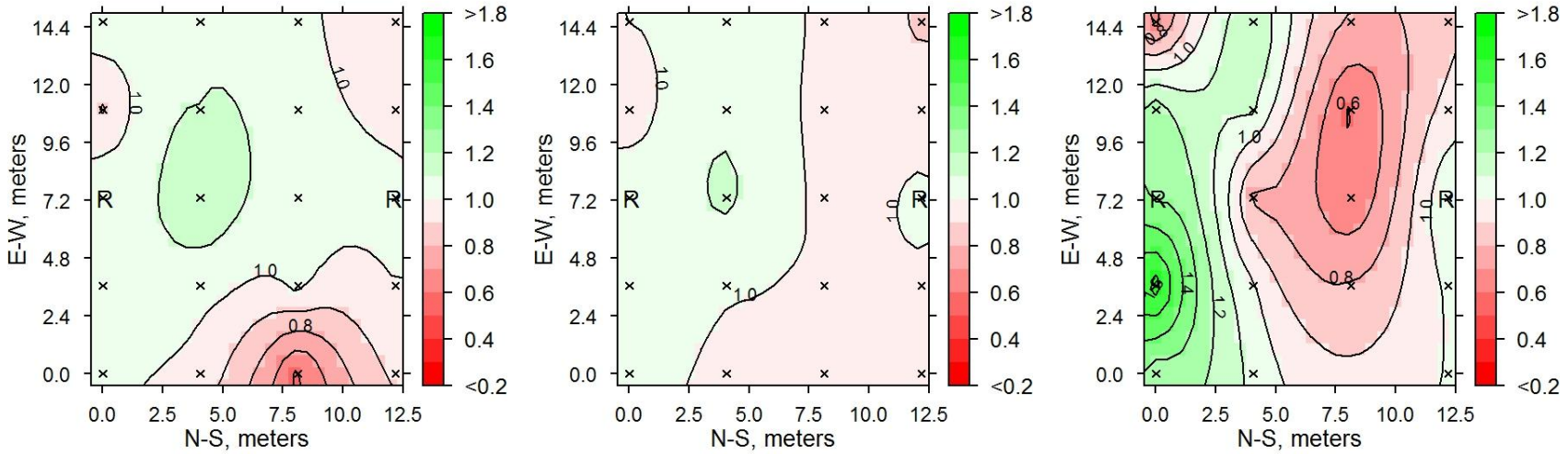

Figures D.42a-c 02 September section G11N masses (left to right) pre and post irrigation and net water gain.

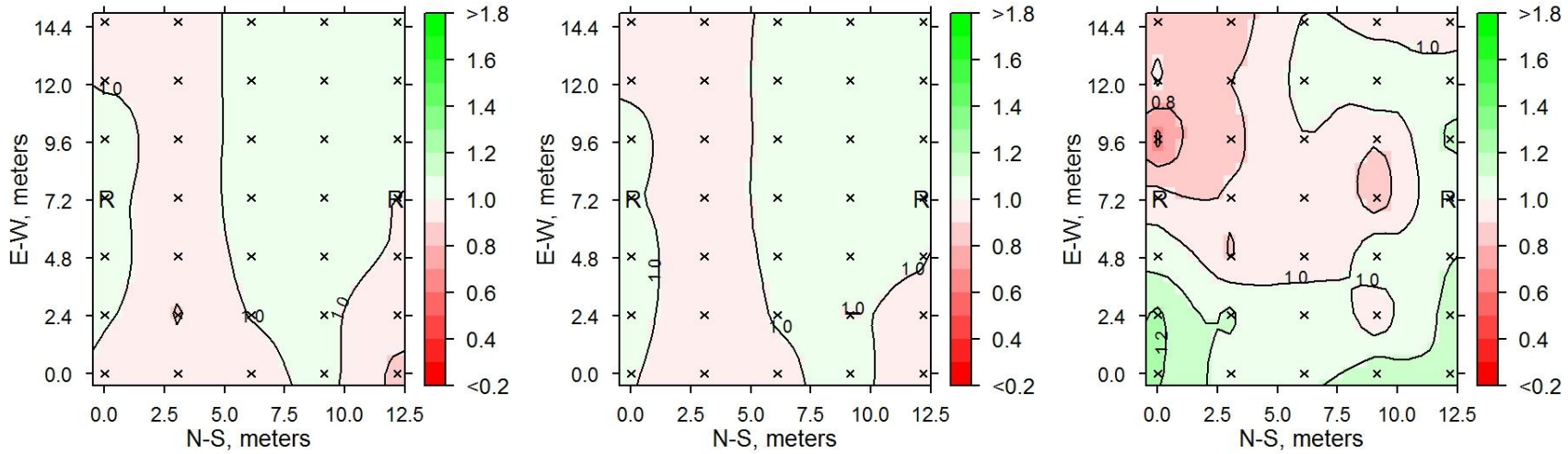

Figures D.43a-c 02 September section G11S masses (left to right) pre and post irrigation and net water gain.

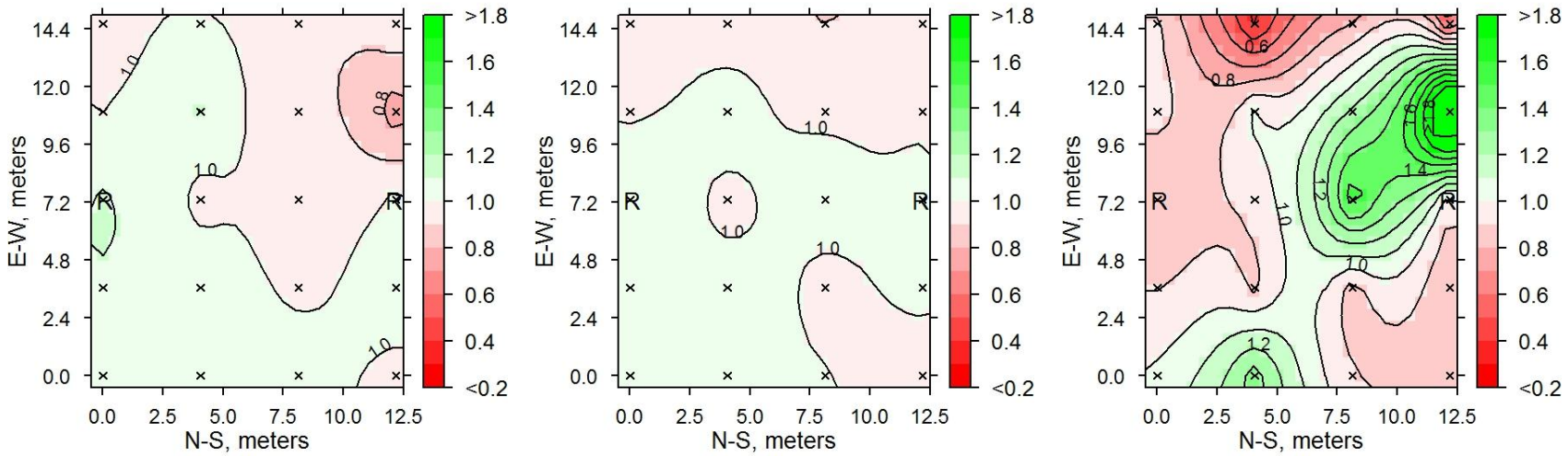

Figures D.44a-c 02 September section G16 masses (left to right) pre and post irrigation and net water gain.

Appendix E

Leaching Fraction Data

Table E.1 Sections used to collect leaching fraction data and summary of data collected.

Date	Section	Plant species	Irrigation duration (minutes)	# monitored buckets	# buckets leaching	Mean in empty bucket (ml)	Mean leachate (Min-Max) (ml)	Mean leaching fraction (Min-Max)
22 July	D5S	*P.J.M.*	122	12	9	444	123 (0-500)	0.27 (0-1.4)
05 Aug	G9S	*Potentilla*	122	18	16	545	214 (0-600)	0.39 (0-0.95)
19 Aug	G16	*Physo.*	120	19	19	476	1376 (475-2550)	3.4 (0.74-6.9)
02 Sept	G16	*Physo.*	135	20	19	495	1308 (0-4925)	2.5 (0-6.0)

In all figures, the ‘R’ is the irrigation riser. The small ‘x’ is a monitored plant.

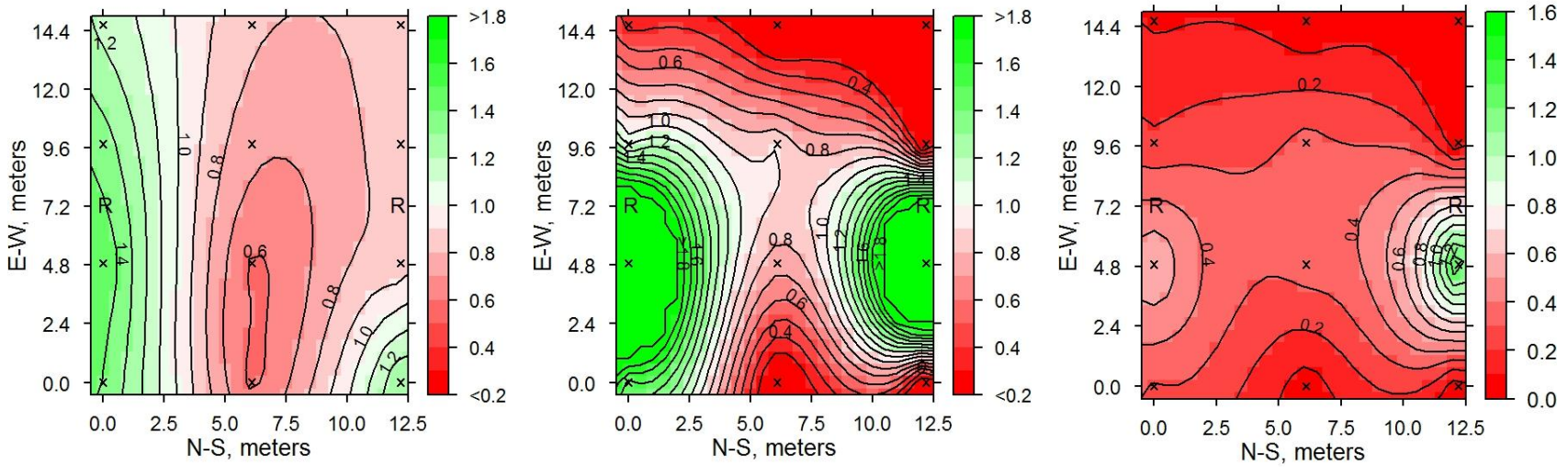

Figures E.1a-c 22 July section D5N catch-can, leachate, and leaching fraction maps (left to right).

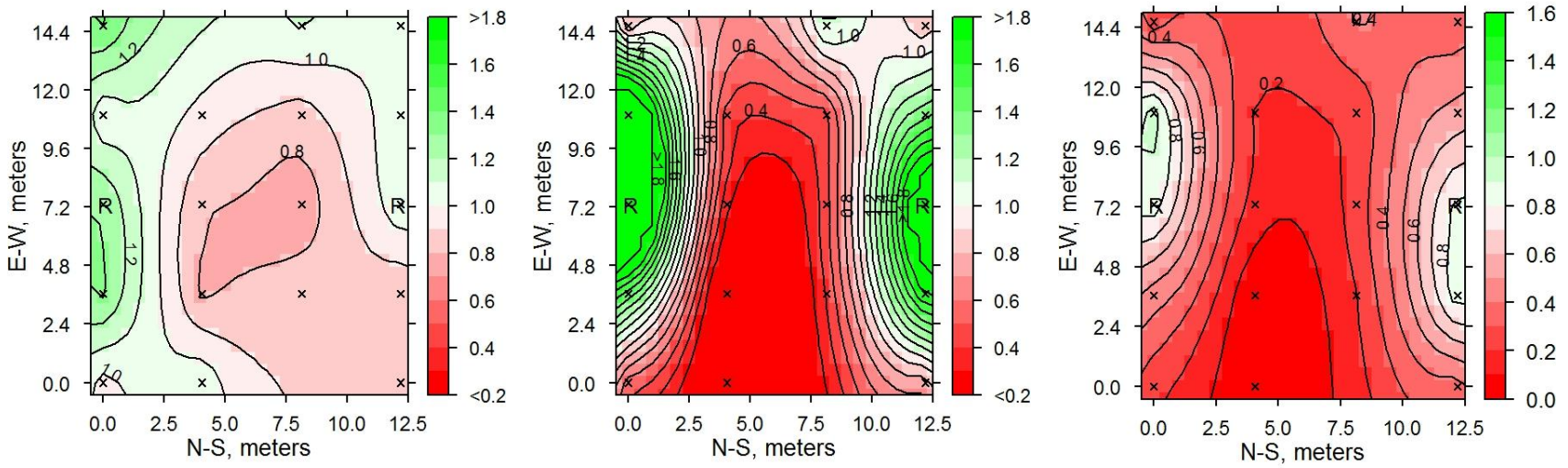

Figures E.2a-c 05 August section G9S catch-can, leachate, and leaching fraction maps (left to right).

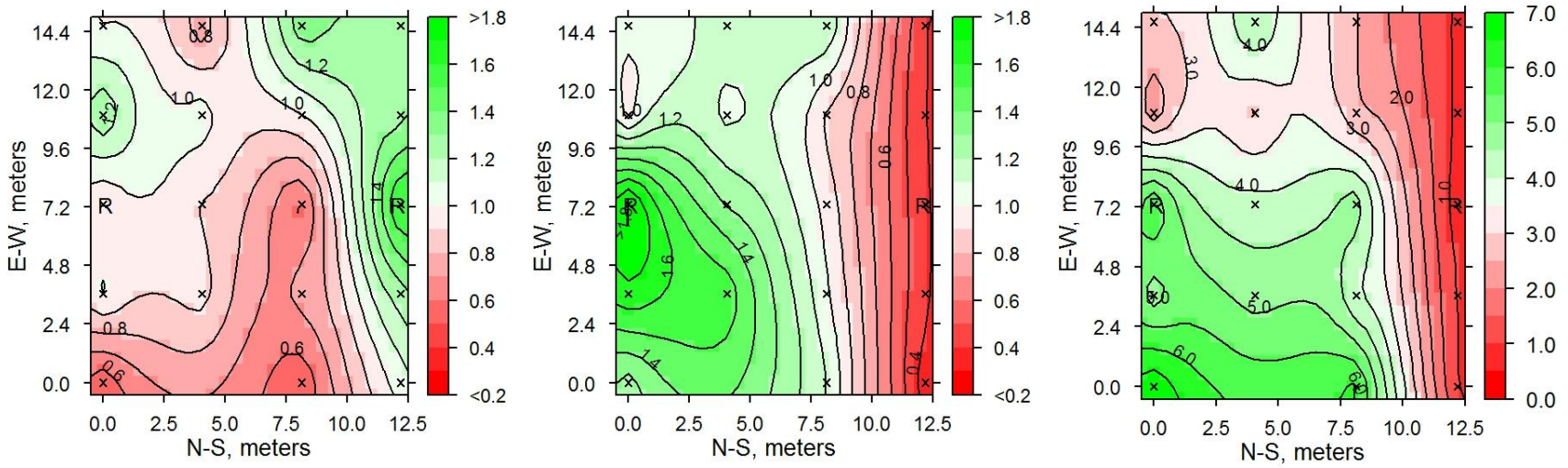

Figures E.3a-c 19 August section G16 catch-can, leachate, and leaching fraction maps (left to right).

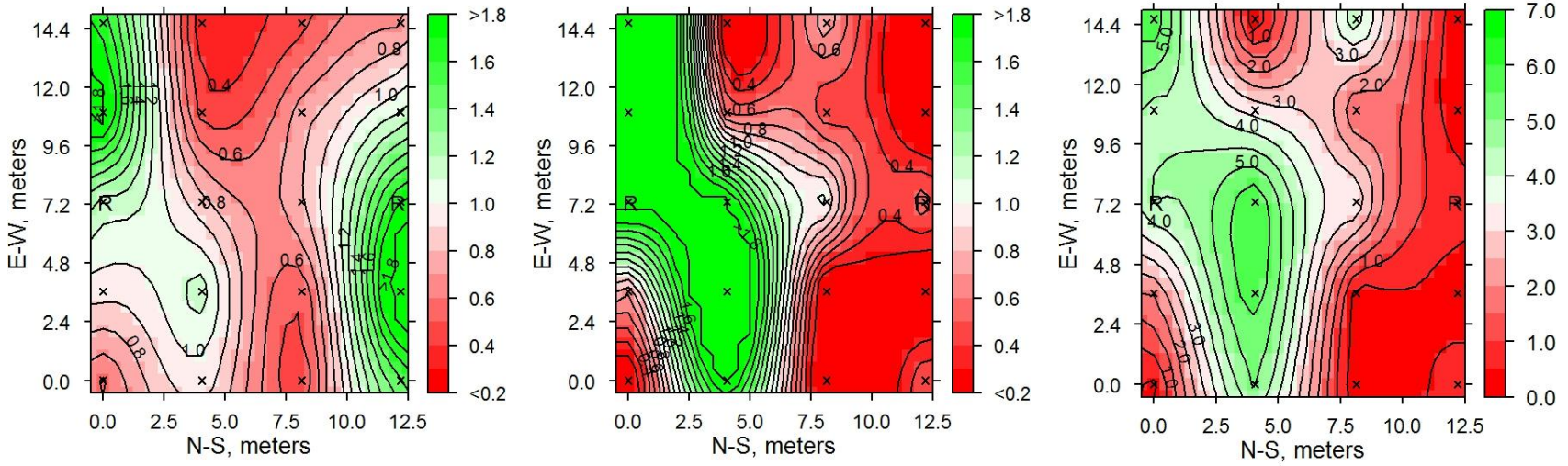

Figures E.4a-c 02 September section G16 catch-can, leachate, and leaching fraction maps (left to right).

Appendix F

Canopy Interaction Data

F.1 Irrigation Distribution

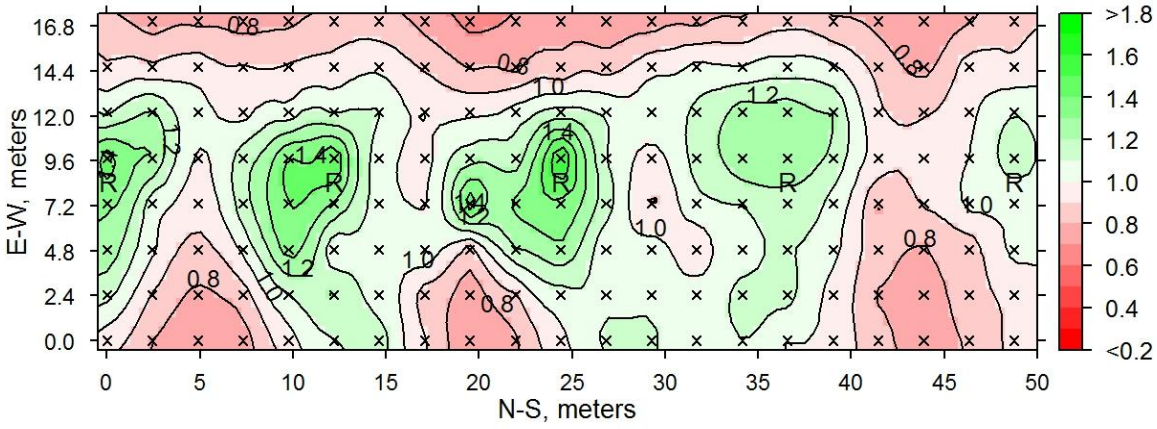

Figure F.1 Irrigation distribution normalized to the mean on 15 September in row F9. 'R' is an irrigation riser; 'x' is a catch-can.

On 15 September, a small rain event occurred during the data collection period bringing into question the accuracy of the data. Therefore the experiment was repeated on 16 September. The data from 16 September were those analyzed.

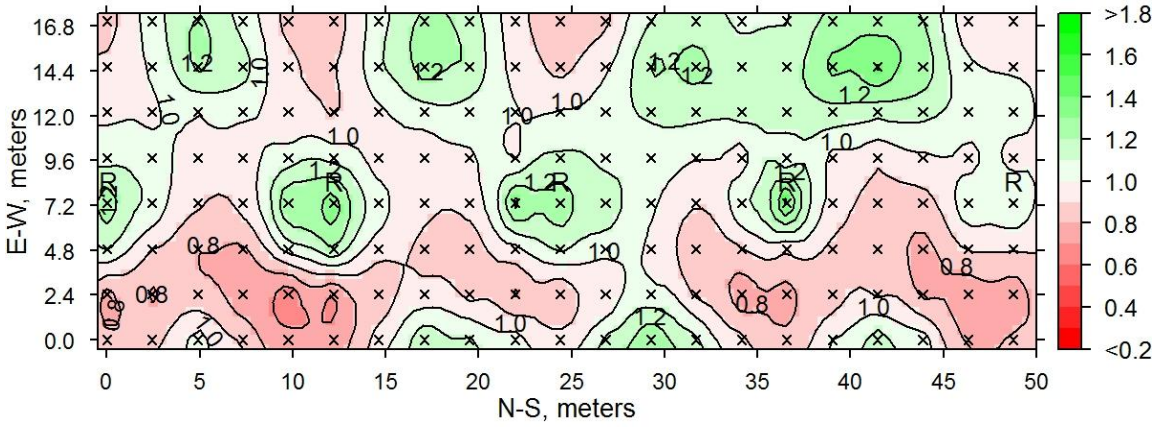

Figure F.2 Irrigation distribution normalized to the mean on 16 September in row F9. 'R' is an irrigation riser; 'x' is a catch-can.

The distribution uniformity was 0.80 on 16 September.

The Christianson Coefficient was 0.86 on 16 September.

F.2 Leaching Fraction

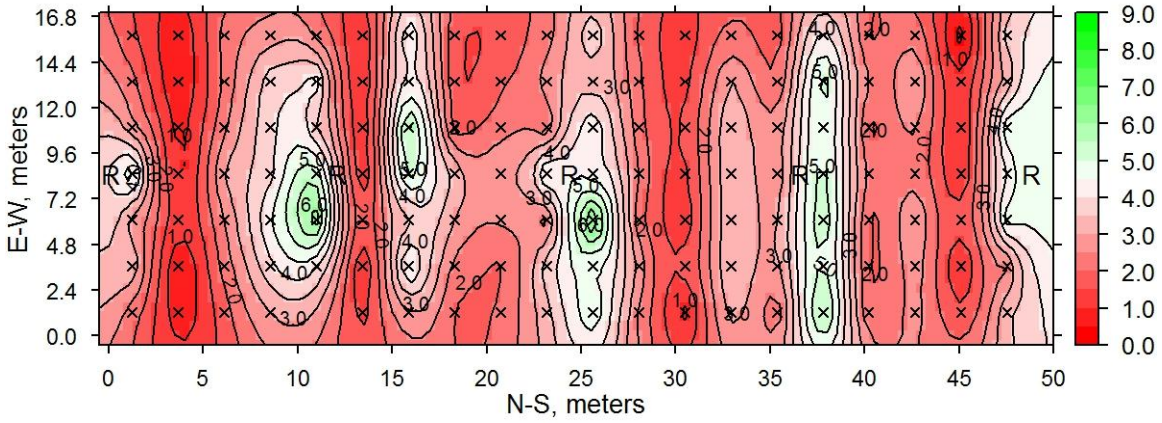

Figure F.3 Leaching fractions of 15 September in row F9. 'R' is an irrigation riser; 'x' is a monitored plant. Notice that the leaching fractions generally align into columns of plants. That is because each column was a single species and size.

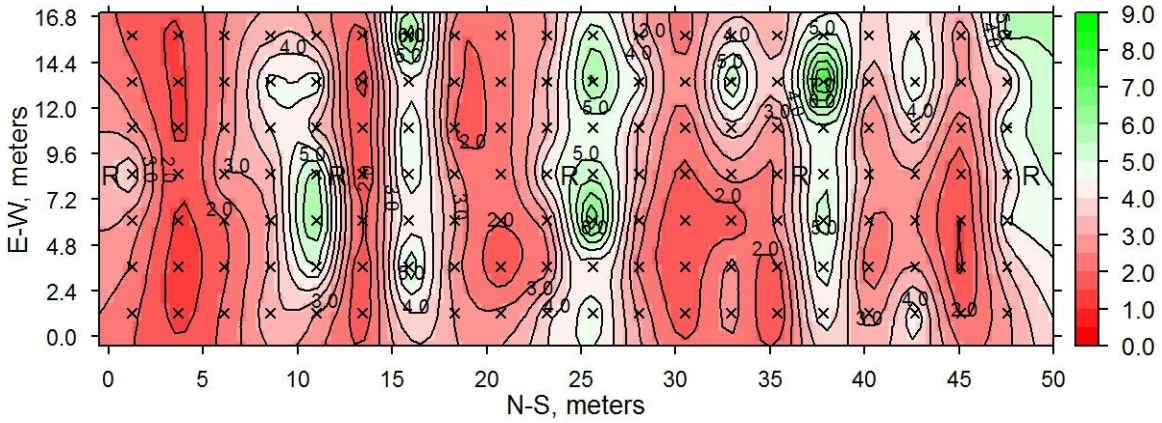

Figure F.4 Leaching fractions of 16 September in row F9. 'R' is an irrigation riser; 'x' is a monitored plant. Notice that the leaching fractions generally align into columns of plants. That is because each column was a single species and size.

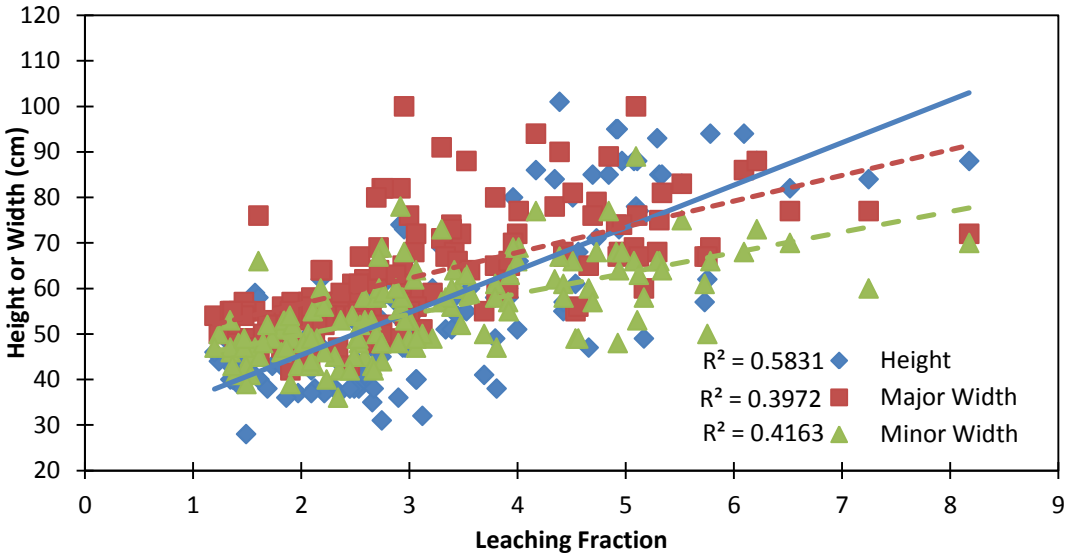

Figure F.5 Leaching fraction versus canopy dimensions. With R-squared values.